# SPECTROSCOPIC CHARACTERIZATION OF SOL-GEL-DERIVED MATERIALS

# PREPARATION AND CHARACTERIZATION OF ORGANICALLY-MODIFIED SOL-GEL-DERIVED MATERIALS: SPECTROSCOPIC AND BIOLOGICAL ASSAY STUDIES FOR THE DEVELOPMENT OF OPTICAL BIOSENSORS USING SOL-GEL IMMOBILIZED PROTEINS AND ENZYMES

By

MICHAEL RAKIC, B.SC.

A Thesis

Submitted to the School of Graduate Studies

in Partial Fulfilment of the Requirements

for the Degree

Master of Science

McMaster University

MASTER OF SCIENCE (1999) McMaster University
(Chemistry) Hamilton, Ontario

Title: Preparation and Characterization of Organically Modified Sol-Gel-Derived Materials: Spectroscopic and Biological Assay Studies for the Development of Optical Biosensors Using Sol-Gel Immobilized Proteins and Enzymes

Author: Michael Rakic, B. Sc. (Brock University)

Supervisor: Dr. John. D. Brennan

Number of Pages: xiv, 169

## Abstract

The goal of this research project was the development of a protocol for preparation of optically clear organic/inorganic hybrid materials that was amenable to entrapment of lipophilic biomolecules. The protocol involved the acid-catalyzed hydrolysis of mixtures of tetraethylorthosilicate (TEOS) with organosilane precursors, including methyltriethoxysilane (MTES), dimethyldimethoxysilane (DMDMS) and propyltrimethoxysilane (PTMS) in the presence and absence of the polymer additives poly(ethylene glycol) or poly(vinyl alcohol).

The effect of organosilane precursors and polymer additives on the optical clarity, hardness and hydration stability of the resulting materials was characterized. It was determined that there was a limit to the amount of organosilane that could be added before the materials exhibited unacceptable characteristics. These limits were 20.0% (v/v) for MTES, 10.0% (v/v) for PTMS, and 5.0% (v/v) for DMDMS. Addition of PEG to these materials at levels up to 10.0% (w/v) resulted in good material characteristics. However, addition of PVA produced opaque materials with poor material properties. The internal environment of the materials was also probed using the environmentally sensitive fluorescent probes 7-azaindole (7AI) and prodan. These studies showed that the method of hydrolysis of the silane precursors and the aging conditions had a dramatic effect on the resulting material.

The hybrid materials were used to entrap human serum albumin (HSA) and lipase to determine the effect of organic content on the biological function of these biomolecules. Both biomolecules retained a portion of their native function when entrapped in sol-gel-derived materials, and it was found that both proteins showed enhanced function in the presence of MTES. In the case of lipase, it was also determined that addition of PEG 600 at 10.0% (w/v in the gelation buffer) provided a dramatic increase in activity compared to materials without this additive, likely owing to a direct effect of the PEG on the stability of the entrapped protein.

Following studies using bulk glasses, a protocol was developed for the preparation of optically clear sol-gel-derived thin films that was amenable to entrapment of biomolecules. The optimal method involved dipcasting of co-hydrolyzed materials containing 1.0 to 3.0% PEG. By careful control of the viscosity of the casting solution and the rate of film deposition, it was possible to form very stable thin films with excellent physical characteristics. These films were used to entrap the pH-sensitive, ratiometric fluorescent probe dextran-SNARF-1, resulting in a prototype of a fluorimetric pH sensor. Co-entrapment of the probe and lipase into sol-gel-derived thin films resulted in a rapid, reagentless biosensor prototype that could monitor changes in pH due to the enzyme-catalyzed hydrolysis of triglycerides. These results demonstrate that species entrapped in sol-gel derived thin films are suitable for biosensor development.

## Acknowledgements

I would like to thank my supervisor, Dr. John Brennan for all of his guidance and support over the last two years. His encouragement was always able to get me through even the blackest of days.

I would also like to extend my gratitude to Kulwinder Flora. She continues to be a good friend and a valuable colleague and she made coming to work enjoyable. Thanks also to the other people that worked diligently in H209 at Brock and ABB-B101 at Mac, Lili Zheng, Cassandra Spong, Emily DiBattista, Amy Jones, Elizabeth Ilnicki, B.J. Frid, Glenda Bendiak, Doris Yan and Lehing Tu. I would also like to thank James Shoemaker, Barb Worman-Purnell and Carl Turner for their friendship and general silliness.

A special thank you goes to Stephanie Reed for her love, understanding, patience and support over the last two years. I can hardly express how wonderful she has been while I conducted my research or how much I appreciate the way she stood by me while I prepared this thesis.

I would also like to thank Dave and Bozena Styczynski for being so helpful and generous and for making my life so much easier over the last year.

Finally, I would like to thank my parents, Drago and Stella Rakic for their continued love and support over the last twenty-six years. They have always taught me that effort and hard work pay off in the end. Thank you for your patience, love and trust.

## Table of Contents

## List of Figures

## List of Tables

# Chapter 1: Introduction and Theory

## 1.1. Introduction

### *1.1.1. Biosensors*

One of the most important areas of analytical chemistry is the development of biosensors. A biosensor is a device that uses a biological sensing element in close proximity to, or directly integrated within, an inorganic signal transducer for the selective detection of targeted analytes.[1] The transducer converts the recognition step into an optical or electrical signal which is directly related to the nature and amount of analyte present.[2,3] The signal derived from the sensor is usually a secondary signal arising from a primary event involving the interaction between the sensing element and the analyte, rather than a direct signal caused by the analyte itself. In such cases, it is the effect that the analyte has upon the sensing element that provides the analytical signal. For the sensor to be effective, the recognition element (generally a biomolecule such as a regulatory protein, enzyme, antibody or oligonucleotide) should show a high degree of specificity for the target analyte. It should also retain its biological function over an extended period of time in an immobilized state, and it should not result in undesirable sample contamination.

There are several advantages to the use of biosensors for detection of analytes. Many biomolecules exhibit a high degree of selectivity for their target analytes, which means that the sensing element is able to detect the desired target even in the presence of other potentially interfering species within a given sample. Due to this selectivity,

biosensors can often be used to detect analytes directly and without the need for separation steps in complex matrices such as blood or natural waters, which often contain a significant amount of organic material. The use of biosensors allows for rapid detection of analytes since there is no need for separation of analytes from their original matrix and response times on the order of one second are common. Biosensor devices can also be quite compact, employing small power sources (e.g. batteries) and in the case of fluorescence-based optical sensors, a light emitting diode (LED) as the source of excitation. These components are quite inexpensive and coupling of the devices with laptop computers allows for remote sensing since the device is readily portable. Biosensors can also be used for detection of a wide variety of analytes, due to the vast number of different biomolecules that exist in nature, each exhibiting specificity for the species with which they interact. Some of the classes of target analytes include biomedical analytes, gases, metal ions, narcotics, pathogens, and viruses.[4] Biosensors have also been used for detection of analytes with concentrations in the sub-nanomolar range, depending on the analyte.[4]

### *1.1.2. Enzymes*

Proteins are molecules composed of a linear sequence of amino acids, the order of which is the primary structure of the protein. The chain of the protein folds to form substructures such as α-helices and β-sheets, which are common elements of protein secondary structure. The various secondary structural elements fold into a compact three-dimensional structure, known as the tertiary structure, which is often the functional

form of the protein. In some cases, two or more of these compact structures can combine to form larger quaternary structures, and these structures may be required for protein functionality. The presence of the correct tertiary or quaternary structure determines whether a protein is functional.[5]

Enzymes are one of the most widely used recognition elements for biosensor development. Enzymes are specialized proteins that catalyze specific reactions, often increasing the rates of given reactions $10^6$ to $10^{12}$-fold, compared to uncatalyzed reaction rates. The key advantage of enzymes is that they usually have very high selectivity for their reactants (known as substrates) and produce specific products with no side-products. Furthermore, enzyme-catalyzed reactions occur under mild temperature and pH conditions, making them amenable to sensing at physiological conditions.[6]

The mechanism of enzyme function varies from molecule to molecule, depending on the type of reaction that the enzyme is catalyzing. There is however, a common feature linking the function of various enzymes. This feature is known as the *active site*. In most enzymes, the active site is an indentation or cleft on a surface of the molecule that is geometrically and electrostatically complementary to the substrate. The substrate associates with specific amino acids in the active site via hydrogen-bonding, electrostatic interactions and van der Waal's and hydrophobic forces. Molecules that differ from the substrate in terms of shape, functional group distribution, or stereochemistry cannot bind effectively to the active site to form an enzyme-substrate complex required for formation of products. This property dictates the selectivity of an enzyme for a given substrate.[6]

There are other advantages to the use of enzymes for sensors compared to the use of other biorecognition elements such as antibodies. Enzymes, being catalysts, are not destroyed during the course of their catalytic function. Because of this, the enzyme-substrate reaction can be considered reversible (though not for the substrate, which is consumed during the course of the reaction), and hence a single enzyme molecule can be reused after it has completed its function. Also, a single enzyme molecule can turn over many substrate molecules during the course of a single measurement, depending on the time per measurement. This provides an inherent amplification of the signal as compared to other protein-based recognition elements, such as antibodies, that can only bind two ligands per antibody, usually irreversibly.

### *1.1.3. Enzyme Immobilization Methods*

For preparation of viable chemical sensors or biosensors, it is necessary to immobilize the chemical recognition element in contact with or integrated within a signal transducer.[3] There are several different types of methods that have been developed for immobilization of reagents.[3,4] These processes fall under three main headings: physisorption, covalent immobilization and entrapment. Physisorption techniques are the simplest to perform since the immobilization is based simply on the electrostatic interactions between the surface and the species being immobilized. However, repeated use of substrates with surface-adsorbed molecules can lead to degradation of the recognition ability of the surface, especially if the surface is rinsed repeatedly, causing protein desorption. Another major drawback of the use of adsorption methods is the

random orientation of the recognition element on the surface being treated. The binding site of the enzyme may be oriented in such a manner that it is not accessible to the target analyte, rendering the sensor at least partially useless.

Covalent immobilization of the recognition element onto a surface avoids the problem of desorption because the reagent is covalently bound to the surface. Covalent immobilization onto a surface can also reduce response time because the sensing element is directly exposed to the sample matrix and hence, the target analyte. However, the use of organic solvents and higher temperatures during immobilization may be too harsh for biological sensing elements such as enzymes. It may also be necessary to chemically modify the biomolecule if it lacks functional groups necessary for binding to the surface. Techniques for this type of modification of proteins have been reviewed.[7] Disadvantages of covalent immobilization include protein unfolding, which may render the protein or enzyme inactive since its binding or active site may be unfolded, preventing binding of target analytes. In addition, random orientation of the immobilized molecules on the surface may limit the accessibility of the target analyte to the sensing element.

The third general method for immobilization of molecules is entrapment of the sensing element within a porous, three-dimensional matrix. Typical matrixes include organic polymers such as nylon or poly(acrylamide).[8] In this case, the protein is not physically bonded to the surface and orientation of the biomolecule is not an issue. The porosity of the matrix allows the flow of small molecules into the region containing the biomolecule but the larger biomolecule remains entrapped. Potential disadvantages include the chemical processing conditions used for polymerization, which may have a

detrimental effect on the recognition element. Also, the polymer material may also be prone to swelling after insertion into different solvents, which can also lead to leaching of the entrapped biomolecule. It is also difficult to control the polarity of the polymer matrix, which can be important for entrapment of lipophilic proteins.

### *1.1.4. Sol-Gel Processing and ORMOSILs*

A recent advancement in protein immobilization is the application of the *sol-gel* process[9,10] for entrapment of molecules into inorganic matrixes. This process allows the encapsulation of molecules without any modification to the immobilized species and the mild reaction conditions make the process amenable to applications using a wide variety of biological molecules.[11,12,13,14,15,16,17]

The sol-gel process is a multi-step process that uses a metal or semimetal alkoxide precursor such as tetraethylorthosilicate (TEOS, $Si(OEt)_4$) or tetramethylorthosilicate (TMOS, $Si(OMe)_4$) to form a solid silicate glass. The alkoxysilane is hydrolyzed in the presence of an acid catalyst, forming hydroxylated silicon species, and an alcohol as a by-product (ethanol if TEOS is the silane precursor). The acid-catalyzed reaction scheme is shown in Figure 1.1.

$$Si(OEt)_4 + n\ H_2O \xrightarrow{H^+} Si(OEt)_{4-n}(OH)_n + n\ EtOH$$

**Figure 1.1. Hydrolysis of TEOS**

The hydroxysilane species interact with each other in multiple condensation reactions, releasing water and forming siloxane bonds. The condensation reaction scheme is shown in Figure 1.2.

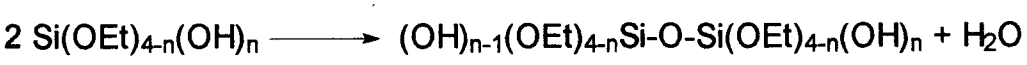

**Figure 1.2. Condensation Reaction Occurring During Sol-Gel Processing**

Condensation and polycondensation reactions continue with time, and when sufficient interconnected siloxane bonds are formed in a region, they respond collectively as colloidal particles or a sol. The size of these particles is on the order of 50 to 100 nm. Condensation and polycondensation reactions are shown in Figure 1.3.

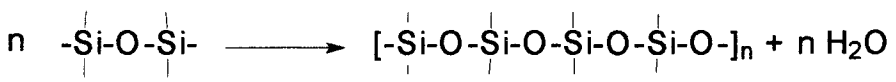

**Figure 1.3. Polycondensation Reactions Forming Colloidal Particles**

Given sufficient time, the colloidal particles and condensed silica species link together to form a solid three-dimensional network. This process can be accelerated by the addition of an aqueous buffer solution to the sol, which increases the pH of the resulting solution. The increase in pH is especially important for entrapment of biomolecules since it can prevent acid denaturation or aggregation or both.[12] Given that the addition of the buffer accelerates polycondensation, it rapidly initiates gelation, turning the liquid into a soft, gel-like solid. During gelation, the viscosity of the buffer/sol mixture increases dramatically, and a solid object results, assuming the shape of the mold containing the

starting materials. After gelation, the condensation and polycondensation reactions continue to occur over the course of days and weeks while the glass ages. During aging, water and ethanol evaporate from the cavities within the glass and the volume of the solid matrix shrinks by a factor of about 2-10.[18] The gel can be aged dry, wet (i.e., in buffer solution) or it can be rinsed with buffer to wash away any excess ethanol formed and then aged wet or dry. It is possible to harden the material by heating the porous gel at high temperature, which causes densification to occur. Densification causes elimination of the pores within the matrix, and the density of the network becomes comparable to that of fused quartz or fused silica. However, such a step is not possible when proteins are entrapped, owing to the potential for denaturation.

There are several advantages to the use of silicon-based precursors for formation of sol-gel-derived materials, as outlined by Lev.[18] The first is that the glass matrix formed is optically clear and non-fluorescent, making sol-gel-derived materials amenable to spectroscopic characterization. Second, the sol-gel-derived glass has a tunable porosity, allowing small molecules to diffuse through the matrix while larger biomolecules or higher molecular weight polymers are immobilized and hence will not leach out of the glass over time. Third, there is a significant amount of interstitial water molecules within the glass matrix, which serve to hydrate the immobilized biomolecules. These waters of hydration are necessary for retention of biological activity upon immobilization.[19] Fourth, sol-gel-derived glass materials are highly stable since the silica matrix is chemically inert, photochemically and thermally stable and resistant to biodegradation. Fifth, the sol-gel process can be performed at ambient temperatures, allowing

incorporation of thermally unstable organic and biological molecules into the matrix. Sixth, the precursor solutions can be molded into a variety of geometries, including blocks, slides, films and fibers.[20] Finally, various precursors such as organically modified silanes or polymers may be incorporated to control the polarity of the matrix.

As indicated above, one of the most attractive features of sol-gel-processed materials is the ease with which molecules can be incorporated into the matrix. This molecular incorporation is accomplished by addition of the desired dopant to the gelation buffer. Fluorescent probes,[21,22] regulatory proteins,[23,24] enzymes,[14,25] antibodies[26,27] and cell extracts[28] have been successfully entrapped in sol-gel-derived matrixes. Such materials have been used for non-linear optics, photochromic glasses, biosensors and bioreactors.

Perhaps the most important feature of sol-gel-derived materials is the fact that it is possible to control the properties of the final matrix by careful manipulation of the processing conditions. For example, the water:Si ratio used in preparation of the materials can have a significant effect on pore sizes and on the physical properties of the resultant materials.[29] Changing the aging and drying conditions (i.e. wet aging vs. dry aging, densification) can also control the pore size and physical properties of the material.

Another method for modification of the material properties of the sol-gel-derived materials is the use of organically modified silanes (ORMOSILs). ORMOSILs are attractive sol-gel precursor materials because of the ability they offer to tailor various desirable materials properties by suitable copolymerizations and because they permit anchoring of organic functionalities directly into the matrix.[30] The use of ORMOSILs for preparation of organic/inorganic hybrid materials from different starting materials

originated from the idea of creating materials having more desirable properties than the two original components. Blending of organic and inorganic components in a material is particularly useful since it allows the development of materials with totally new properties. The use of these types of materials in sol-gel processing has been reviewed.[31]

Work has been done previously[22,30,32] to probe the internal environment of hybrid organic/inorganic materials using optical spectroscopy. However, the processing conditions used for these studies were not amenable to entrapment of biomolecules due to the addition of excess ethanol (a protein denaturant) as a co-solvent, or heating at temperatures exceeding 80°C. Both of these processing conditions can cause denaturation of proteins, which can cause partial or total loss of function. More recently,[29,33] work has been done to probe the internal environment of TEOS and TMOS-derived materials prepared using room temperature processing conditions. Bright's research used the fluorescent probes pyrene and rhodamine-6G (R6G) to map out the local dipolarity and dopant mobility within the sol-gel composites, respectively.

An alternate method for preparation of organic/inorganic hybrid sol-gel-derived materials is the incorporation of organic polymers into the sol-gel matrix via entrapment. Bright and co-workers[33] doped poly(ethylene glycol), of different molecular weights and concentrations, into TEOS and ORMOSIL-derived sol-gel materials for the purpose of using fluorescent probes to study the effect of the polymer additives on the internal polarity and dynamics of these materials. The incorporation of various polymers into sol-gel-derived materials was also recently reviewed.[34]

Most of the work done for entrapment of enzymes, as described above, has involved the use of TEOS or TMOS as the silane precursor for preparation of sol-gel-derived materials. Also, the enzymes used have been water-soluble and hence, were suitable for entrapment in polar silica matrixes derived from TEOS or TMOS. However, these materials are not suitable for entrapment of lipophilic enzymes such as lipase.[35] Recent work has focused on entrapment of lipases in organic/inorganic hybrid materials.[36,37] It was found in these studies that the use of methylated ORMOSIL precursors, such as methyltrimethoxysilane (MTMS, $CH_3$-Si$(OMe)_3$), was necessary for enhanced activity of the entrapped lipases. One of these studies[37] also showed that the addition of polymer additives such as poly(vinyl alcohol), improved the activity of the entrapped lipase.

The immobilization methods employed in the studies described above involved mixing the silane, catalyst, additives, protein and water without pre-hydrolysis of the silane. A significant drawback of the described method was that the resulting sol-gel-derived material was a soft, white gel. The opaque material afforded by these processing conditions was not amenable to fluorescence studies. The resulting gel was dried, then crushed into a powder and the activity of the entrapped lipase was tested in this form. This method of preparation was used since the purpose of using the immobilized enzyme was for esterification reactions in a bioreactor. The format chosen was not suitable for sensing applications since the powder could not readily be coupled with an optical signal transduction device.

### *1.1.5. Purpose of Research and Experimental Approach*

The purpose of the current research project is the preparation and characterization of both the material properties and the behaviour of biomolecules entrapped in *optically clear*, sol-gel-derived organic/inorganic hybrid materials. Such materials were prepared by the two-step method of silane hydrolysis and buffer addition to promote gelation that is amenable to encapsulation of lipophilic enzymes. The mechanical properties of the sol-gel-derived materials were examined by evaluating properties such as optical clarity, hardness and dehydration/rehydration stability. This was done using samples prepared by mixing TEOS with various organically modified silanes as precursors. The glasses were formed in three different formats. Monoliths refer to sol-gel-derived materials that are roughly cubic in shape (with dimensions of ~0.8 cm x 0.8 cm x 0.8 cm). Slides refer to flat, rectangular solid sol-gel-derived materials with dimensions of ~1.5 cm x 0.8 cm x 0.2 cm. Thin films refer to materials cast on solid supports at a thickness of less than 1 μm. The mechanical properties of monoliths and slides prepared using TEOS and ORMOSILs, with or without polymer additives, were also examined. The polymer additives used in this work were poly(vinyl alcohol), PVA, and poly(ethylene glycol), PEG. The structures of these two polymers are shown in Figure 1.4.


**Figure 1.4. Structures of PVA (Left) and PEG (Right)**

The internal polarity of the sol-gel-derived materials was monitored using two fluorescent probes, 7-Azaindole (7AI)[38,39,40,41] and 6-propionyl-2-dimethylaminonaphthalene (prodan),[21,42,43] whose emission characteristics are sensitive to the polarity of their surroundings. The structures of these probes are shown in Figure 1.5. In this work, these probes were incorporated into sol-gel-derived materials prepared using TEOS and mixtures of ORMOSILs with TEOS in the presence and absence of polymer additives.

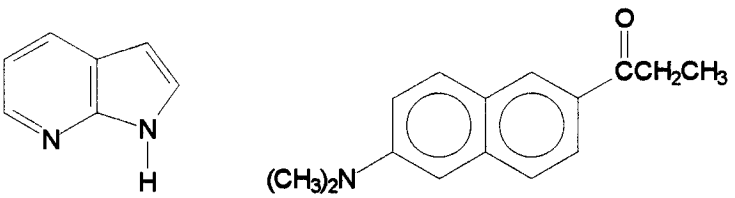


**Figure 1.5. Structures of 7AI (Left) and Prodan (Right)**

After the mechanical properties of these materials were characterized, the function of biomolecules entrapped in these materials was investigated. This was accomplished using two model proteins, lipase (from *Candida Rugosa*) and human serum albumin (HSA). Lipase was used in this study because it has been previously demonstrated[37] that the hydrolytic activity of the entrapped enzyme is highly dependent on the characteristics of sol-gel-derived materials. Lipases are enzymes that catalyze a variety of esterification, interesterification and ester hydrolysis reactions,[37] and hence are potentially useful for the development of optical biosensors for triglycerides.

HSA is an abundant human blood protein and has the ability to bind several ligands, including small aromatic and heterocyclic carboxylic acids, such as nonsteroidal anti-

inflammatory drugs (NSAIDs).[23] HSA was a useful protein for this study because it has a fluorescence-based assay of protein function which requires optically transparent hybrid materials for spectroscopic studies to be performed. HSA is a single-tryptophan protein formed from a single polypeptide chain of 585 residues,[44] which is divided into three major domains. The structure of tryptophan is shown in Figure 1.6.

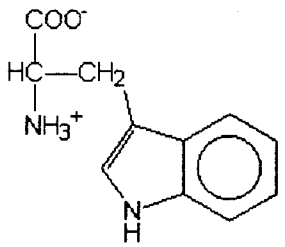


**Figure 1.6. Structure of Tryptophan**

The fluorescence of the single Trp residue in HSA has been used previously[23] to provide information on the conformation of the protein in solution and should be useful for probing how the structure of entrapped HSA is affected by matrix composition.

Both lipase and HSA were entrapped into various types of organic/inorganic hybrid materials and either the catalytic activity of lipase or the ligand-binding ability of HSA was monitored. The activity of lipase was monitored by measuring the amount of free fatty acids produced in the enzyme-catalyzed hydrolysis of glyceryl tributyrate using titrimetric methods.[45] A reaction scheme for this hydrolysis reaction is shown in Figure 1.7.

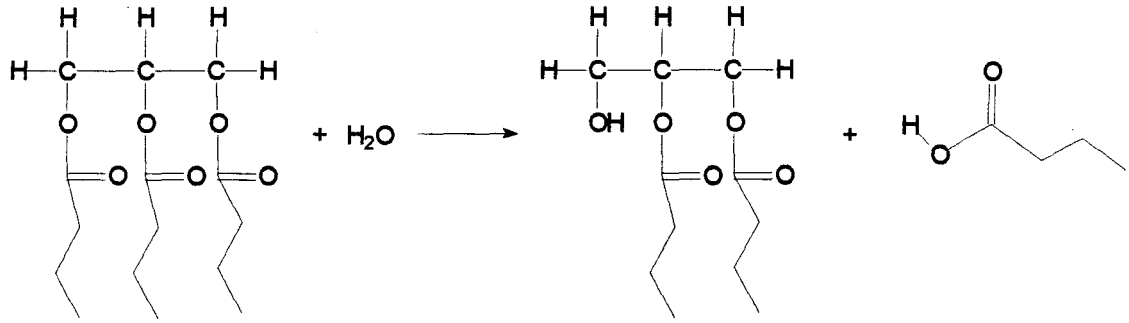

**Figure 1.7. Reaction Scheme for the Hydrolysis of Glyceryl Tributyrate**

The ligand-binding ability of HSA was monitored by measuring the fluorescence quenching of the single tryptophan residue of HSA upon binding of salicylate.

After the initial characterization of these proteins was completed using bulk sol-gel-derived materials, the materials were prepared in a different format, namely sol-gel-derived thin films dipcast onto glass slides. This method of fabrication was chosen since the ultimate goal of this research project was the development of an evanescent wave biosensor.

There are several advantages to the use of thin films for sensor development and biomolecule entrapment. First, dipcasting of protein-loaded thin films allows the recognition element to be put in intimate contact with a physicochemical transduction device, such as a planar waveguide or an optical fiber, facilitating excitation of fluorescence and detection of emission from the immobilized recognition element.[4] Second, the use of thin films rather than slides or monoliths greatly reduces the diffusion path for analytes, providing faster response times and reducing the dependence on

diffusion kinetics of the reaction kinetics. Third, thin films are simple to prepare using a variety of methods, which will be discussed in detail in Section 1.2.2. Finally, the preparation, aging and drying processes for thin films are complete in much shorter spans of time, relative to those of monoliths or slides. This shorter processing time allows much quicker turnaround of samples, which can be prepared and tested within a period of days, rather than having to wait several weeks for samples to age and dry. Shorter aging and drying times also result in reduced exposure of entrapped proteins to ethanol, thereby reducing the likelihood of protein denaturation due to ethanol. Although the faster aging and drying times make the use of thin films an attractive method for entrapping proteins, it is not known what effect these processing conditions will have on the function of the entrapped proteins.

There are also some disadvantages to the use of thin sol-gel-derived films for molecular entrapment. Due to the reduced pathlength and a reduced number of probe molecules deposited onto a surface, it is necessary to use solutions of fluorescent probes or biomolecules that have higher concentrations than those used for preparation of monoliths and slides. The lower concentration of reporter groups on the surface also results in a reduction of signal-to-noise ratio since the fluorescent signal from probe-doped films is much lower. However, these problems can be largely overcome by using more concentrated probe or biomolecule solutions for film processing or by using evanescent excitation of the immobilized fluorophores.[46]

One of the other goals of this research project was the development of a reagentless sensing system for detection of triglycerides using lipase. In order to make the system

reagentless, the reporter group (i.e. a pH indicator to detect changes in pH due to formation of fatty acid products) needed be co-entrapped with lipase in thin films for development of a prototypical fluorescence-based optical biosensor. A new method for monitoring lipase activity was investigated, using two pH-sensitive fluorescent probes, fluorescein,[47,48,49] and carboxyseminaphtharhodafluor-1 (SNARF-1).[50,51] The structures of these probes are shown in Figure 1.8. The pH sensitivity of these two probes was to be examined both in solution and entrapped in thin sol-gel-derived films.

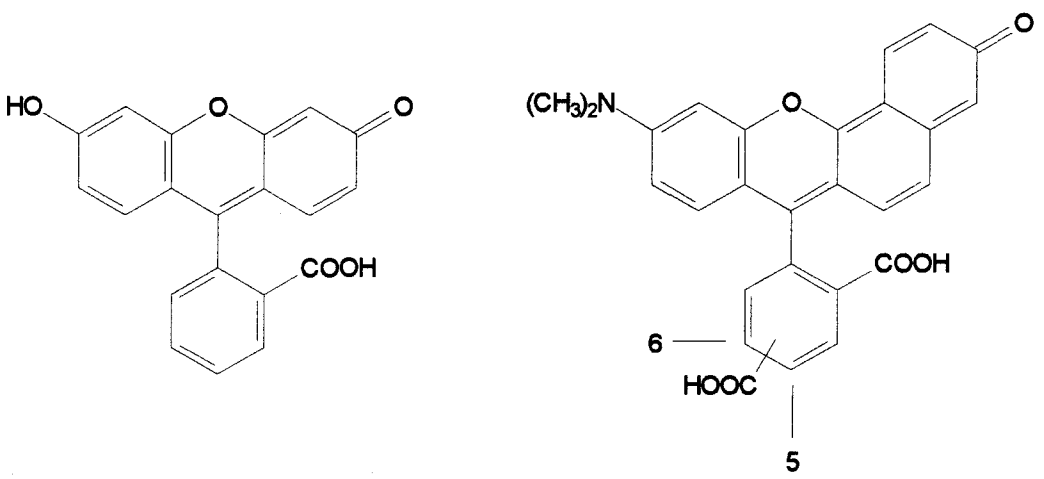


**Figure 1.8. Structures of Fluorescein (Left) and SNARF-1 (Right)**

Fluorescein is a useful probe for pH determination because it has a high quantum yield that is pH dependent in solution, is inexpensive, and can be excited at visible wavelengths, allowing the use of inexpensive excitation sources such as light emitting diodes (LED's). SNARF-1 is a useful probe for monitoring pH changes because it can be excited using a wide range of wavelengths (ranging from 442 to 531 nm) and its emission undergoes a pH-dependent wavelength shift. SNARF-1 emits at two different

wavelengths, the intensity of each corresponding to the relative amount of the protonated and deprotonated forms of the probe. The intensity of the emission from these forms of the probe is dependent on their concentrations and hence, the pH of the surrounding solution. Monitoring the ratio of the intensity of the two forms of the probe, which changes as a function of pH, allows spectroscopic determination of pH in solution. The signal derived from SNARF-1 is ratiometric and therefore, spectroscopic drift due to photobleaching of the probe or changes in excitation source intensity are not major problems since both forms of the probe are affected to the same degree. Unlike fluorescein, whose pH-dependent emission intensity is dependent on the concentration of the basic form alone, and hence on probe concentration, the signal from SNARF-1 is not dependent on the concentration of the probe. The $pK_a$ of both fluorescein and SNARF-1 are within the biological pH range and hence may be used for monitoring pH changes due to enzyme-catalyzed formation of acidic or basic products.

The final portion of this research project focussed on the entrapment of biomolecules in sol-gel-derived thin films for the purpose of developing optical biosensors. HSA was immobilized in TEOS-derived films for the purpose of examining its ability to bind salicylate, once entrapped in a thin film. Lipase and SNARF-1 were co-entrapped in TEOS and ORMOSIL-derived thin films in the presence and absence of polymer additives for the initial characterization of a reagent biosensor for triglycerides.

## 1.2. Theory

### *1.2.1. Fluorescence-Based Methods of Probing Sol-Gel Internal Environment*

A Jablonski diagram, shown in Figure 1.9, best illustrates the processes involved in fluorescence emission.

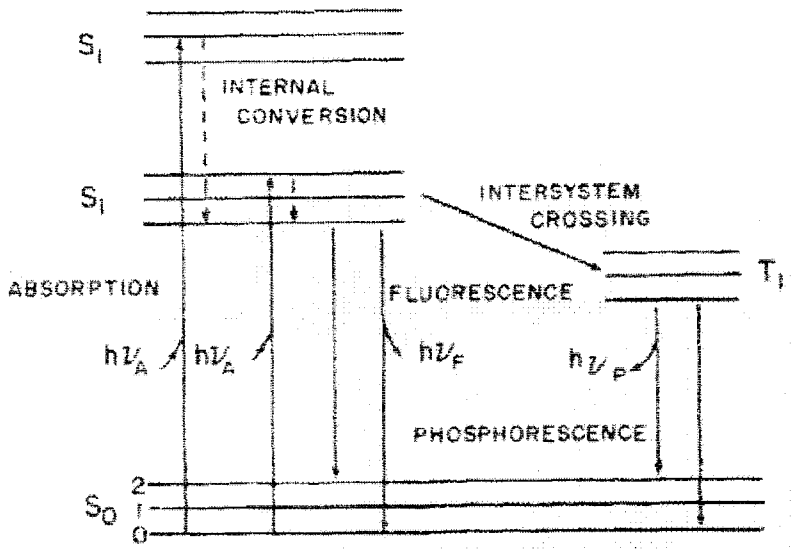


**Figure 1.9. Jablonski Diagram[52]**

In this diagram, the ground state and the first excited, singlet electronic state are labeled $S_0$ and $S_1$, respectively. After light absorption, the fluorophore is usually excited to some higher vibrational level of $S_1$. Molecules in these excited vibrational states relax to the lowest vibrational state of $S_1$ in a process known as internal conversion. This process occurs in about $10^{-12}$ s. Since fluorescence emission occurs in about $10^{-8}$ s, vibrational relaxation is generally complete before emission occurs. The electronic transition down to the lowest electronic level can also result in an excited vibrational

state. Molecules in the $S_1$ state can also undergo conversion to the first triplet state, $T_1$, in a process known as intersystem crossing. Emission from $T_1$ is termed phosphorescence and is generally shifted to longer wavelengths (lower energy) relative to fluorescence.[52]

One of the most important parameters of fluorescence emission is the intensity. The intensity of fluorescence emission is dependent upon several parameters, as shown in the following relationship:

$$F(\lambda) = 2.303P_0k\varepsilon bc\Phi \qquad (1)$$

where $F(\lambda)$ is the intensity of the emitted radiation at a particular wavelength, $\lambda$; $P_0$ is the intensity of the exciting radiation; k is a wavelength dependent instrument correction factor; $\varepsilon$ is the molar extinction coefficient of the fluorophore; b is the optical pathlength; c is the molar concentration of the fluorophore and $\Phi$ is the wavelength independent quantum yield. This relationship shows that fluorescence intensity depends on the ability of a fluorophore to absorb and emit light. If $P_0$, k, $\varepsilon$, b, and c are constant (as in most protein studies), F is directly proportional to $\Phi$.

The fluorescence quantum yield is the ratio of the number of photons emitted to the number absorbed and describes the probability of an excited molecule emitting radiation as fluorescence. Relaxation of the excited state can be described by two types of processes, each with its own rate constant, $k_r$ and $\Sigma\ k_{nr}$. $k_r$ describes relaxation by emission of photons (radiative decay) whereas $\Sigma\ k_{nr}$ is a sum of the rates of all non-radiative processes including internal conversion, intersystem crossing and solvent relaxation.[53] The quantum yield can therefore be defined as:

$$\Phi = \frac{k_r}{k_r + \Sigma k_{nr}} \qquad (2)$$

In the context of this research project, changes in intensity of the Trp residue of HSA due to salicylate binding depend on changes in the quantum yield of the Trp owing to quenching of tryptophan fluorescence by bound salicylate.

Monitoring the wavelength of emission of a fluorophore as it returns to the ground state allows the derivation of other physical information. For most fluorophores in solution, there is a general shift to longer wavelength (lower energy) of emission relative to absorption. This red shift is known as a Stoke's shift. A common cause of the Stoke's shift is the rapid decay of the excited vibrational state to the lowest vibrational state of $S_1$. Since there is a loss of vibrational energy, the fluorophore emission occurs at a longer wavelength. Also, excited fluorophores often decay to excited vibrational levels of $S_0$, leading to further loss of vibrational energy, further increasing the Stoke's shift. Further relaxation to lower vibrational levels of an excited fluorophore can also occur due to the transfer of vibrational energy to solvent molecules.

The fluorescence emission of many fluorophores is also sensitive to the polarity of the solvent. The general trend indicates that red shifts occur for fluorophores in solvents of increasing polarity. The shifts result from the interactions of the dipole moment of the fluorophore with the dipole moments of the solvent molecules, and from specific chemical interactions between the fluorophore and one or more solvent molecules. Solvent-dependent shifts in emission wavelength involve the reorientation of the solvent shell surrounding the fluorophore and as a result, are time dependent. The basis for shifts

in emission wavelengths is conceptually quite simple. The absorption of light generally occurs in about $10^{-15}$ s, a time frame that is adequate for redistribution of the electronic structure of the fluorophore. The electronically excited states of aromatic compounds tend to have a larger dipole moment ($\mu^*$) relative to the dipole moment of the ground electronic state ($\mu$). The absorption of a photon by the fluorophore involves the instantaneous creation of a dipole, which disrupts the environment surrounding the fluorophore. As a result, the solvent responds by reorganization of the solvent cage around the fluorophore. This reorganization of the solvent cage induces a stabilization of the dipole moment of the excited fluorophore, $\mu^*$, lowering its energy. Relaxation of the fluorophore by emission returns the dipole moment to its original ground state configuration, $\mu$. After emission, the solvent molecules are oriented as they were with the excited state dipole moment. This serves to destabilize the dipole moment of the ground electronic state of the fluorophore, raising its energy. The result of these solvent restabilizations is a decreased energy of emission and a shift to longer wavelength.[54] A diagram of this process is shown in Figure 1.10.

This figure shows that the interaction between the solvent and fluorophore molecules affects the difference between the ground and excited states. In general, fluorophores dissolved in polar solvents tend to exhibit larger red shifts, relative to fluorophores dissolved in non-polar solvents. A good approximation of the energy difference between the absorption and emission bands is described in the Lippert Equation, shown below. This energy difference between the absorbance maximum ($\bar{\nu}_a$) and the emission maximum ($\bar{\nu}_f$) is a function of the refractive index (n, measure of

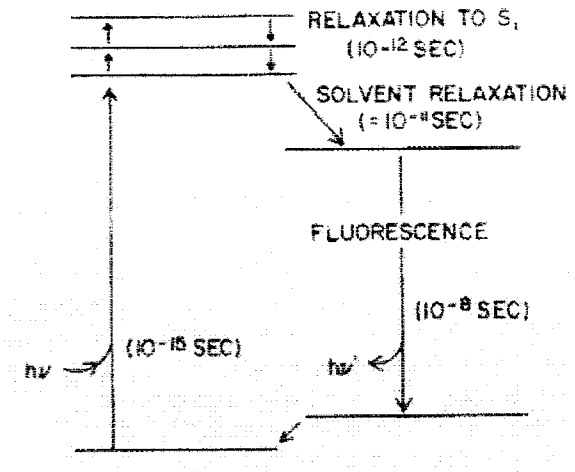


**Figure 1.10. Jablonski Diagram Illustrating Solvent Effect[54]**

electronic polarizability) and the dielectric constant (ε, measure of orientational polarizability) of the solvent.

$$\bar{\nu}_a - \bar{\nu}_f = \frac{2}{hc}\left(\frac{\varepsilon - 1}{2\varepsilon + 1} - \frac{n^2 - 1}{2n^2 - 1}\right)\frac{(\mu^* - \mu)^2}{a^3} + \text{constant} \qquad (3)$$

where h is Planck's constant; c is the speed of light; a is the radius of the cavity in which the fluorophore resides and the constant is the inherent Stoke's shift. This equation indicates that higher values of n or ε result in larger shifts in wavenumbers and therefore, wavelengths.

Another consideration regarding the fluorescence emission spectrum of a solute dissolved in a particular solvent is the fact that fluorescence spectroscopy involves the interrogation of large numbers of molecules, rather than a single molecule. At any instant in time, different molecules exist in many different solvent microenvironments. As a result, the fluorescence spectra of solutes in liquid solvents are broadened as a result of the different environments experienced by the different solute molecules comprising the

ensemble of solute molecules. This effect has been termed inhomogeneous broadening[55] and is important in the context of this work since it will provide a method for monitoring the distribution of local microenvironments inside the sol-gel-derived material.

The Lippert equation given above describes a general effect and wavelength shift that all dissolved species experience, and that is dependent on the dipolarity of the solvent. However, there are also other more specific interactions between the solvent and the dissolved probe molecules that result in further wavelength shifts. These types of interactions are important in that they can provide information about the local environment surrounding the probe molecules. Specifically, interactions between polar functional groups in a solute with some solvents (such as hydrogen bonding or complex formation) are the dominating factors affecting the absorption and fluorescence wavelengths of the solute.[56]

The probes used in this research project demonstrate these types of specific interactions that lead to significant shifts in emission maxima. 7-Azaindole (7AI) in water exhibits an emission maximum at ~385 nm when excited at 289 nm.[38] However, it is known that 7AI is able to form dimers and cyclic hydrogen-bonded complexes with solvent molecules and that these dimers and complexes exhibit significantly red-shifted emission maxima. Examples of these types of dimers and complexes are shown in Figure 1.11.

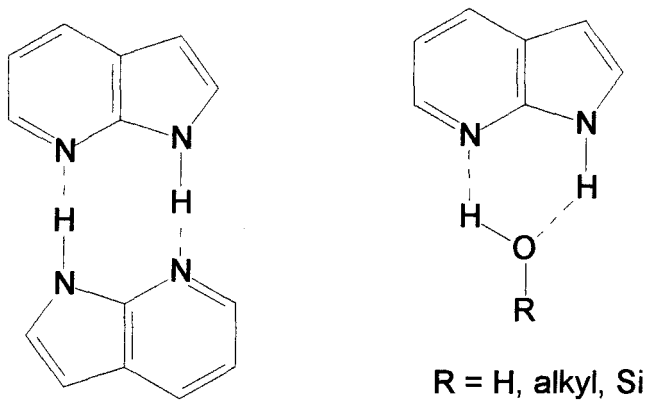


**Figure 1.11. Dimer (Left) and Solvent-Complexed (Right) Forms of 7AI[38]**

These red shifts are greater than those that result from interaction between the dipole moments of the solute and the solvent molecules alone. Hence, the resulting red shift is a sum of the solvent dipolar relaxation and hydrogen bonding effects. The use of 7AI in probing the internal environment of sol-gel-derived materials therefore allows a qualitative determination of the surface silanol content, based on the presence of significant red shifts due to adsorbed forms of the probe on the interior surfaces of the sol-gel-derived material.[57]

Prodan is a probe whose emission characteristics are highly sensitive to the polarity of its local environment, and hence is useful for examining the polarity of the internal environment of sol-gel-derived materials. Prodan has previously been used for examination of the internal environment of sol-gel-derived materials prepared using TMOS as the silane precursor.[21] The probe exhibits emission maxima ranging from 401 nm in cyclohexane to 530 nm in water.[42] It has also been recently reported[43] that prodan forms dimers and higher-order aggregates in supersaturated solution (concentrations of

greater than 1 μM in pure water). These aggregates exhibit an emission maximum near 420 nm that is often present as a shoulder on the monomer peak. Due to the solvent dependent emission characteristics of prodan, it is a well-suited probe for monitoring the internal polarity of the ORMOSIL-derived and polymer-doped sol-gel-derived materials. The occurrence of the aggregate peak at 420 nm can also provide a semi-quantitative method for monitoring the rate of drying of the sol-gel-derived materials.

Another type of specific interaction that can affect the emission wavelength of a particular probe dissolved in a solvent is protonation. In this case, a chemical bond is formed between the probe and the proton, resulting in dramatic differences in the electronic structure of the probe. Hence, the spectroscopic properties of the protonated and deprotonated forms of the probe are very different.[58] For two species or two forms of a fluorescent probe (such as SNARF-1, which emits at two different wavelengths depending on its state of protonation), the fluorescence intensity is a function of the sum of the electronic properties of both forms of the probe. This relationship can be expressed as:

$$F(\lambda_1, \lambda_2) = 2.303P_0[(\varepsilon_1 bc_1\Phi_1) + (\varepsilon_2 bc_2\Phi_2)] \qquad (4)$$

In the case of fluorescein, the wavelength of maximum emission is not pH dependent. Instead, the quantum yields of the monoanionic ($\Phi_m = 0.37$) and dianionic ($\Phi_d = 0.93$) forms of the probe are different, and hence the emission intensity is dependent upon the concentrations of the dianionic form of the probe as described in Equation 1. Equation 4 shows that the resulting fluorescence spectrum of a probe such as SNARF-1 will be a combination of the spectra of the protonated and deprotonated forms. The relative

concentrations of these forms will also have an effect on the resulting spectrum. Changes in these relative concentrations allow the use of SNARF-1 for pH determination due to the inherent sensitivity of the probe to proton concentration. In the context of this work, the use of pH-sensitive probes provides a fluorimetric method for monitoring the lipase-catalyzed formation of acidic hydrolysis products.

### *1.2.2. Preparation of Sol-Gel-Derived Thin Films*

There are three main methods for formation of sol-gel-derived, protein-doped thin films: dip-casting,[59,60,61] spin casting[62] and aerosol deposition.[63,64] Spin casting involves the deposition of a small amount of a sol-gel/buffer mixture directly to the surface of a planar substrate such as a glass slide. The slide is then spun briefly at high speed, which causes spreading of the solution on the surface, and resulting in a uniform, featureless film. This method is simple to implement and is useful for preparation of crack-free films, but is limited to applications that employ planar substrates. Aerosol deposition involves the spraying of the sol-gel precursor solution, which has been nebulized by an ultrasonic humidifier. Nitrogen gas is introduced into the flask containing the mist, forcing the mist onto the surface. The thickness of the film can be controlled by adjusting the vapour deposition time or the water:silane ratio used in forming the precursor solution. Although aerosol deposition of sol-gel-derived films can also be applied for non-planar substrates, it is difficult to use this method for preparation of uniform films on cylindrical or low surface area surfaces such as optical fibers.

The final casting method, which was employed in this research project, is dip-casting. In this method, the substrate is immersed into the coating sol, which contains polymeric or colloidal species in suspension along with the protein. The substrate is then withdrawn from the sol at a constant rate.[60] This process is shown schematically in Figure 1.12.

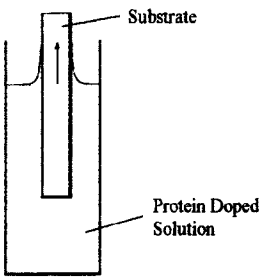


**Figure 1.12. Schematic of Dip Casting Process for Preparation of Sol-Gel-Derived Films**

As the substrate is withdrawn from the sol, a liquid film adsorbs to the surface of the moving substrate. The film becomes thinner by evaporation of solvent (i.e. water and ethanol) and gravitational draining. Spatially resolved fluorescent spectroscopy[60] using the ethanol-sensitive fluorescent probe pyranine has shown that ethanol evaporates preferentially from the film, changing the profile of the film. In thin films, gelation, aging and drying occur within a few minutes, compared to days or weeks for bulk sol-gel-derived materials. The film profile appears to be wedge-shaped but magnification revealed[60] that two parabolic shapes corresponding to the preferential evaporation of ethanol create a water-rich film which dries to produce the deposited film. The schematic of the double parabolic shape of a film during casting is shown in Figure 1.13.

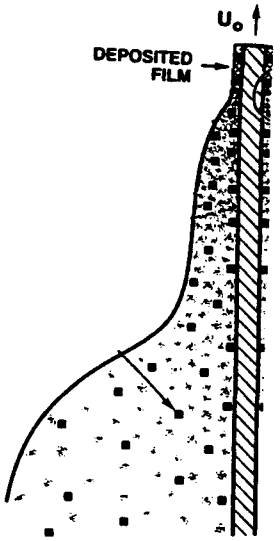


**Figure 1.13. Schematic of the Profile of a Dip Cast Sol-Gel-Derived Film During Casting[60]**

The thickness of the film deposited onto a substrate is dependent on the properties of the coating solution and the rate at which the film is withdrawn. The relationship between these properties and film thickness is shown in Equation 1.[59]

$$t = 0.944\left(\frac{\eta U}{\sigma}\right)^{1/6}\left(\frac{\eta U}{\rho g}\right)^{1/2} \qquad (5)$$

In this equation, t is the film thickness; $\eta$ is the viscosity of the solution; $\sigma$ is the surface tension of the solution; $\rho$ is the density of the solution; U is the withdrawal speed and g is the gravitational acceleration constant. This equation shows that it is possible to manipulate the film thickness by altering the properties of the solution being cast or altering the withdrawal speed. Dipcasting is a useful technique for preparation of thin films because it is simple to perform and can be applied with substrates of any size or shape, including optical fibers. However, there is a great deal of waste in preparing thin

films by dipcasting because only a small fraction of the casting solution is actually used for formation of the film.

A variety of optical sensing applications using thin sol-gel-derived films have been demonstrated. These applications have involved the entrapment of metal complexes[65,66,67,68] and fluorescent probes[64,69] for oxygen sensing, fluorescent probes such as bromophenol blue,[70,71] fluorescein[47] and fluorescein-labeled dextrans[48,49] for pH sensing and biomolecules[63,72,73] for stability studies. These applications used spincasting techniques with planar substrates only and used added ethanol in preparation of the sol-gel-derived thin films. These conditions were not amenable to the preparation of protein-doped films on optical fibers due to the presence of excess ethanol (a protein denaturant) and the fact that spin coating cannot be used for preparation of films on optical fibers. This research project represents one of the first times that thin film immobilization techniques have been used for preparation of thin films using conditions that are amenable to entrapment of proteins for biosensing applications.

# Chapter 2: Experimental

## 2.1. Chemicals

Tetraethylorthosilicate (TEOS, 98%, 99.9%), methyltriethoxysilane (MTES, 99%), dimethoxydimethylsilane (DMDMS, 95%), poly(ethylene glycol) (PEG, molecular weights 400 and 600), and poly(vinyl alcohol) (PVA, 98% hydrolyzed, average molecular weight 13 000 to 23 000) were purchased from Aldrich. n-Propyltrimethoxysilane (PTMS, 99%) was purchased from Petrarch Silanes and Silicones (Bristol, PA). All silanes and polymers were used without further purification. Glyceryl tributyrate, (approximately 99%), phenol red (phenolsulfonphthalein), fluorescein, 7-azaindole (7AI), human serum albumin (HSA, 99%, essentially fatty acid free), lipase (from *Candida rugosa*), and poly(styrene) and poly(methacrylate) cuvettes were purchased from Sigma. All chemicals and proteins listed above were used as received. 6-Propionyl-2-dimethylaminonaphthalene (prodan), 5-(and-6)-seminaphtharhodafluor-1 (SNARF-1), 5-(and-6)-chloromethyl-SNARF-1 acetate (mixed isomers), dextran-SNARF-1 (70 000 molecular weight, anionic), and dextran-fluorescein (70 000 molecular weight, polyanionic) were purchased from Molecular Probes (Eugene, Oregon) and were used as received. All solutions were made with distilled water that had been deionized using a Milli-Q filtration system. All other chemicals and solvents were of analytical grade and were used as received.

## 2.2. Procedures

### *2.2.1. Preparation of Sol-Gel Precursor Solutions*

The method used for preparation of sol-gel-derived materials has been described previously.[74] TEOS was hydrolyzed by mixing 4.5 mL TEOS, 1.4 mL distilled, deionized water and 0.1 mL of 0.1 M HCl. The resulting molar ratio of $H_2O$:Si (*R*-value) was 4:1. The mixture was contained in a glass vial which was placed in an ultrasonic bath for an hour or until a visibly homogenous solution was obtained.

Hydrolysis of organically modified silane (ORMOSIL) precursors for preparation of organically modified sol-gel-derived glasses was accomplished using two methods. In the separate hydrolysis method, MTES or PTMS were hydrolyzed as described above for TEOS, resulting in *R*-values of 3.7 and 3.3, respectively. DMDMS could not be hydrolyzed alone, as it would not form one clear phase, regardless of how long it was sonicated. Hence, DMDMS samples were prepared exclusively by the co-hydrolysis method (described below).

In the co-hydrolysis method, an appropriate amount of ORMOSIL (MTES, PTMS or DMDMS) was added directly to TEOS to provide organosilane:TEOS ratios ranging up to 40.0% (v/v) for MTES, up to 10.0% (v/v) for DMDMS and up to 20.0% (v/v) for PTMS. A total of 4.5 mL of the silane mixture was then mixed with 1.4 mL of distilled, deionized water and 0.1 mL of 0.100 M HCl and sonicated as described above. These conditions provided *R*-values between 4.1 and 3.9 for all samples with the *R*-values decreasing as the proportion of ORMOSIL increased.

For both methods, the solutions were then stored at -20°C for a period of 24 hours (for preparation of thin films), or for between one or two weeks (for monoliths and slides) to allow complete hydrolysis of the alkoxy groups to occur. Litmus paper was used to determine that the pH of the hydrolyzed solutions was approximately 2.

### *2.2.2. Preparation of Sol-Gel-Derived Monoliths and Slides*

For preparation of sol-gel-derived monoliths and slides, samples were kept at 0°C until the final mixing steps occurred. For separately hydrolyzed samples, appropriate volumes of hydrolyzed TEOS and ORMOSIL were mixed in a poly(styrene) cuvette to give a total of 1.0 mL of solution for monoliths or 300 μL for slides. Volume ratios of organosilane:TEOS ranged from 0 to 40.0% (v/v) for MTES (0 to 0.43 mole ratio), or 0 to 20.0% (v/v) for PTMS (0 to 0.24 mole ratio). Alternatively, 1.0 mL or 300 μL of co-hydrolyzed silane was placed into the cuvette with volume ratios of 0 to 40.0% (v/v) for MTES, 0 to 20.0% (v/v) for PTMS or 0 to 10.0% (v/v) for DMDMS (0 to 0.15 mole ratio).

Buffer solutions used for gelation contained either 2.3 ± 0.1 μM prodan or 33.8 ± 0.7 μM 7AI. The absorbance spectrum of the probe solution was collected for determination of probe concentration. For prodan, the absorbance value at 365 nm was used to determine the concentration using a molar absorbtivity of 14 500 $M^{-1}cm^{-1}$ and a pathlength of 1.0 cm. For 7AI, the absorbance value at 290 nm was used to determine the concentration using a molar absorbtivity of 8100 $M^{-1}cm^{-1}$ and a pathlength of 1.0 cm. All ultraviolet/visible absorbance measurements were obtained using either an ATI-Unicam

UV-4 Spectrophotometer operated by Vision Software or a Varian Cary 300 Spectrophotometer operated by Cary WinUV Software. In both instruments, the ultraviolet light source was a deuterium lamp and the visible source was a tungsten lamp.

For preparation of fluorophore-doped materials, an equivalent amount of buffer solution (0.010 M PBS with 0.100 M KCl at pH 7.2), containing either prodan or 7AI, was added to the cuvette containing the hydrolyzed silane. The cuvette was then sealed with Parafilm, gently shaken until the contents were thoroughly mixed, and allowed to gel at room temperature. Monoliths (containing a total of 2.0 mL of liquid) gelled with the cuvette standing in an upright position, whereas slides (containing a total volume of 600 μL of liquid) gelled after the cuvette was laid on its side. TEOS and ORMOSIL-derived samples were also prepared with fluorescent probes and polymer additives co-entrapped to determine the effect of polymer additives on the internal environment of sol-gel-derived glasses. For these samples, PEG or PVA were added to the buffered probe solutions in concentrations of 5.0 or 10.0% (w/v, in the buffer solution). Hydrolyzed solutions containing varying types and amounts of ORMOSILs were added directly to these polymer and probe-doped solutions to induce gelation.

For preparation of lipase solutions, an appropriate amount of buffer solution was added directly to the vial containing the lyophilized powder. These solutions were then diluted to an appropriate concentration in separate containers and frozen or the stock solution was frozen until used. For HSA solutions, an appropriate amount of protein was dissolved in buffer to produce a solution of the approximate desired concentration. The concentration of HSA was determined by collecting the absorbance spectrum of the HSA

solution, using the corresponding buffer in the reference cell. The absorbance value at 277 nm was used to determine the concentration using a molar absorbtivity, ε, of 36 000 $M^{-1}cm^{-1}$ and a pathlength of 1.0 cm. The concentration of HSA used for preparation of HSA-doped slides was 10.5 ± 0.2 μM. The concentration of lipase was calculated based on the weight of protein provided by the supplier on the stock vial. Based on these values, the concentration of lipase used for entrapment and solution-based assays was either 0.12 mg/mL or 0.06 mg/mL. In most cases, the activity values obtained for entrapped lipase were reported as a fraction of the activity of lipase in solution. Activity values were obtained using an identical amount of the same enzyme solution for both solution assays and assays in which the enzyme was entrapped.

For protein entrapment into monoliths or slides, the buffer solution containing lipase or HSA was added to the hydrolyzed silane in a 1:1 volume ratio. PEG, at average molecular weights of 400 and 600 and PVA, with average molecular weight of 13 000 to 23 000 were added to the buffered lipase solutions and co-entrapped with the enzyme to determine the effect of polymer additives on enzyme activity. PEG concentrations were 5.0 or 10.0% (w/v in the buffer solution) or 10.0% (w/v in the buffer solution) PVA. Proteins were entrapped only into materials derived from the co-hydrolysis method on the basis of fluorescence results (to be discussed) and to allow the use of DMDMS. Protein samples were prepared only as slides to allow for more rapid diffusion of analytes into the porous glass matrix, and later on, as thin films (described below).

Following gelation of the samples containing probes or proteins, the monoliths or slides were either dry-aged without washing or were washed with 2.0 mL of buffer twice

to remove entrapped ethanol (24 h for the first wash, 30 min. for the second wash) and then dry-aged. For fluorescent probe-doped samples, the washing solution contained 7AI or prodan in a concentration identical to that used for entrapment to prevent leaching of the probe from the sol-gel-derived glass. Samples that contained polymer additives were washed with solutions that contained the appropriate probe and polymer in concentrations identical to those used for entrapment. Protein and enzyme samples were rinsed with buffer solution only.

For aging, a syringe was used to punch a small hole in the Parafilm covering the cuvette to allow slow evaporation of water and ethanol. All samples were aged at 4°C until tested.

### *2.2.3. Preparation of Sol-Gel-Derived Thin Films*

Thin films were prepared by dipcasting on to substrates using a Kibron Layer-X film lift (Kibron, Inc., Helsinki, Finland). Substrates (glass or quartz slides cut to an appropriate size) were placed in a removable metal holder which attached to the magnetic film lift arm. The film lift had a variable speed controller, which allowed the casting rate to be adjusted. In most cases, 1.0 to 1.2 cm of the substrate was coated owing to the depth of the casting well.

For thin films, storage at –20°C for 24 hours after sonication of silane precursors was sufficient to prepare high quality films. The sample was then mixed rapidly using a vortex mixer and poured into a Teflon casting well approximately 1.5 cm long, 0.5 cm wide and 1.2 cm deep. The substrate (glass microscope slide or quartz plate) was

mounted in the metallic sample holder of the Kibron Layer-X film lift and suspended over the sol/buffer solution. Glass and quartz slides were cleaned by placing them in a solution of 1.00 M NaOH for 24 hours. The samples were then washed with copious amounts of tap water and then distilled, deionized water. The slides were then wiped dry using a Kimwipe and placed in a box until used. The substrate was then lowered into the sol-gel/buffer solution at a rate of 10 mm/minute and withdrawn at 4 mm/minute until the bottom edge of the substrate was suspended about 1 mm above the top edge of the casting well. The metal sample holder was then removed and the substrate was suspended, in air, perpendicular to the benchtop using an alligator clip. A Kimwipe was touched to the bottom edge of the coated glass or quartz slide to draw any excess solution collected at the bottom of the slide. A new, uncoated substrate was then placed in the sample holder and the process was repeated. The time required for deposition of the film was $7.0 \pm 0.5$ minutes. Coated samples were suspended in air for approximately 10 minutes, after which time they were placed (bottom coated edge down) into a sealed scintillation vial and aged for 24 hours and tested.

Fluorescent probe or protein-doped sol-gel-derived thin films were prepared as described above using fluorescein, SNARF-1, dextran-fluorescein, dextran-SNARF-1 or protein, dissolved in pH 7.2, 10.0 mM Tris buffer. Dextran-conjugated forms of fluorescein and SNARF-1 were used to reduce leaching of the probes from within the porous films. The concentration of fluorescein and dextran-fluorescein solutions used for entrapment in thin films were $2.8 \pm 0.1$ μM and $2.3 \pm 0.1$ μM, respectively, using the absorbance at 492 nm with a molar absorbtivity of 83 000 $M^{-1}cm^{-1}$ and a pathlength of

1.0 cm. The concentration of SNARF-1 and dextran-SNARF-1 used for entrapment in thin films were 1.21 ± 0.02 μM and 1.18 ± 0.02 μM, respectively, using the absorbance at 548 nm with a molar absorbtivity of 27 000.

Films were also prepared that were doped with PEG 400 and PEG 600 in concentrations of 0 to 10.0 % (w/v in the buffer) in the absence of probes to determine the effect of polymer doping on the properties of the films.

For preparation of HSA-doped thin films, 400 μL of 66.6 ± 1.3 μM HSA was mixed with 400 μL of TEOS and cast onto quartz slides. Only 400 μL of each precursor solution were used for casting onto quartz slides due to the larger size of the quartz slides relative to glass slides, which caused greater displacement of the contents of the casting well.

Lipase (1.5 mg/mL) was used to prepare films made from TEOS, 20.0% MTES or 5.0% DMDMS. TEOS-derived films containing lipase were also prepared with 1.0, 2.0 or 3.0% (w/v in the buffer) PEG having molecular weight of either 400 or 600.

Lipase (0.75 mg/mL), 0.59 ± 0.01 μM dextran-SNARF-1 and 3.0% PEG 600 (w/v in the lipase/dextran-SNARF-1 mixture) were used to prepare films that contained lipase co-entrapped with dextran-SNARF-1 and 3.0% PEG 600. The cast films were stored in a sealed vial for 24 hours before being tested.

### *2.2.4. Characterization of the Physical Properties of Sol-Gel-Derived Materials*

#### 2.2.4.1. Optical Clarity of Slides

Optical transmittance values of various ORMOSIL and polymer-doped sol-gel-derived glasses were collected 23 and 180 days after gelation for neat ORMOSIL-derived samples and 23 and 80 days after gelation for polymer-doped samples. The instrument was zeroed using empty poly(styrene) cuvettes in the sample and reference light paths. All transmittance values were collected with an empty poly(styrene) cuvette in the reference path. Slides were placed in the sample cuvette at an angle perpendicular to the direction of the light beam. Transmittance values for all samples were collected using light at a wavelength of 400 nm. This wavelength was used since it is at the lower extremity of the visible region of the spectrum where scattering is highest, and is suitable for spectroscopic studies. This wavelength also allowed the use of both poly(styrene) and poly(methacrylate) cuvettes.

#### 2.2.4.2. Hardness

The hardness of 180-day-old ORMOSIL-derived glasses was evaluated qualitatively using the Moh's hardness scale. This was accomplished by scratching the surface of the slides with various substances. The substances used were talc (1), gypsum (2), calcite (3), copper (3.5), fluorite (4), apatite (5), a glass plate (5.5), orthoclase (6) and quartz (7). The number given in parentheses increases as the hardness of the material increases. The number assigned to the sol-gel-derived material was based on the substance for which

both the sol-gel-derived glass and the substance scratched each other, or neither scratched the other.

The hardness of 40-day-old ORMOSIL samples doped with PVA or PEG was measured using a LECO M-400-H2 hardness-testing machine. Samples were tested 40 days after gelation rather than after 180 days (as for neat ORMOSIL-derived samples) due to time constraints. This method of hardness testing was chosen to provide a quantitative measure of hardness values of the sol-gel-derived materials. This method of hardness testing was unavailable at the time of preparation of the original ORMOSIL samples. Washed and unwashed sol-gel-derived monoliths were placed on their sides on a block on a movable stage. A square pyramid-based diamond tip was carefully lowered to a position just above the surface of the monolith and the machine was started. The diamond tip was slowly lowered to the surface until contact was achieved and a 10.0 g load was applied for 20.0 seconds. The diamond tip was then raised again and the resulting indentation was examined using a microscope connected to a video screen. The hardness of the sample was determined by measuring the size of the diamond-shaped indentation on the surface of the monolith. The average length of the two diagonals of the diamond-shaped indentation was measured by adjusting the distance between two calibrated lines within the viewfinder. The distance between the points of the diamond was directly related to the hardness of the sample as measured using the Vickers scale. The indentation experiment was performed three times per sample on different areas on the surface.

2.2.4.3 Dehydration/Rehydration Stability of Sol-Gel-Derived Glasses

A simple, qualitative classification of dehydration stability was adopted by counting the number of cracks formed in the sol-gel-derived slides as they aged. Samples were examined at various times, including day 21, the same day that protein samples were tested. Samples that did not crack were classified as excellent, those with 1 or 2 cracks were considered good, those with 3-5 cracks were considered moderate and samples with more than 5 cracks were considered poor. Rehydration stability was evaluated by quickly adding 2.0 mL of buffer solution to the cuvette containing the slide and counting the number of cracks formed. The rehydration stability was quantified using the same scale as that used for dehydration stability.

*2.2.5. Fluorescence Spectroscopy*

2.2.5.1. 7AI and Prodan

The instrument used for all fluorescence measurements was an SLM Aminco 8100 spectrofluorimeter. Light from a 450-W xenon arc lamp was passed through a double grating excitation monochromator and then through a 1 $cm^2$ cuvette (poly(styrene) for visible wavelengths, poly(methacrylate) or quartz for UV wavelengths) containing the sample. Emission was collected at right angles and passed through a single grating emission monochromator and detected using a R928 photomultiplier tube in a Peltier cooled housing operating in current mode. The sample emission intensity was divided by the signal from a reference channel containing a quantum counter solution of 3.0 g/L of

Rhodamine B in ethanol to account for fluctuations resulting from deviations in the power output of the lamp.

7AI-doped samples were excited at 295 nm with emission collected from 310 to 560 nm. Prodan samples were excited at 370 nm with emission collected from 385 to 650 nm. All fluorescence emission spectra were collected in 1 nm increments with an integration time of 0.3 seconds/nm and with a 4 nm bandpass in the excitation path and an 8 nm bandpass in the emission path unless otherwise indicated. Spectra were corrected to account for deviations in emission monochromator throughput and photomultiplier response. Blank subtraction from 7AI and prodan-doped samples was not done since the signal from the blank was less than 0.5% of the signal derived from the probe-doped samples. Emission spectra were collected on several occasions from day 1 after gelation up to 180 days for neat ORMOSIL-derived samples and from 1 day after gelation up to 74 days for polymer-doped samples. Spectra were not collected past day 74 for polymer-doped samples due to time constraints.

2.2.5.2. Human Serum Albumin (HSA)

Tryptophan emission spectra of HSA were collected with excitation at 295 nm and emission collected from 310 to 450 nm. Solution samples of 10.5 ± 0.2 μM HSA (native and denatured using 5.0 M guanidine hydrochloride) were collected in pH 7.2, 10.0 mM PBS. TEOS and ORMOSIL-derived slides doped with 10.5 ± 0.2 μM HSA were mounted in 2.0 mL of pH 7.2, 10 mM PBS for spectral acquisition.

2.2.5.3. Salicylate Titrations of HSA

All titrations of salicylate into HSA were performed using sol-gel-derived slides (approximate dimensions: 15 mm x 8 mm x 0.2 mm) that had been aged for 21 days. Slides were mounted in a holder at the bottom of a poly(methacrylate) cuvette and oriented at 45° relative to the excitation beam so that intensity from reflected excitation radiation was minimized using collection from the left emission channel. This sample orientation is shown in Figure 2.1.

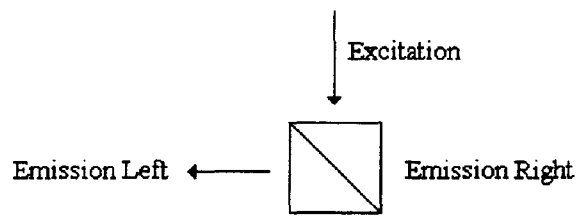


**Figure 2.1. Orientation of Slides Mounted in Fluorimeter Optical Path**

The samples were titrated with 100 mM salicylic acid dissolved in 10.0 mM PBS at pH 7.2 in 17.5 μL aliquots. Fluorescence spectra of entrapped HSA were collected ~12 minutes after each addition of salicylic acid to allow equilibration of the sample. Stirring was not possible since the slide was mounted at the bottom of the cuvette. The HSA samples were excited at 295 nm and emission was collected from 310 to 450 nm to monitor the quenching of tryptophan fluorescence by salicylate. Spectra were collected for blank contributions using a solution containing salicylate but no protein and a 10 nm window centered at the Trp emission maximum of 335 nm was integrated to provide intensity values for the protein at each salicylate concentration. Linear regression was

performed on each curve to quantitate the relative degree of binding of salicylate to HSA.[75] These experiments were repeated using native and denatured HSA in solution (denatured using 5.0 M guanidine hydrochloride) with appropriate blank subtraction, instrument and dilution corrections applied.

Salicylate binding experiments using HSA entrapped in TEOS-derived thin films were performed in a similar manner to that used for slides. The excitation spectral bandpass used was 4 nm and the emission spectral bandpass used was 16 nm to increase the signal intensity collected by the detector. Quartz slides coated with TEOS-derived films containing HSA were suspended in 2.0 mL of 10.0 mM PBS at pH 7.2, so that the film was within the optical path of the fluorimeter, in the same orientation as shown in Figure 2.1. 100 μM salicylic acid was titrated into the solution surrounding the film-coated quartz slide in 5 μL aliquots. An uncoated quartz slide was suspended in a similar manner in a solution that did not contain salicylic acid. This was done to allow subtraction of scattered excitation radiation from the spectra of the HSA-doped films.

2.2.5.4. Fluorescein and SNARF-1

Fluorescence-based methods for monitoring pH were investigated using the pH sensitive probes fluorescein and SNARF-1 (in their free and dextran conjugated forms). The pH response of fluorescein was examined only when the probe was entrapped in thin films, whereas the pH response of SNARF-1 was examined both in solution and when entrapped in thin films.

TEOS-derived thin films doped with fluorescein, dextran-fluorescein, SNARF-1 or dextran-SNARF-1 were prepared as described above. Film were stored dry for 24 hours after which time, the samples were rinsed with distilled, deionized water to wash away any surface-adsorbed probe molecules. The samples were then placed in cuvettes containing 2.5 mL of 1.0 mM, pH 9.0 PBS for 24 hours. The slides were removed from the buffer and the emission spectra of these solutions were collected. Solutions from cuvettes containing slides prepared using fluorescein and dextran-fluorescein were excited at 460 nm and emission was collected from 480 to 600 nm. Solutions from cuvettes containing SNARF-1 or dextran-SNARF-1 were excited at 531 nm and emission was collected from 550 to 800 nm.

TEOS-derived thin films doped with dextran-fluorescein were mounted in 2.0 mL of pH 7.2, 10.0 mM PBS in the optical path of the fluorimeter in an orientation as shown in Figure 2.1. HCl (0.100 M) was added to the solution containing the dextran-fluorescein film in 5 μL aliquots. The solution was allowed to stand for 10 minutes after each addition before collection of the spectrum. Time traces were also performed to monitor the pH-dependent spectroscopic change of fluorescein with time. The samples were excited at 460 nm and the emission at 520 nm was continuously monitored with an integration time of 0.99 seconds. Aliquots (50 μL) of 0.100 M HCl or 0.100 M NaOH were added to the solution containing the slide to determine the effect of changing the pH on the emission of fluorescein.

The pH response of SNARF-1 in solution was determined by dissolving dextran-SNARF-1 to a concentration of 1.20 ± 0.02 μM in solutions of 10.0 mM PBS at various

pH values ranging from 4.0 to 10.0 and collecting the emission spectra of the solutions. The emission intensities at 588 and 640 nm were integrated over a 10 nm window centered at these wavelengths and their ratio ($I_{588}/I_{640}$) was plotted as a function of pH to determine the $pK_a$ of the probe in solution. The spectra of SNARF-1 in pH 4.0 and 10.0 buffers were also collected using different excitation wavelengths. The wavelengths used for excitation were 442 nm, 488 nm, 514 nm and 531 nm.

Time traces were also collected to monitor the response of dextran-SNARF-1 to changes in pH as a function of time. Dextran-SNARF-1 (2.0 mL of 0.85 ± 0.02 μM in 1.0 mM pH 9.0 PBS) was placed in the fluorimeter and was stirred continuously throughout the course of the time trace. In this experiment, the dextran-SNARF-1 solution was excited at 531 nm with spectral bandpasses of 8 nm in the excitation and both the right and left emission paths. The signal monitored was a ratio of the detector response from the left emission detector (set at 588 nm) and the right emission detector (set at 640 nm). The signals from each detector were monitored simultaneously, which was possible using the T-format optical layout of the SLM 8100. Aliquots (5 μL) of 0.100 M HCl or NaOH were added to the solution at various times throughout the course of the time trace.

Dextran-SNARF-1-doped films derived from TEOS were suspended in 2.0 mL of pH 9.0 PBS in an orientation as shown in Figure 2.1 to allow the simultaneous monitoring of the signals from the right and left detectors. This was done using the same conditions as described above for dextran-SNARF-1 solution with the exception of the use of 8 nm and 16 nm bandpasses in the excitation and emission paths, respectively.

Time traces were run with an integration time of 0.99 seconds with additions of aliquots of 0.100 M HCl or NaOH throughout the course of the time trace.

Another method was also used for monitoring the pH response of dextran-SNARF-1 entrapped in a TEOS-derived film. In this method, the film was mounted (Figure 2.1) in a slide holder at the bottom of a cuvette containing 2.0 mL of 1.0 mM, pH 9.0 PBS. The entrapped dextran-SNARF-1 was excited at 531 nm with spectral bandpasses of 4 nm and 16 nm in the excitation and emission paths, respectively. The ratio of emission intensities at 588 and 640 nm were calculated using a 10 nm window centered at these wavelengths. 2.5 or 5 μL aliquots of 0.100 M HCl were added to the solution and the sample was allowed to stand for 5 minutes before spectral acquisition. This process was repeated until the ratio of emission intensities had reached a maximum value, at which time similarly sized aliquots of 0.100 M NaOH were added instead of HCl.

### *2.2.6. Enzyme Activity Assays*

#### 2.2.6.1. Titrimetric Assays of Lipase Activity

Samples tested were made of TEOS or combinations of TEOS with organically modified silanes. Samples were also prepared that had lipase co-entrapped with polymer additives (PEG at concentrations of 5.0 and 10.0% (w/v in the buffer) or PVA at a concentration of 10.0% PVA (w/v in the buffer)). All samples were tested as intact slides and were not crushed into powders. The assay involved incubating the lipase-doped slide in a solution prepared by mixing 500 μL of distilled, deionized water with 500 μL of glyceryl tributyrate ($1.7 \times 10^{-4}$ mol). The reaction was run for 30.0 minutes at room

temperature with continuous stirring. The reaction was quenched by rapid addition of 2.0 mL of a 1:1 (v/v) mixture of ethanol and acetone and allowed to stir for an additional 5.0 minutes. After quenching, the free fatty acids were titrated to a phenolphthalein endpoint using 0.050 M NaOH. Assays were also run using sol-gel-derived glass slides that were lipase-free to account for the non-enzymatic hydrolysis of glyceryl tributyrate. The volume of NaOH required to reach the endpoint for the blanks was subtracted from the volume required to reach the endpoint for the lipase-doped samples. The average activity values (over 3 to 5 samples) was determined from the volume of NaOH added and reported as activity relative to a solution containing an identical amount of lipase and assayed in an identical manner. For assays performed using neat ORMOSIL-derived samples and samples containing 10.0% PVA, the concentration of lipase was 0.12 mg/mL (for solution and immobilization studies). All samples were washed with buffer only. For assays performed using ORMOSIL-derived samples doped with PEG, the concentration of lipase used was 0.06 mg/mL (for solution and immobilization studies). Samples were either washed or unwashed with buffer that did not contain any polymer additives to determine the effect of washing on lipase activity.

2.2.6.2. Spectroscopic Assays of Lipase Activity

A colorimetric assay was also performed using phenol red as a pH indicator. Phenol red dissolved 3.0 mL of 1.0 mM, pH 9.0 PBS was placed in a poly(styrene) cuvette. The assay was performed by continuously monitoring the change in absorbance at 560 nm using thin films derived from TEOS, 20.0% MTES and 5.0% DMDMS and doped with

1.5 mg/mL lipase and PEG 400 and 600 in concentrations ranging from 1.0 to 3.0% (w/v in the buffer). The instrument was zeroed with the lipase-doped, thin-film-coated slide suspended from the top of the sample cuvette to allow stirring. After the instrument was zeroed, 100 μL of glyceryl tributyrate was added rapidly to the reference and sample cuvettes and the assay was commenced.

An alternate method of monitoring lipase activity was developed to allow the eventual development of a fluorescence based sensor for triglycerides. Dextran-SNARF-1 (2.0 mL of 0.85 ± 0.02 μM dissolved in pH 9.0, 1.0 mM PBS) was placed in a cuvette with a stirring flea and 100 μL of glyceryl tributyrate was added to the stirred solution. The solution was excited at 531 nm and emission was collected using simultaneous detection of emission at 588 and 640 nm. A 4 nm bandpass was used in the excitation path, with an 8 nm bandpass in both of the emission paths. Time traces were collected that spanned 60 minutes with an integration time of 0.99 seconds per point. After 120 seconds, 50 μL of 1.5 mg/mL lipase dissolved in 10.0 mM, pH 7.2 Tris was added to the dextran-SNARF-1 solution and the ratio of emission intensities was monitored continuously.

The assay was also performed using lipase/dextran-SNARF-1 and 3.0% PEG 600 (w/v in the buffer solution) co-entrapped in a thin film. In this experiment, the film was suspended from the top of the cuvette (Figure 2.1) in 2.0 mL of 1.0 mM, pH 9.0 PBS to allow stirring of the solution. Thin film immobilized dextran-SNARF-1 was excited at 531 nm with simultaneous detection of emission at 588 and 640 nm. A spectral bandpass of 8 nm was used in the excitation path while spectral bandpasses of 16 nm were used in

both emission paths. Once the signal had reached a constant value, the sample compartment was opened and 100 μL of glyceryl tributyrate was added to the solution. The sample compartment was then closed and the time trace continued for 30 minutes.

# Chapter 3: Results and Discussion

## 3.1. Characterization of Organically Modified Sol-Gel-Derived Materials

### *3.1.1. Physical Properties of TEOS and ORMOSIL-Derived Monoliths*

#### 3.1.1.1. Gelation Time

The gelation time was defined as the period of time required for the sol-gel/buffer mixture to become so viscous that it would not flow if the cuvette was tilted from the position it was placed in for gelation. It is desirable to control the gelation time since extended gelation times can cause denaturation of proteins or enzymes being entrapped due to the presence of ethanol.[76] However, if the gelation times are too short, it is not possible to prepare thin films by dip-casting. It was necessary to have gelation times that were between 20 and 60 minutes to minimize exposure to ethanol while allowing the formation of high quality films.

The major factors that affected the rate of gelation were the type and ratio of organosilane used in the silane solution, the type and concentration of buffer used and the temperature at which the samples were formed. It was found that separately hydrolyzed and co-hydrolyzed samples required a similar amount of time for gelation. The gelation time increased as the amount of organosilane was increased. The gelation time also increased when going from MTES to PTMS to DMDMS. This result suggests that steric effects partially control the gelation kinetics.[77] The gelation time decreased for samples containing greater than 7.5% DMDMS, suggesting a separation of the organic and

inorganic phases, which gelled independently of one another. This point is discussed in more detail later in this chapter.

The temperature of the solutions also had a significant impact on the gelation time. If the silane and buffer solutions were both held at room temperature (i.e. 22 ± 1°C) prior to mixing and were allowed to gel at room temperature, the gelation times were generally rather short. For example, samples prepared using TEOS and 10.0 mM phosphate buffer at pH 7.2 gelled in less than 5 minutes. In cases where both solutions were held at 0°C before mixing and allowed to gel at room temperature, the gelation times tripled, generally ranging from 10 to 15 minutes. Gelation at 0°C increased the gelation time even further to about 30 minutes but the resulting slides were uneven. Hence, the precursor solutions were held at 0°C prior to mixing and samples were allowed to gel at room temperature. Under these conditions, it was possible to achieve gelation times of 5 to 60 minutes, with adjustment of the buffer concentration allowing control over the rate of gelation.

Phosphate buffer (10.0 mM with 100 mM KCl at pH 7.2) was also found to provide gelation times that were between 5 and 60 minutes. Tris buffer (concentration of 10.0 mM with 100 mM KCl at pH 7.2) dramatically increased the gelation time compared to PBS at an identical concentration and pH. For samples derived from TEOS, the time required for gelation using Tris buffer was approximately sixty minutes.

3.1.1.2. Optical Clarity

For development of optical biosensors using sol-gel-derived materials, it is important that the material used for immobilization of the biological sensing element is optically clear to allow the transmission of light to and from the signal transducer. Transmittance values at 400 nm for separately and co-hydrolyzed monoliths aged for 180 days are given in Tables 3.1 and 3.2, respectively. The data indicates that the method by which the silane precursors were hydrolyzed, the sample preparation temperature and whether or not the samples were washed after gelation all affected the optical clarity of the materials. The overall clarity was improved when the solutions were held at 0°C prior to mixing, when silane solutions had been stored in the freezer for seven days before use rather than a shorter period of time (i.e. one hour) and when silanes were prepared by co-hydrolysis. Storage in the freezer likely resulted in a relatively slow rate of condensation, which likely occurred in a more ordered manner, and hence, the materials were more homogeneous and transparent.

Samples prepared from separately hydrolyzed silanes were more transparent than samples prepared from co-hydrolyzed silanes, regardless of ORMOSIL content. Washing of the samples resulted in a decrease in the clarity of the glass. The decrease in clarity may be due to the forcing out of ethanol, which acted as a co-solvent for the TEOS. This washing out of ethanol may also have caused an increase in the phase separation behaviour in the early stages of monolith formation.

The other main factors influencing the clarity of the glass included the type and content of organosilane and, for separately hydrolyzed samples, the order of addition of

**Table 3.1. Physical Properties of Monoliths Prepared by Separate Hydrolysis of Silane Precursors**

| Sample | Optical Transmittance (%), Washed/Unwashed | Dehydration Stability | Rehydration Stability | Hardness (Moh's Scale) |
|---|---|---|---|---|
| TEOS | 70/80 | Excellent | Good | 4 |
| 5% MTES | 69/81 | Excellent | Good | 3.5 |
| 10% MTES | 72/80 | Excellent | Moderate | 3 |
| 15% MTES | 71/80 | Excellent | Poor | 2.5 |
| 20% MTES | 67/79 | Excellent | Poor | 2.5 |
| 25% MTES | 65/78 | Excellent | Poor | 2.5 |
| 30% MTES | 58/70 | Moderate | Poor | 2.5 |
| 35% MTES | 50/63 | Poor | - | 2.5 |
| 40% MTES | 21/29 | Poor | - | 2.5 |
| 5% PTMS | 52/63 | Good | Moderate | 2 |
| 10% PTMS | 27/36 | Moderate | Poor | 2 |
| 15% PTMS | 0/0 | Poor | - | < 1 |
| 20% PTMS | 0/0 | Poor | - | < 1 |

**Table 3.2. Physical Properties of Monoliths Prepared by Co-Hydrolysis of Silane Precursors**

| Sample | Optical Transmittance (%), Washed/Unwashed | Dehydration Stability | Rehydration Stability | Hardness (Moh's Scale) |
|---|---|---|---|---|
| TEOS | 67/78 | Excellent | Excellent | 4 |
| 5% MTES | 66/78 | Excellent | Good | 3.5 |
| 10% MTES | 69/80 | Good | Poor | 3 |
| 15% MTES | 64/81 | Good | Poor | 3 |
| 20% MTES | 66/83 | Good | Poor | 3 |
| 25% MTES | 65/81 | Good | Poor | 2.5 |
| 30% MTES | 60/72 | Moderate | Poor | 2.5 |
| 35% MTES | 51/60 | Moderate | Poor | 2.5 |
| 40% MTES | 28/33 | Poor | - | 2 |
| 2.5% DMDMS | 62/71 | Good | Moderate | 3.5 |
| 5% DMDMS | 51/66 | Poor | - | 3 |
| 7.5% DMDMS | 24/33 | Poor | - | 3 |
| 10% DMDMS | 0/0 | Poor | - | 2 |
| 5% PTMS | 49/60 | Moderate | Poor | 2.5 |
| 10% PTMS | 29/31 | Poor | - | 1.5 |
| 15% PTMS | 0/0 | Poor | - | < 1 |
| 20% PTMS | 0/0 | Poor | - | < 1 |

the components. The optimal mixing method was to first add the required volume of buffer, followed by ORMOSIL and finally TEOS. Regardless of the order of addition, the transparency decreased with increasing ORMOSIL content. The type of organosilane also affected the clarity of the resulting glass. Samples containing up to 25.0% MTES were quite transparent, however 10.0% DMDMS or 15.0% PTMS samples were opaque. The difference in transparency between samples composed of a particular ORMOSIL was quite abrupt in most cases, and was likely due to separation of the organic and inorganic phases within the slides. Prior to gelation, the less polar organically modified silanes likely preferentially associated with each other, forming organic pockets within the non-polar TEOS. It is likely that there exists a critical concentration, similar to a critical micelle concentration, at which the radius of the non-polar regions is on the order of the wavelength of visible light. If the concentration of ORMOSIL exceeds this critical concentration, the visible light is scattered by these non-polar agglomerations, and the material appears opaque. The maximum ratio before the drop in transparency correlated approximately with the miscibility of the ORMOSIL in TEOS (i.e. 25.0% MTES, 10.0% PTMS or 7.5% DMDMS).

3.1.1.3. Hardness

The hardness values for TEOS and ORMOSIL-derived glasses are summarized in Tables 3.1 and 3.2. Hardness values for the various organosilane-derived glasses prepared by co-hydrolysis and separate hydrolysis and aged for 180 days indicated that increased ORMOSIL content caused a decrease in the hardness of the resulting glass. Co-

hydrolyzed and separately hydrolyzed samples showed no significant difference in their hardness. TEOS-derived glasses exhibited a hardness value of 4 while ordinary glass has a hardness of 5.5. Ordinary glass is densified by heat treatment, a process that was not possible for samples doped with protein since proteins denature after exposure to even mild temperatures (on the order of 75 °C or less).

In general, the hardness of the samples decreased with increasing organosilane content and with increasing length or number of alkyl chains present. The hardness decreased smoothly going from 5.0% MTES to 40.0% MTES, 2.5% DMDMS to 10.0% DMDMS and 5.0% PTMS to 20.0% PTMS (for co-hydrolyzed samples). For separately hydrolyzed samples, the hardness also decreased smoothly with increased ORMOSIL content for all samples tested. The hardness values of samples containing PTMS or DMDMS were significantly lower than those of samples containing the equivalent amount of MTES. This result suggested that the presence of more organic components (either longer chain length or more alkyl groups per Si atom) weaken the siloxane bond network, resulting in softer materials.

3.1.1.4. Dehydration Stability

The dehydration stability for the ORMOSIL-derived samples is also provided in Tables 3.1 and 3.2. In general, increases in the number or chain length of the alkyl group resulted in poorer dehydration stability, likely due to reduced cross-linking between silicon atoms (especially for DMDMS) and phase separation (for all organosilanes). For MTES, the degree of cracking increased with increased organic content and there was an

obvious decrease in dehydration stability above 20.0% MTES. This discontinuity was consistent with the reduction in optical clarity and hardness of MTES levels above 20.0% (v/v), and supports the presence of phase separation due to the formation of hydrophobic pockets within the TEOS-derived matrix.

Glasses prepared using co-hydrolyzed or separately hydrolyzed silanes followed the same general trend of increased cracking with increased organosilane content. However, slides that were prepared using separately hydrolyzed silanes showed better dehydration stability than the corresponding slides prepared using co-hydrolyzed silanes. The difference in the dehydration stability between separately and co-hydrolyzed samples was likely due to differences in the colloid structure of the different silanes. Separate hydrolysis of silane precursors forms colloids of pure composition (i.e. pure TEOS and pure ORMOSIL colloid particles) which were mixed together to form a hybrid organic/inorganic material. Materials derived from TEOS exhibited excellent dehydration stability and high optical clarity since the colloid particles are of a pure composition. This result indicated that materials made with colloidal particles of pure composition are relatively durable. Co-hydrolysis of silane precursors forms colloids of mixed composition. It was assumed that the composition of the colloids formed by co-hydrolysis of the silanes were homogeneous, with each colloidal particle containing the same degree of organic content. Materials made with colloidal particles of mixed composition are less durable than those derived from colloids of pure composition. Hence, separate hydrolysis of the precursors allowed better control over the colloid

properties of the sol, which allowed control of the properties of the resulting sol-gel-derived materials.

Another explanation for cracking of the materials is the uneven drying of the slides. This uneven drying may have resulted in the formation of hydrostatic pressure gradients within the slides, which exert stress on the glass at different regions in the slide. The uneven drying of slides may be alleviated by optimization of the drying conditions, which must be done in the future.

3.1.1.5. Rehydration Stability

The rehydration stability for the TEOS and ORMOSIL-derived samples is shown in Tables 3.1 and 3.2. The rehydration behaviour of the slides generally follows the trends observed for dehydration, despite the rapid change in water content relative to dehydration, which occurred over a period of several weeks. Rehydration was first done on day 21 when some water was still trapped within the pores of the silica matrix. This aging time also corresponded to the day on which protein testing was done. Samples were also tested on day 180, when the samples were fully dried. Rehydration of partially dried slides did not result in further cracking of slides that had not already cracked due to dehydration. Slides could be prepared with up to 20.0% MTES or 10.0% PTMS with reduced cracking during dehydration at day 21, regardless of the method used for silane hydrolysis. Above these levels, samples showed extensive cracking during dehydration by day 21 and further cracking upon rehydration.

The rehydration behaviour of fully dried samples at day 180 was much worse than that of partially dried samples. Rapid addition of buffer to the samples caused the slides of almost all compositions to shatter, regardless of the preparation method, likely due to capillary stresses within the glass matrix.[78] 5.0% MTES samples (co-hydrolyzed), and 10.0% MTES samples (separately hydrolyzed) exhibited reasonable rehydration behaviour, relative to the other compositions, suggesting that modification of the materials using low ORMOSIL compositions allows retention of desirable physical properties such as fracture resistance.

Overall, separate hydrolysis of precursors resulted in materials that exhibited higher optical clarity and resistance to fracture (due to dehydration or rehydration) than samples prepared by co-hydrolysis of silane precursors. Regardless of the method of hydrolysis, there was a limit to the amount of ORMOSIL that could be incorporated into the sol-gel-derived material before the materials exhibited poor mechanical properties. Materials with compositions above 20.0% MTES, 5.0% PTMS, and 5.0% DMDMS (in the case of samples prepared by co-hydrolysis of precursors) exhibited extensive cracking upon dehydration and further cracking upon rehydration and dramatic reductions in optical clarity. The relatively poor physical properties of the materials with compositions greater than 20.0% MTES, 5.0% PTMS or 5.0% DMDMS was likely due to the separation of the organic and inorganic phases. Above these concentrations, visible light was likely scattered by the non-polar regions, and the material appeared opaque. The poor interaction of these organic and inorganic regions also caused the materials to be more easily fractured upon dehydration or rehydration.

### *3.1.2. Spectroscopic Studies of TEOS and ORMOSIL-Derived Derived Monoliths Using Environmentally-Sensitive Fluorescent Probes*

#### 3.1.2.1. 7-Azaindole (7AI) Fluorescence

In order to further examine the potential of phase separation in the hybrid materials, and to probe the internal polarity of the sol-gel-derived materials, fluorescent probes were entrapped into the materials. The first probe used to examine the materials was 7AI. This probe is sensitive to its local environment and is useful for providing qualitative information on the surface silanol content of the sol-gel-derived materials.[57] Representative fluorescence emission spectra of 7AI entrapped in unwashed and washed, co-hydrolyzed MTES-derived monoliths that had been dried for 180 days are shown in Figure 3.1, parts a and b, respectively. Significant differences were apparent between samples depending on their organosilane content, whether or not they were washed, and on the method by which the silane precursors were hydrolyzed.

The emission maximum of 7AI samples also changed as a function of time. The emission maxima (as a function of time) for 7AI samples prepared by the co-hydrolysis and separate hydrolysis methods (washed and unwashed) are summarized in Tables 3.3 and 3.4, respectively.

One day after gelation, all samples exhibited 7AI emission spectra with a maximum intensity between 360 and 380 nm, regardless of whether they were washed or unwashed. The spread of the initial maxima (spectra not shown) was much larger for co-hydrolyzed samples (20 nm), relative to that of separately hydrolyzed samples (4 nm). The wide range of wavelengths found in co-hydrolyzed samples suggested that the internal

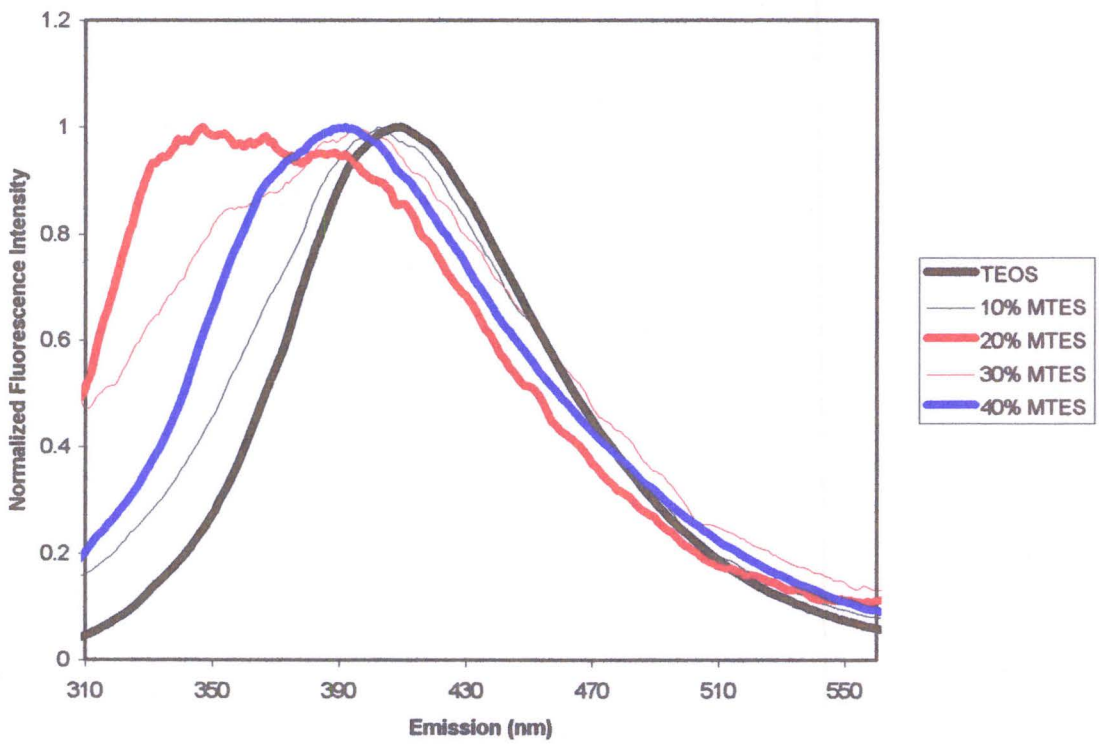


**Figure 3.1a. Fluorescence Emission Spectra of 7AI in Unwashed, Co-Hydrolyzed Monoliths Prepared Using Various Concentrations of MTES**

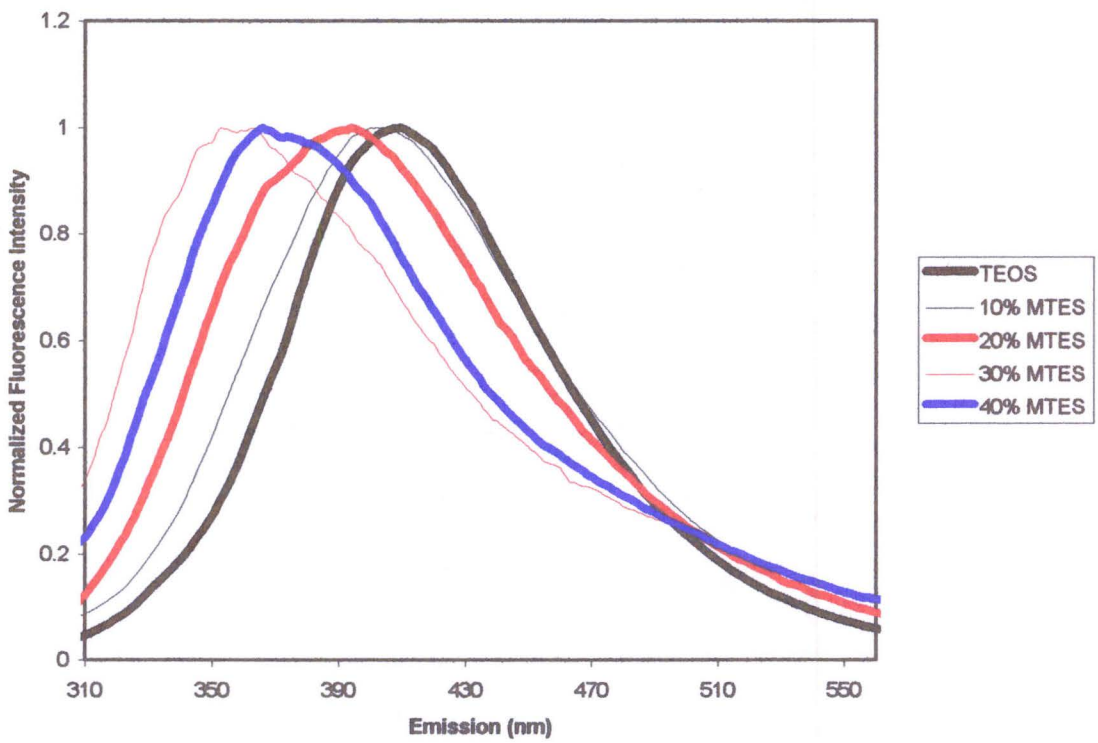


**Figure 3.1b. Fluorescence Emission Spectra of 7AI in Washed, Co-Hydrolyzed Monoliths Prepared Using Various Concentrations of MTES**

**Table 3.3. Emission Maximum Wavelengths of Entrapped 7AI in Sol-Gel-Derived Monoliths Prepared Using Co-Hydrolyzed Silane Precursors**

| Sample | Day 1 | Day 10 | Day 23 | Day 34 | Day 50 | Day 64 | Day 106 | Day 180 |
|---|---|---|---|---|---|---|---|---|
| **Washed** | | | | | | | | |
| TEOS | 366 | 370 | 371 | 369 | 370 | 382 | 402 | 409 |
| 5% MTES | 367 | 374 | 373 | 375 | 378 | 385 | 399 | 401 |
| 10% MTES | 367 | 371 | 371 | 370 | 378 | 376 | 395 | 406 |
| 15% MTES | 366 | 372 | 370 | 369 | 371 | 364 | 379 | 395 |
| 20% MTES | 367 | 369 | 369 | 371 | 370 | 372 | 375 | 394 |
| 25% MTES | 364 | 366 | 366 | 364 | 365 | 363 | 365 | 393 |
| 30% MTES | 365 | 369 | 367 | 367 | 366 | 368 | 364 | 393 |
| 35% MTES | 362 | 362 | 360 | 362 | 360 | 353 | 349 | 353 |
| 40% MTES | 365 | 364 | 363 | 364 | 360 | 359 | 354 | 356 |
| 2.5% DMDMS | 370 | 372 | 370 | 372 | 385 | 385 | 401 | 406 |
| 5% DMDMS | 369 | 372 | 369 | 372 | 370 | 373 | 396 | 399 |
| 7.5% DMDMS | 369 | 368 | 369 | 367 | 368 | 368 | 382 | 399 |
| 5% PTMS | 382 | 381 | 380 | 386 | 386 | 388 | 394 | 394 |
| 10% PTMS | 380 | 376 | 378 | 381 | 377 | 383 | 392 | 389 |
| 15% PTMS | 379 | 377 | 377 | 381 | 371 | 374 | 386 | 363 |
| 20% PTMS | 372 | 375 | 380 | 381 | 387 | 383 | 386 | 359 |
| **Unwashed** | | | | | | | | |
| TEOS | 366 | 368 | 370 | 375 | 388 | 398 | 410 | 410 |
| 5% MTES | 366 | 370 | 369 | 374 | 377 | 394 | 407 | 402 |
| 10% MTES | 366 | 363 | 366 | 371 | 379 | 386 | 403 | 402 |
| 15% MTES | 368 | 367 | 369 | 367 | 363 | 368 | 396 | 401 |
| 20% MTES | 367 | 366 | 367 | 364 | 366 | 365 | 365 | 396 |
| 25% MTES | 364 | 364 | 365 | 363 | 364 | 362 | 366 | 395 |
| 30% MTES | 366 | 365 | 366 | 364 | 357 | 347 | 361 | 392 |
| 35% MTES | 360 | 360 | 363 | 359 | 351 | 348 | 349 | 386 |
| 40% MTES | 365 | 364 | 363 | 364 | 357 | 361 | 364 | 381 |
| 2.5% DMDMS | 368 | 370 | 369 | 371 | 388 | 402 | 408 | 409 |
| 5% DMDMS | 368 | 369 | 367 | 368 | 378 | 385 | 402 | 404 |
| 7.5% DMDMS | 366 | 367 | 367 | 366 | 367 | 368 | 388 | 404 |
| 5% PTMS | 378 | 381 | 386 | 380 | 387 | 391 | 396 | 397 |
| 10% PTMS | 371 | 376 | 377 | 379 | 384 | 387 | 389 | 378 |
| 15% PTMS | 371 | 377 | 373 | 372 | 369 | 374 | 374 | 364 |
| 20% PTMS | 367 | 375 | 373 | 377 | 369 | 361 | 361 | 361 |

**Table 3.4. Emission Maximum Wavelengths of Entrapped 7AI in Sol-Gel-Derived Monoliths Prepared Using Separately Hydrolyzed Silane Precursors**

| Sample | Day 1 | Day 10 | Day 23 | Day 34 | Day 50 | Day 64 | Day 106 | Day 180 |
|---|---|---|---|---|---|---|---|---|
| **Washed** | | | | | | | | |
| TEOS | 366 | 370 | 371 | 369 | 370 | 382 | 402 | 409 |
| 5% MTES | 367 | 371 | 373 | 374 | 379 | 392 | 401 | 405 |
| 10% MTES | 366 | 369 | 371 | 369 | 382 | 381 | 395 | 400 |
| 15% MTES | 367 | 371 | 371 | 372 | 374 | 381 | 390 | 399 |
| 20% MTES | 369 | 369 | 370 | 374 | 369 | 381 | 387 | 404 |
| 25% MTES | 368 | 369 | 369 | 371 | 369 | 370 | 364 | 393 |
| 30% MTES | 366 | 368 | 368 | 368 | 369 | 369 | 347 | 390 |
| 35% MTES | 366 | 365 | 367 | 363 | 366 | 361 | 341 | 339 |
| 40% MTES | 366 | 366 | 368 | 365 | 350 | 334 | 338 | 339 |
| 5% PTMS | 368 | 375 | 379 | 375 | 380 | 382 | 386 | 389 |
| 10% PTMS | 368 | 370 | 369 | 369 | 368 | 369 | 369 | 369 |
| 15% PTMS | 368 | 367 | 367 | 365 | 367 | 367 | 365 | 363 |
| 20% PTMS | 368 | 365 | 366 | 364 | 366 | 364 | 359 | 360 |
| **Unwashed** | | | | | | | | |
| TEOS | 366 | 368 | 370 | 375 | 388 | 398 | 410 | 410 |
| 5% MTES | 368 | 369 | 369 | 374 | 383 | 398 | 406 | 404 |
| 10% MTES | 368 | 369 | 373 | 372 | 380 | 391 | 404 | 403 |
| 15% MTES | 366 | 369 | 368 | 372 | 379 | 391 | 401 | 396 |
| 20% MTES | 366 | 367 | 367 | 369 | 371 | 393 | 400 | 395 |
| 25% MTES | 367 | 366 | 366 | 365 | 363 | 354 | 343 | 397 |
| 30% MTES | 365 | 364 | 365 | 365 | 365 | 363 | 345 | 403 |
| 35% MTES | 366 | 366 | 367 | 365 | 366 | 365 | 352 | 395 |
| 40% MTES | 365 | 366 | 364 | 362 | 358 | 352 | 338 | 351 |
| 5% PTMS | 367 | 367 | 367 | 371 | 367 | 369 | 369 | 360 |
| 10% PTMS | 366 | 368 | 366 | 366 | 365 | 365 | 366 | 364 |
| 15% PTMS | 367 | 369 | 366 | 365 | 366 | 365 | 364 | 360 |
| 20% PTMS | 367 | 365 | 366 | 368 | 366 | 363 | 363 | 358 |

environment of these materials was dominated by the amount of ORMOSIL present, whereas in separately hydrolyzed samples, the probe was likely in an environment composed predominantly of TEOS.

In MTES and DMDMS samples, the wavelength of maximum emission was not dependent on the concentration of the ORMOSIL used, suggesting that the internal solvent environment rather than the dipolarity of the matrix dominated the spectral characteristics. However, for PTMS samples, the emission wavelength blue-shifted with increasing PTMS content. This observation suggested that the internal environment of PTMS-derived glasses was much less polar in the presence of increased levels of PTMS.

As the monoliths aged and dried, the wavelength of maximum intensity tended to red shift for samples with a low proportion of ORMOSIL (i.e. 20.0% MTES or less) and to broaden and blue shift in samples containing a higher proportion of ORMOSIL (i.e. greater than 30.0% MTES or 5.0% PTMS). The red shift at lower organosilane content is consistent with the probe adsorbing onto the silanol groups present on the internal surfaces of the monoliths.[29,57] This conclusion is supported by the fact that washed samples exhibit smaller red shifts in the maximum emission wavelength due to reduced silanol content. The silanol content is reduced in washed samples owing to the presence of excess water, which promotes dissolution and reprecipitation of small silica particles onto larger, less soluble silica particles, increasing the degree of cross-linking and reducing the overall silanol content within the matrix.[9]

The blue shift for samples having higher organosilane content is consistent with the probe partitioning into organic rich regions, rather than adsorbing to the hydroxylated

surface. The probe likely partitions into the organic regions, which serve to solvate the probe, favouring the presence of individual molecules rather than dimers or hydrogen bonded probe-solvent complexes. As a consequence, the spectra were dominated by the contributions of the solvated form of the probe rather than the adsorbed or dimerized forms. Previous work[38] has shown that 7AI exhibits an emission maximum at 378 nm when dissolved in methanol, whereas the emission maximum when the probe is dissolved in water is 385 nm. As discussed in the introduction, the emission at lower wavelengths is from free probe molecules, while emission at higher wavelengths is due to emission from complexed probe molecules. The spectra of entrapped 7AI were also rather broad, exhibiting large full-width-at-half-maximum values. This spectral broadening was indicative of a distribution of microenvironments within the glass, providing further evidence for microscopic phase separation of the organic and inorganic regions.

After aging was completed, 7AI in co-hydrolyzed and separately hydrolyzed samples containing MTES did not show significantly different spectral properties. Both types of samples tended to show a fairly consistent trend of more blue-shifted emission maxima with increased MTES content and also showed similar emission maxima for samples containing low amounts of DMDMS relative to similar samples containing double the amount of MTES. Significantly different spectral characteristics were observed for samples containing PTMS. These different results were somewhat expected based on the lower miscibility of PTMS with TEOS and, thus, the higher likelihood of phase separation when samples were prepared using separately hydrolyzed precursors. Phase separation was also consistent with the observed physical characteristics of the

PTMS-derived samples (i.e. poor optical clarity, hardness and dehydration/rehydration stability).

The largest differences in 7AI spectral characteristics were observed between washed and unwashed samples made from co-hydrolyzed or separately hydrolyzed silanes. These differences were most pronounced for co-hydrolyzed samples. Spectra collected from unwashed samples showed increased spectral broadening as the level of MTES was increased. The full-width-at-half-maximum values for 7AI entrapped in TEOS and MTES-derived monoliths prepared by co-hydrolysis hydrolysis of precursors, aged for 180 days, washed and unwashed are given in Table 3.5.

**Table 3.5. Full-Width-at-Half-Maximum Values for 7AI Entrapped in Materials Derived from Co-Hydrolyzed MTES, Aged 180 Days**

| Composition | Full-Width-at-Half-Maximum (nm) |
|---|---|
| **Washed** | |
| TEOS | 97 |
| 10% MTES | 110 |
| 20% MTES | 116 |
| 30% MTES | 112 |
| 40% MTES | 108 |
| **Unwashed** | |
| TEOS | 97 |
| 10% MTES | 111 |
| 20% MTES | 142 |
| 30% MTES | 153 |
| 40% MTES | 118 |

As the MTES content increased, the spectra changed in a manner consistent with the appearance of a new peak in the region of 340 to 350 nm accompanied by the gradual loss of intensity of the main peak at 370 to 380 nm. The emission spectra of 7AI in glasses of increasing MTES content (co-hydrolyzed, unwashed) are shown in Figure 3.1a.

The width of the spectral profiles was consistent with partitioning of the probe between a hydrophobic, ORMOSIL-rich region and a second region of higher dipolarity, composed mainly of silica. The spectral breadth may also have been indicative of the presence of peaks corresponding to the adsorbed and soluble forms of 7AI.

In the case of samples that were washed for 24 hours prior to drying, the spectra were much narrower and exhibited a much more gradual change to shorter emission wavelength maxima. There are several explanations for this observation. The presence of excess water from washing over the first 24 hours removed any excess ethanol produced as a by-product of the hydrolysis process. Since ethanol was removed, reesterification and any resulting spectral changes in the internal environment were avoided. It was also plausible that the presence of excess water during the initial stages of aging reduced the proportion of free silanol groups on the interior surfaces of the glass. As a result, 7AI was less likely to adsorb to free silanol groups so the contribution of the adsorbed form of the probe to the spectrum was reduced. Finally, the presence of water during the early stages of aging may have provided more favourable conditions for partitioning of the probe from the aqueous solvent into the hydrophobic regions of the monolith (since little or no ethanol was present), resulting in a narrower distribution of probe environments.

The spectra of washed or unwashed samples prepared using separately hydrolyzed silanes (not shown) exhibited trends similar to those from similarly aged co-hydrolyzed samples. However, there were some notable differences in the spectra. The spectral width of separately hydrolyzed samples was much larger than that from co-hydrolyzed

samples, in general. Unwashed, separately hydrolyzed samples containing MTES provided spectra that were quite broad, with full-width-at-half-maximum values as great as 150 nm as compared to about 100 nm for the corresponding co-hydrolyzed samples. The spectra were also quite flat at their maxima, indicative of a large distribution of environments with differing polarity. This spectral broadening was likely due to the differences in the colloidal properties of materials prepared from separately hydrolyzed silanes. In materials prepared using separately hydrolyzed silanes, the colloids were composed of pure TEOS and pure ORMOSIL. Hence, an emission spectrum of 7AI entrapped in these materials is a combination of the spectral profiles of 7AI associated with TEOS colloids and also with ORMOSIL colloids. Conversely, in materials prepared by co-hydrolysis of precursors, each colloid is of mixed composition and assumed to be homogeneous from colloid to colloid. Therefore, the emission spectrum of 7AI in the region of a colloid reports on a single, homogeneous environment rather than a combination of two different environments.

In summary, both separately hydrolyzed and co-hydrolyzed samples exhibited controllable decreases in the internal polarity with increasing organosilane content. Samples prepared from co-hydrolyzed silanes provided a narrower distribution of environments. This narrow distribution indicated that it is possible to exert some degree of control over the internal environment of the sol-gel-derived glass. It was also evident that washing of monoliths after gelation resulted in better control of the final internal environment. This latter finding was useful, especially considering that the resulting removal of ethanol was likely to be beneficial for biomolecule entrapment.[79]

3.1.2.2. Prodan Fluorescence

As with 7AI, significant differences in the spectral properties of prodan were observed, dependent upon organosilane content, sample washing and hydrolysis method. Representative emission spectra of prodan in unwashed and washed glasses made with various concentrations of co-hydrolyzed MTES are shown in Figures 3.2a and 3.2b, respectively.

As with 7AI, the emission maximum of entrapped prodan changed as a function of ORMOSIL content and aging time. The wavelengths of maximum emission (as a function of time) for prodan entrapped in sol-gel-derived materials prepared by co-hydrolysis and separate hydrolysis of precursors, washed and unwashed, are shown in Tables 3.6 and 3.7, respectively. Entries in the tables that have multiple wavelength values are indicative of spectra that had more than one peak and the values are the maximum wavelengths of the multiple peaks.

On day 1 after gelation, the emission maximum of prodan ranged from 511 nm (TEOS) to 505 nm (40% MTES). The general trend of shorter emission wavelength with higher organosilane content was also observed for PTMS and DMDMS samples. The lower wavelength of maximum emission indicated that the internal environment, reported by prodan, was determined both by the internal solvent content and the number of organic groups present. After aging was complete, both separately and co-hydrolyzed samples exhibited blue shifts in emission maxima with increased organosilane content. The emission maxima generally shifted to about 506 nm (TEOS) and about 468 nm (40%

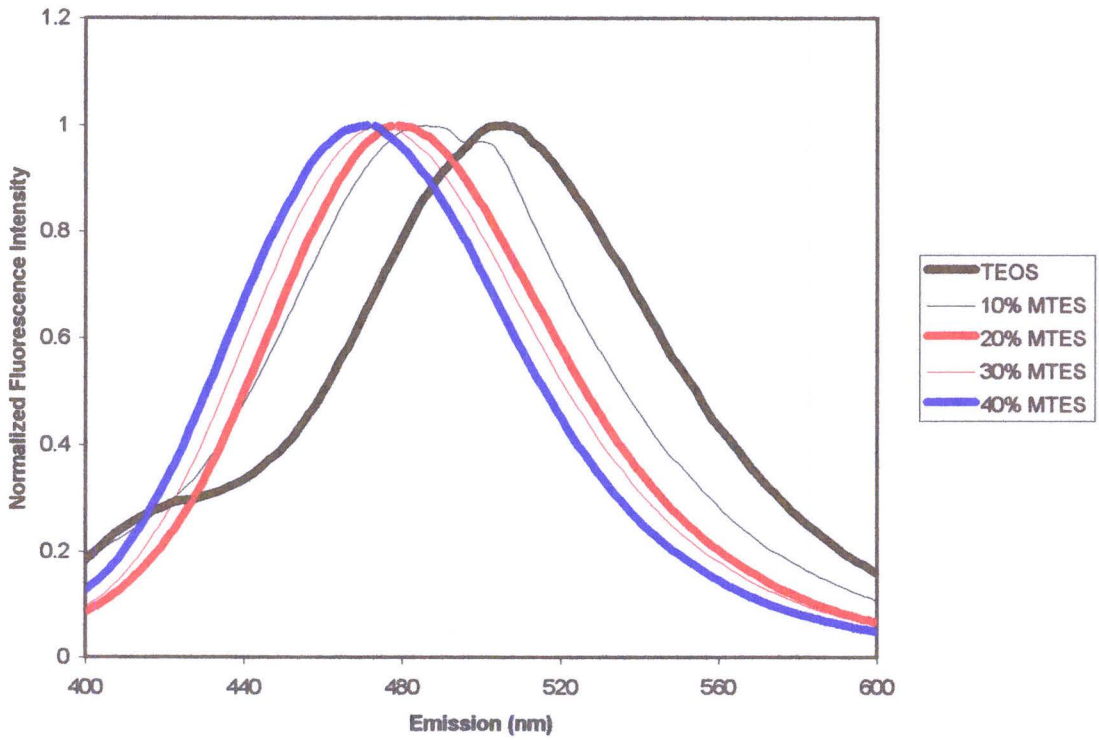


**Figure 3.2a. Fluorescence Emission Spectra of Prodan in Unwashed, Co-Hydrolyzed Monoliths Prepared Using Various Concentrations of MTES (Aged 180 Days)**

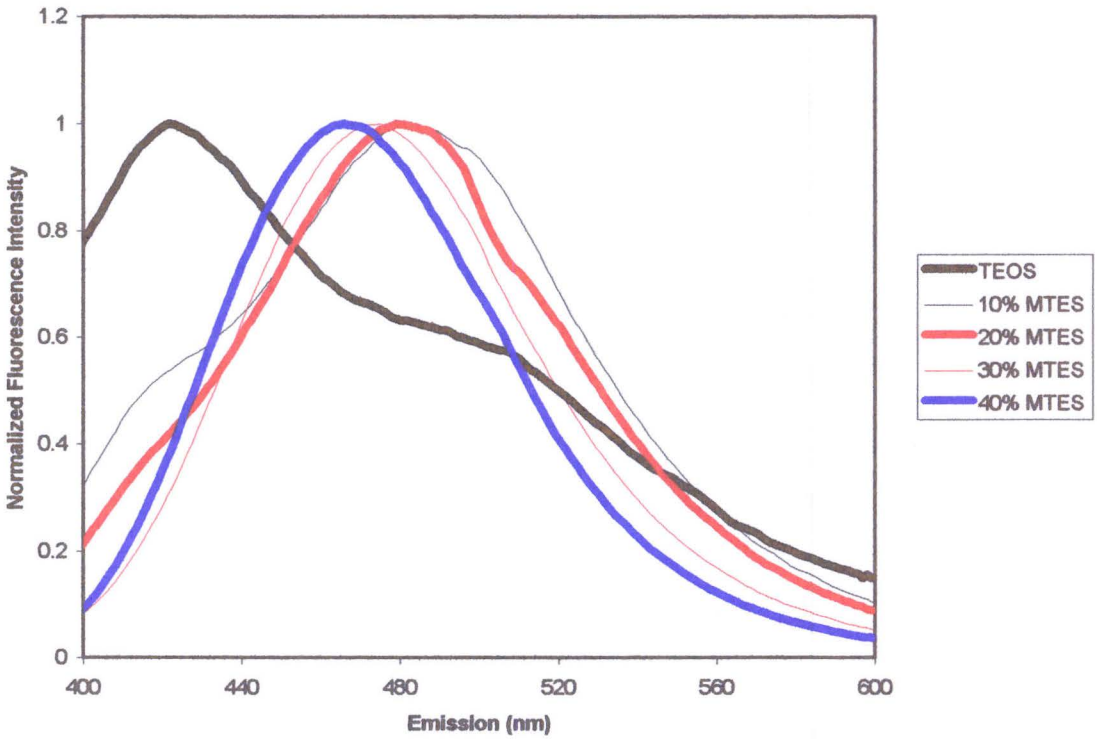


**Figure 3.2b. Fluorescence Emission Spectra of Prodan in Washed, Co-Hydrolyzed Monoliths Prepared Using Various Concentrations of MTES (Aged 180 Days)**

**Table 3.6. Emission Maximum Wavelengths of Entrapped Prodan in Sol-Gel-Derived Monoliths Prepared Using Co-Hydrolyzed Silane Precursors**

| Sample | Day 1 | Day 10 | Day 23 | Day 34 | Day 50 | Day 64 | Day 106 | Day 180 |
|---|---|---|---|---|---|---|---|---|
| **Washed** | | | | | | | | |
| TEOS | 510 | 515 | 516/434 | 512/432 | 509/426 | 514/425 | 505/424 | 506/424 |
| 5% MTES | 511 | 514 | 514/436 | 508/429 | 501/428 | 505/423 | 503/427 | 487/426 |
| 10% MTES | 510 | 510 | 509 | 508 | 508/424 | 508/424 | 492/424 | 482/425 |
| 15% MTES | 508 | 508 | 505 | 505 | 492/424 | 488/424 | 479/425 | 474/424 |
| 20% MTES | 509 | 507 | 504 | 498 | 494 | 490 | 480 | 473 |
| 25% MTES | 507 | 505 | 500 | 497 | 490 | 485 | 480 | 470 |
| 30% MTES | 507 | 503 | 498 | 495 | 489 | 485 | 479 | 469 |
| 35% MTES | 504 | 495 | 491 | 490 | 485 | 482 | 478 | 468 |
| 40% MTES | 505 | 498 | 494 | 493 | 484 | 482 | 477 | 468 |
| 2.5% DMDMS | 511 | 514 | 514/434 | 512/431 | 506/432 | 504/429 | 500/425 | 485/424 |
| 5% DMDMS | 508 | 507 | 505 | 504 | 497 | 492 | 489 | 482 |
| 7.5% DMDMS | 508 | 503 | 501 | 498 | 490 | 488 | 482 | 481 |
| 5% PTMS | 516 | 510 | 507 | 505 | 505 | 504 | 502 | 486 |
| 10% PTMS | 508 | 504 | 498 | 495 | 493 | 489 | 490 | 479 |
| 15% PTMS | 498 | 489 | 485 | 484 | 481 | 480 | 480 | 473 |
| 20% PTMS | 494 | 484 | 484 | 482 | 481 | 483 | 479 | 484 |
| **Unwashed** | | | | | | | | |
| TEOS | 511 | 512 | 514 | 513/435 | 516/425 | 516/428 | 508/425 | 504/426 |
| 5% MTES | 510 | 511 | 509 | 512/426 | 515/424 | 511/423 | 505/425 | 489/418 |
| 10% MTES | 512 | 509 | 508 | 506 | 502/424 | 502/423 | 488/424 | 487/425 |
| 15% MTES | 509 | 508 | 507 | 507 | 502 | 495 | 485 | 478 |
| 20% MTES | 509 | 507 | 507 | 503 | 501 | 499 | 488 | 478 |
| 25% MTES | 507 | 506 | 504 | 503 | 496 | 492 | 479 | 477 |
| 30% MTES | 506 | 504 | 502 | 503 | 492 | 491 | 479 | 474 |
| 35% MTES | 506 | 503 | 501 | 496 | 488 | 489 | 478 | 471 |
| 40% MTES | 505 | 503 | 499 | 495 | 492 | 493 | 479 | 471 |
| 2.5% DMDMS | 511 | 510 | 513 | 508/428 | 512/425 | 511/426 | 503 | 491 |
| 5% DMDMS | 509 | 507 | 506 | 505 | 500 | 500 | 489 | 486 |
| 7.5% DMDMS | 510 | 506 | 506 | 505 | 497 | 492 | 486 | 481 |
| 5% PTMS | 511 | 508 | 508 | 507 | 506 | 505 | 504 | 485 |
| 10% PTMS | 509 | 507 | 504 | 503 | 500 | 494 | 492 | 482 |
| 15% PTMS | 507 | 501 | 497 | 495 | 491 | 489 | 486 | 477 |
| 20% PTMS | 504 | 498 | 495 | 492 | 488 | 486 | 486 | 482 |

**Table 3.7. Emission Maximum Wavelengths of Entrapped Prodan in Sol-Gel-Derived Monoliths Prepared Using Separately Hydrolyzed Silane Precursors**

| Sample | Day 1 | Day 10 | Day 23 | Day 34 | Day 50 | Day 64 | Day 106 | Day 180 |
|---|---|---|---|---|---|---|---|---|
| **Washed** | | | | | | | | |
| TEOS | 510 | 515 | 516/434 | 512/432 | 509/426 | 514/425 | 505/424 | 506 |
| 5% MTES | 511 | 512 | 514 | 510/424 | 510/424 | 512/422 | 504 | 488 |
| 10% MTES | 510 | 510 | 509 | 507 | 505/423 | 503/422 | 492 | 484 |
| 15% MTES | 509 | 508 | 506 | 505 | 501 | 494 | 482 | 477 |
| 20% MTES | 509 | 505 | 504 | 502 | 497 | 489 | 482 | 475 |
| 25% MTES | 508 | 504 | 503 | 497 | 491 | 489 | 477 | 471 |
| 30% MTES | 509 | 501 | 501 | 491 | 487 | 481 | 473 | 464 |
| 35% MTES | 508 | 498 | 495 | 494 | 487 | 483 | 471 | 466 |
| 40% MTES | 508 | 500 | 494 | 489 | 488 | 483 | 475 | 466 |
| 5% PTMS | 495 | 489 | 490 | 485 | 481 | 478 | 474 | 474 |
| 10% PTMS | 491 | 483 | 481 | 478 | 475 | 474 | 464 | 466 |
| 15% PTMS | 486 | 478 | 474 | 470 | 469 | 470 | 458 | 487 |
| 20% PTMS | 488 | 481 | 480 | 475 | 473 | 464 | 453 | 481 |
| **Unwashed** | | | | | | | | |
| TEOS | 511 | 512 | 514 | 513/435 | 516/425 | 516/428 | 508/425 | 504/426 |
| 5% MTES | 511 | 511 | 512 | 509/424 | 511/424 | 509/424 | 505/425 | 501 |
| 10% MTES | 509 | 508 | 508 | 506 | 494/423 | 499/422 | 501 | 480 |
| 15% MTES | 511 | 507 | 508 | 506 | 503 | 499 | 485 | 475 |
| 20% MTES | 509 | 507 | 504 | 504 | 499 | 494 | 485 | 476 |
| 25% MTES | 508 | 506 | 504 | 503 | 499 | 489 | 480 | 468 |
| 30% MTES | 509 | 505 | 503 | 500 | 494 | 487 | 479 | 469 |
| 35% MTES | 508 | 504 | 502 | 499 | 488 | 485 | 470 | 463 |
| 40% MTES | 507 | 502 | 500 | 495 | 487 | 481 | 464 | 454 |
| 5% PTMS | 512 | 510 | 507 | 506 | 505 | 503 | 485 | 482 |
| 10% PTMS | 509 | 505 | 505 | 501 | 489 | 493 | 478 | 471 |
| 15% PTMS | 508 | 503 | 501 | 497 | 492 | 489 | 474 | 474 |
| 20% PTMS | 508 | 502 | 499 | 483 | 475 | 478 | 472 | 475 |

MTES). Prodan exhibits emission maxima ranging from 401 nm in cyclohexane to 530 nm in water.[42]

Prodan emission spectra collected from samples prepared using separately hydrolyzed silanes tended to be broader than the corresponding spectra for co-hydrolyzed samples. This observation was in agreement with results obtained from 7AI spectra. This trend was consistent with partitioning of the probe between regions that were organosilane rich and deficient. The broadening of the prodan spectra offered further evidence that the internal environment of samples prepared using separately hydrolyzed silanes has a much wider distribution of local polarities suggesting that segregation of organosilane components may have occurred.

The most pronounced difference in prodan emission spectra was based on whether or not the samples were washed during the early stages of aging. In all cases, samples with low ORMOSIL content showed two distinct peaks in their emission spectra, one near 500 nm and the other near 420 nm. In washed TEOS-derived samples, the peak at 420 nm was dominant and was also evident in samples containing up to 20.0% MTES. In unwashed samples, the peak at 420 nm was less prominent and was only evident in samples consisting of up to 10.0% MTES. Recent reports have attributed the emission at 420 nm to be due to prodan forming microcrystals, higher-order aggregates and/or dimers in water when the probe concentration exceeds about 1 μM.[43] Hence, it was expected that increases in the content of MTES should cause the intensity at 420 nm to decrease due to the increased solubility of prodan in the organic phase. The larger dimer peaks in washed and dried monoliths suggested that higher levels of water present during the

initial stages of aging promoted aggregation of the probe, due to the removal of ethanol (which solvated prodan) from the interior of the glass. The aggregates, once formed, were quite stable, since the dimer/aggregate peak did not disappear, even after 180 days of drying.

The spectral full-width-at-half-maximum values for prodan entrapped in materials prepared using co-hydrolysis with various levels of MTES, washed and unwashed and aged 180 days are shown in Table 3.8. It is important to note that the large full-width-at-half-maximum value for prodan in washed TEOS-derived samples was likely due to the presence of aggregates rather than phase separation.

**Table 3.8. Full-Width-at-Half-Maximum Values for Prodan Entrapped in Materials Derived from MTES, Aged 180 Days**

| Composition | Full-Width-at-Half-Maximum (nm) |
|---|---|
| **Washed** | |
| TEOS | >119 |
| 10% MTES | 119 |
| 20% MTES | 99 |
| 30% MTES | 86 |
| 40% MTES | 85 |
| **Unwashed** | |
| TEOS | 93 |
| 10% MTES | 94 |
| 20% MTES | 85 |
| 30% MTES | 86 |
| 40% MTES | 85 |

An interesting aspect of the peaks that corresponded to the monomer and aggregate forms of prodan was that the ratio of their intensities changed over time, as shown in Figure 3.3. Examination of the ratio of aggregate to monomer provided a qualitative method of probing the amount of water remaining within the monoliths of high polarity.

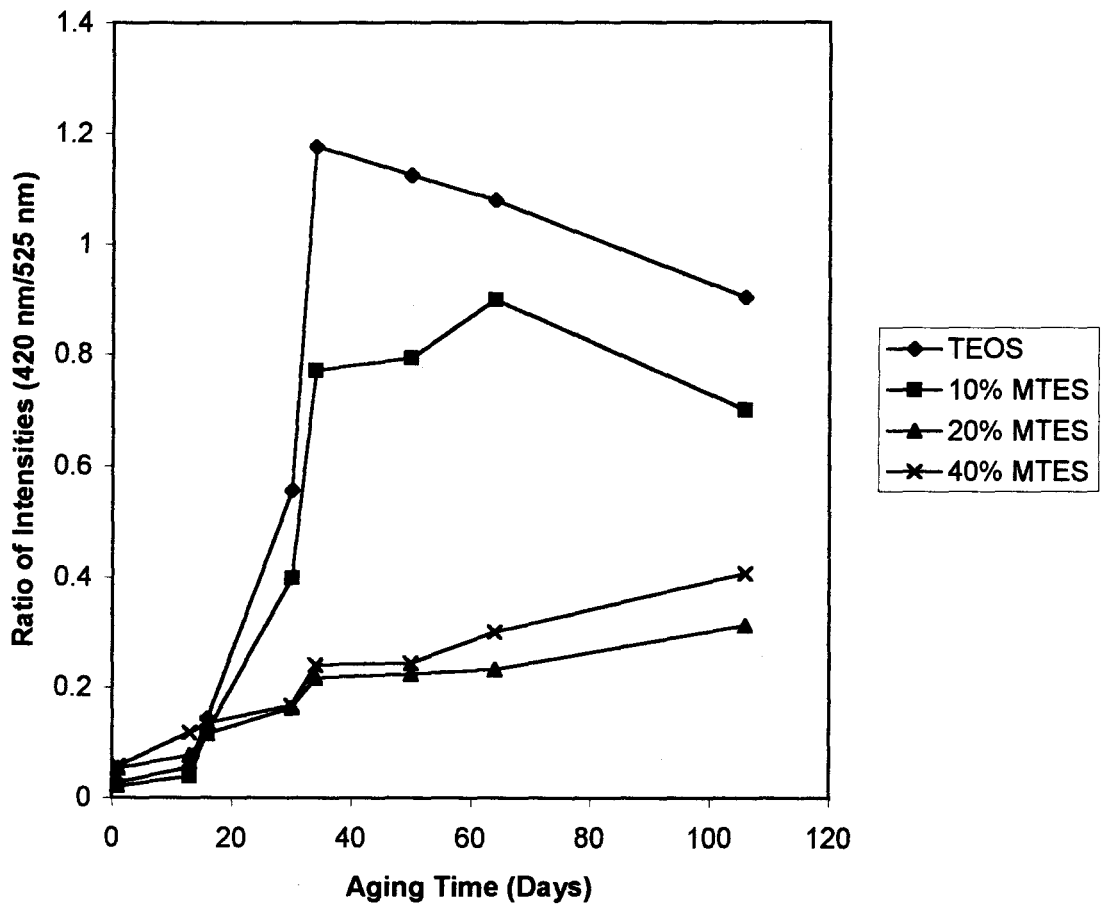


**Figure 3.3. Ratio of Aggregate and Monomer Peaks of Prodan in MTES:TEOS Monoliths as a Function of Aging Time**

The intensity ratio of the aggregate and monomer peaks increased rapidly over the first 30 days for most samples and then remained relatively constant or decreased slightly as aging and drying proceeded. The initial increases were largest for samples with low organosilane content. The initial increases in the aggregate to monomer ratio, and the shift to lower wavelength for the monomer peak during aging were consistent with ethanol and water being removed over the first 30 days. The smaller change in the ratio observed after day 30 was consistent with a slow repartitioning of the probe between the dimer and monomer forms, free and adsorbed states and possibly between MTES-rich and MTES-deficient regions, when MTES was present.

## 3.2. Characterization of Polymer-Doped Sol-Gel-Derived Materials

### *3.2.1. Physical Properties of Polymer-Doped Sol-Gel-Derived Monoliths*

#### 3.2.1.1. Optical Clarity

The optical clarity at 400 nm of washed and unwashed 80-day-old PEG and PVA-doped samples are provided in Table 3.9. Entries of N/A in the table correspond to samples that had broken so the transmittance could not be measured. In almost all cases, there were differences in the transmittance of washed versus unwashed samples. However, washing the samples did not necessarily result in a reduction in clarity of the sample as was the case for ORMOSIL-derived samples. In general, transmittance values of around 75% or greater were observed for samples containing PEG, regardless of the concentration or molecular weight of the PEG added. On the other hand, all of the samples doped with 10.0% (w/v in the buffer) PVA exhibited reduced transmittance and in some cases were opaque. This reduction in transmittance was due to the fact that the PVA used was of a high molecular weight, and was a solid in its native state. Drying of the materials therefore caused entrapped PVA to precipitate, making the samples opaque. Unfortunately, PVA at a lower molecular weight was not commercially available to aid in the preparation of transparent materials. PEG 400 was a viscous liquid and PEG 600 was a moist solid at room temperature. These additives resulted in materials that were quite transparent, even after drying for 80 days. PEG was also found to make MTES-derived samples more transparent, possibly due to the alleviation of phase separation.

**Table 3.9. Physical Properties of Polymer-Doped Sol-Gel-Derived Slides Prepared Using Co-Hydrolyzed Silane Precursors at Day 84**

| Sample | Optical Transmittance (%), Washed/Unwashed | Hardness (Vicker's Scale, Washed/Unwashed) |
|---|---|---|
| **TEOS** | | |
| 5% PEG 400 | 81.76±0.02/74.87±0.02 | 0.35±0.07/2.03±0.70 |
| 10% PEG 400 | 71.05±0.01/75.58±0.02 | 0.95±0.78/1.40±0.00 |
| 5% PEG 600 | 80.99±0.00/76.60±0.00 | 0.73±.0.42/0.80±0.40 |
| 10% PEG 600 | 79.94±0.01/80.45±0.01 | 0.70±0.44/1.15±0.49 |
| 5% PVA | 57.69±0.01/72.51±0.03 | N/A / 1.50±0.82 |
| 10% PVA | N/A | N/A |
| **5% MTES** | | |
| 5% PEG 400 | 63.16±0.02/80.89±0.02 | 0.75±0.07/3.13±2.97 |
| 10% PEG 400 | 41.45±0.02/78.88±0.01 | N/A /0.63±0.59 |
| 5% PEG 600 | 79.17±0.01/78.59±0.01 | 0.70±0.30/0.70±0.42 |
| 10% PEG 600 | 35.77±0.02/79.52±0.00 | 0.55±0.07/0.87±0.64 |
| 5% PVA | 74.01±0.01/70.65±0.01 | 6.97±4.69/0.73±0.61 |
| 10% PVA | 37.58±0.01/67.47±0.02 | N/A / 2.53±1.70 |
| **10% MTES** | | |
| 5% PEG 400 | 71.58±0.01/61.83±0.02 | 0.30±0.10/0.83±0.35 |
| 10% PEG 400 | 73.91±0.02/77.92±0.01 | 0.65±0.49/0.67±0.35 |
| 5% PEG 600 | 60.30±0.01/85.23±0.02 | 0.33±0.06/0.80±0.42 |
| 10% PEG 600 | 76.37±0.02/69.01±0.02 | 0.77±0.31/0.37±0.12 |
| 5% PVA | 53.20±0.01/77.16±0.66 | 1.60±0.40/0.83±0.06 |
| 10% PVA | 0.15±0.00/N/A | N/A |
| **1% DMDMS** | | |
| 5% PEG 400 | 68.89±0.01/82.25±0.01 | 0.45±0.07/0.67±0.21 |
| 10% PEG 400 | 79.10±0.02/78.00±0.01 | 0.57±0.21/0.25±0.07 |
| 5% PEG 600 | 67.28±0.06/78.09±0.00 | 0.90±0.75/1.23±0.31 |
| 10% PEG 600 | 69.14±0.02/73.63±0.00 | 0.30±0.10/0.30±0.26 |
| 5% PVA | 42.61±0.03/80.29±0.01 | 1.00±0.28/0.55±0.35 |
| 10% PVA | 41.31±0.01/65.71±0.03 | N/A |
| **5% DMDMS** | | |
| 5% PEG 400 | 81.50±0.01/75.10±0.01 | N/A / 0.60±0.36 |
| 10% PEG 400 | 77.34±0.03/75.15±0.58 | 0.87±0.23/1.07±0.57 |
| 5% PEG 600 | 63.91±0.01/74.72±0.03 | 0.70±0.26/0.40±0.17 |
| 10% PEG 600 | 78.41±0.02/89.83±0.03 | 1.00±0.42/1.17±0.60 |
| 5% PVA | 45.59±0.01/71.37±0.03 | 0.97±0.38/1.07±0.15 |
| 10% PVA | 0.02±0.00/N/A | N/A |

3.2.1.2. Hardness

The hardness of the 40-day-old polymer-doped samples was evaluated using a diamond indentation instrument and the values are summarized in Table 3.9. The samples were tested on day 40 rather than day 180 after gelation due to time constraints, and also because day 40 was closer to the amount of time after gelation that testing of protein samples was done. It was found that there was no statistical difference between the hardness values for all of the samples at day 40. It is interesting to note that for some samples containing PVA, hardness values could not be obtained since the indentation on the surface was not well defined and could not be resolved using the viewfinder. The hardness of an 8-month-old TEOS-derived sample was also examined to determine the effect of aging time on the hardness of aged sol-gel-derived materials. The hardness value for the 8-month-old sample was 1.57 ± 0.78. This result showed that there was no statistical difference between the hardness values of the 40-day-old and 8-month-old samples, suggesting that long-term aging of monoliths did not necessarily increase the hardness of the samples. This result was unexpected since sol-gel-derived materials should become harder due to increased cross-linking and collapse of the pores within the material over time. It may be possible that the instrument used for determination of the hardness of the sol-gel-derived samples may not be appropriate for these types of samples. The samples may have been too soft to provide an accurate determination of material hardness.

The large errors associated with some of the samples were likely due to the fact that opposite surfaces of the roughly cubic monoliths may not have been perfectly parallel,

hence, the diamond tip may not have come in contact with the surface evenly, resulting in distortions of the indentation. It would be beneficial to retest the samples once they had aged further or to perform scratch tests like those done for samples made from ORMOSILs only.

3.2.1.3. Dehydration /Rehydration Stability

The dehydration stabilities of polymer-doped samples (unwashed and washed) were also examined on days 21 and 80 after gelation and are summarized in Tables 3.10 and 3.11, respectively. The presence of PEG at concentrations of 5.0 and 10.0% (w/v in the buffer) appeared to have a positive effect on the dehydration behaviour of TEOS, 20.0% MTES and 5.0% DMDMS. In general, these materials exhibited enhanced dehydration stability on day 21 and day 80, relative to the corresponding materials prepared in the absence of added PEG, regardless of whether they were washed or not.

The rehydration stabilities were also examined for TEOS, 20.0% MTES and 5.0% DMDMS samples doped with PEG and PVA on days 21 and 80 and are summarized in Tables 3.10 and 3.11. The rehydration stability for these samples followed the same general trend as the dehydration stability. In general, the addition of PEG to the samples resulted in good rehydration stabilities, compared to samples that were prepared in the absence of PEG.

**Table 3.10. Dehydration/Rehydration Stability on Day 21 and Day 80 For PEG-Doped Materials (Unwashed)**

| Sample | Dehydration Stability (Day 21) | Dehydration Stability (Day 80) | Rehydration Stability (Day 21) | Rehydration Stability (Day 80) |
|---|---|---|---|---|
| **TEOS** | | | | |
| 5% PEG 400 | Excellent | Good | Excellent | Good |
| 10% PEG 400 | Excellent | Good | Excellent | Good |
| 5% PEG 600 | Excellent | Good | Excellent | Good |
| 10% PEG 600 | Excellent | Good | Excellent | Good |
| 5% PVA | Excellent | Excellent | Excellent | Excellent |
| 10% PVA | Poor | Poor | Poor | Poor |
| **20% MTES** | | | | |
| 5% PEG 400 | Good | Excellent | Good | Excellent |
| 10% PEG 400 | Good | Excellent | Good | Good |
| 5% PEG 600 | Good | Excellent | Good | Good |
| 10% PEG 600 | Excellent | Excellent | Excellent | Good |
| 5% PVA | Excellent | Excellent | Excellent | Excellent |
| 10% PVA | Good | Good | Poor | Poor |
| **5% DMDMS** | | | | |
| 5% PEG 400 | Good | Good | Good | Good |
| 10% PEG 400 | Excellent | Moderate | Excellent | Moderate |
| 5% PEG 600 | Excellent | Good | Excellent | Good |
| 10% PEG 600 | Excellent | Poor | Excellent | Poor |
| 5% PVA | Good | Good | Good | Good |
| 10% PVA | Poor | Poor | Poor | Poor |

**Table 3.11. Dehydration/Rehydration Stability on Day 21 for PEG-Doped Materials (Washed)**

| Sample | Dehydration Stability (Day 21) | Dehydration Stability (Day 80) | Rehydration Stability (Day 21) | Rehydration Stability (Day 80) |
|---|---|---|---|---|
| **TEOS** | | | | |
| 5% PEG 400 | Excellent | Excellent | Excellent | Good |
| 10% PEG 400 | Excellent | Excellent | Excellent | Excellent |
| 5% PEG 600 | Excellent | Excellent | Excellent | Good |
| 10% PEG 600 | Excellent | Good | Excellent | Good |
| 5% PVA | Excellent | Excellent | Excellent | Excellent |
| 10% PVA | Excellent | Poor | Excellent | Poor |
| **20% MTES** | | | | |
| 5% PEG 400 | Excellent | Excellent | Excellent | Excellent |
| 10% PEG 400 | Excellent | Excellent | Excellent | Excellent |
| 5% PEG 600 | Good | Excellent | Good | Good |
| 10% PEG 600 | Excellent | Excellent | Excellent | Excellent |
| 5% PVA | Excellent | Excellent | Excellent | Excellent |
| 10% PVA | Excellent | Excellent | Excellent | Good |
| **5% DMDMS** | | | | |
| 5% PEG 400 | Excellent | Excellent | Excellent | Excellent |
| 10% PEG 400 | Excellent | Excellent | Excellent | Good |
| 5% PEG 600 | Excellent | Excellent | Excellent | Excellent |
| 10% PEG 600 | Excellent | Excellent | Excellent | Good |
| 5% PVA | Excellent | Excellent | Excellent | Excellent |
| 10% PVA | Excellent | Excellent | Excellent | Excellent |

### *3.2.2. Spectroscopic Studies of Polymer-Doped Sol-Gel-Derived Monoliths Using Environmentally-Sensitive Fluorescent Probes*

#### 3.2.2.1. 7AI Fluorescence

Spectra of unwashed, co-hydrolyzed samples prepared using TEOS and doped with different concentrations and molecular weight PEG and PVA are shown in Figure 3.4a. Those for washed samples are shown in Figure 3.4b. The wavelength of maximum emission for unwashed and washed samples are provided in Tables 3.12 and 3.13, respectively.

For unwashed and washed samples prepared using TEOS, 5.0 and 10.0% MTES and 1.0 and 5.0% DMDMS, increased concentrations of PEG led to a blue shift in the emission maximum, regardless of the molecular weight of the PEG used. These results suggest that the presence of polymer molecules provided an increased degree of hydrophobicity to the material and hence, the 7AI molecules may have been solvated more efficiently in this type of environment. As a result, the spectra of the probe were more like those of individual probe molecules, rather than those of surface adsorbed or solvent-complexed forms. It should be noted that in order to form probe-solvent complexes, the probe must be dissolved in a protic solvent that possesses an exchangeable hydrogen atom.

For washed and unwashed samples prepared using TEOS, 5.0 and 10.0% MTES and 1.0 and 5.0% DMDMS, increased concentrations of PVA led to a red shift in the emission maximum of 7AI. Increased concentrations of PVA would have caused an increase in the number of free hydroxyl groups within the material. 7AI molecules would be expected to exist in an adsorbed form in samples containing higher concentrations of

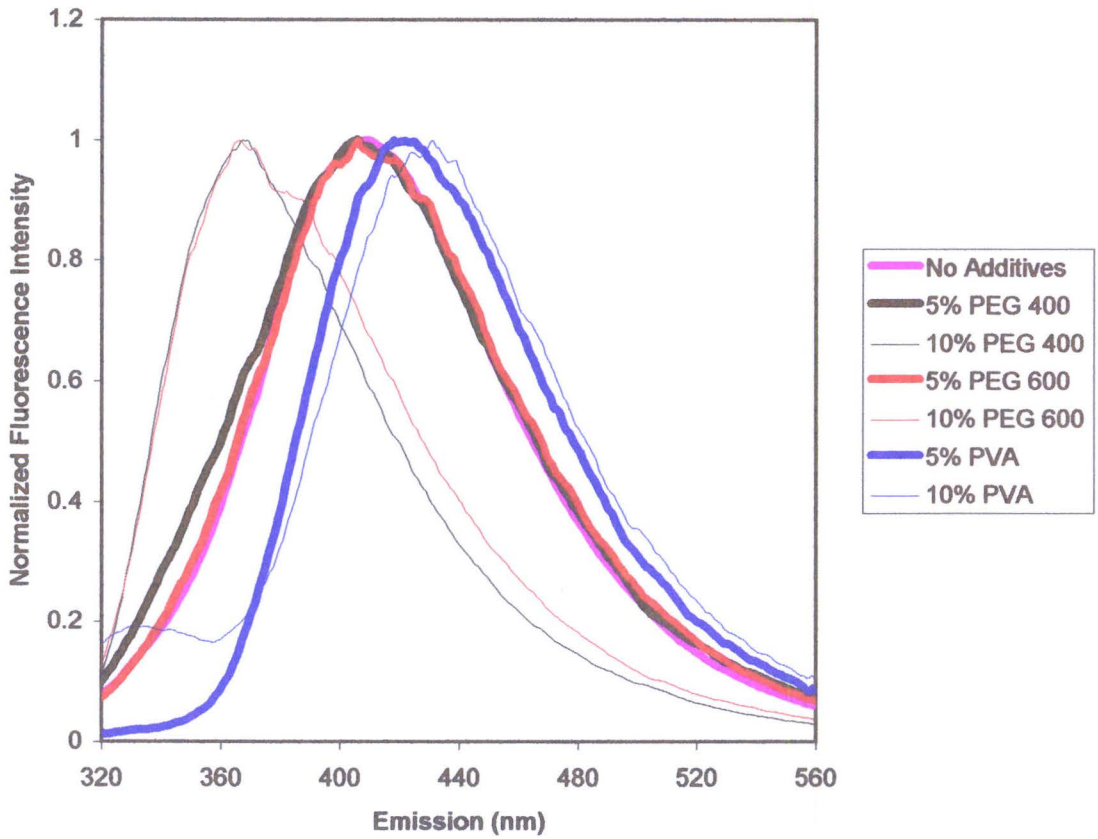


**Figure 3.4a. Emission Spectra of 7AI Entrapped in Unwashed, Polymer-Doped Materials Prepared Using TEOS**

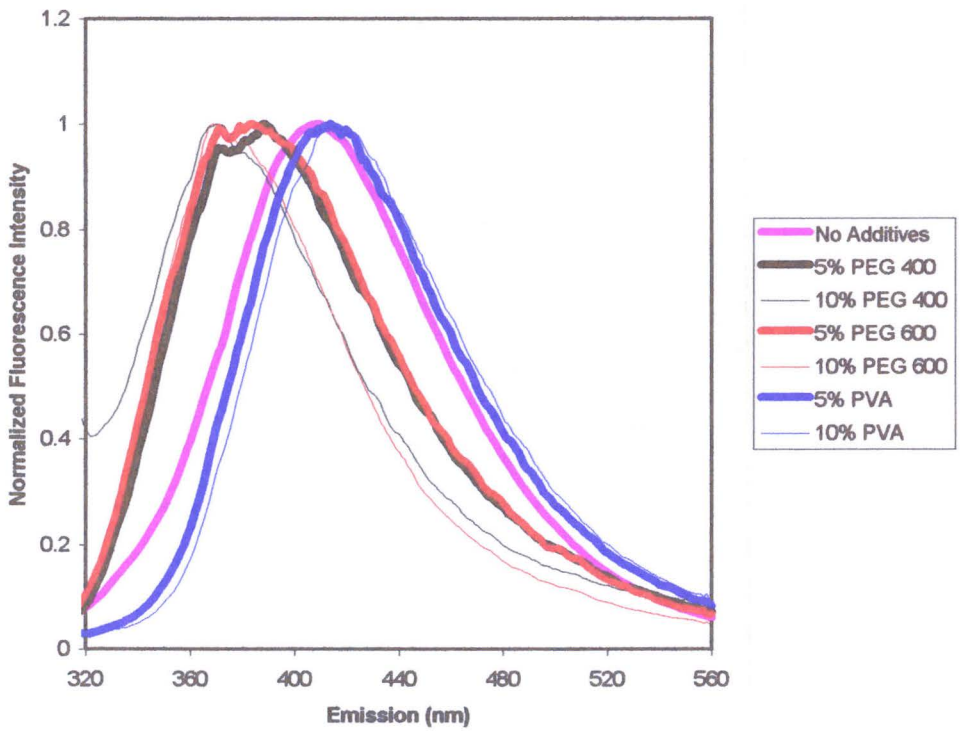


**Figure 3.4b. Emission Spectra of 7AI Entrapped in Washed, Polymer-Doped Materials Prepared Using TEOS**

**Table 3.12. Wavelengths of Maximum Emission of 7AI in Unwashed, Polymer-Doped Sol-Gel-Derived Monoliths Prepared Using Co-Hydrolyzed Silanes**

| Sample | Day 1 | Day 10 | Day 23 | Day 34 | Day 60 | Day 74 |
|---|---|---|---|---|---|---|
| **TEOS** | | | | | | |
| Polymer Free | 366 | 368 | 370 | 375 | 398 | - |
| 5% PEG 400 | - | 371 | 376 | 385 | 406 | 406 |
| 10% PEG 400 | - | 369 | 376 | 379 | 367 | 367 |
| 5% PEG 600 | - | 371 | 373 | 374 | 397 | 406 |
| 10% PEG 600 | - | 369 | 372 | 375 | 389 | 371 |
| 5% PVA | - | 377 | 383 | 385 | 419 | 421 |
| 10% PVA | - | 384 | 388 | 391 | 426 | 431 |
| **5% MTES** | | | | | | |
| Polymer Free | 366 | 370 | 369 | 374 | 394 | - |
| 5% PEG 400 | 370 | 372 | 375 | 379 | 407 | 403 |
| 10% PEG 400 | 367 | 370 | 372 | 374 | 378 | 382 |
| 5% PEG 600 | 368 | 372 | 375 | 377 | 395 | 403 |
| 10% PEG 600 | 366 | 369 | 374 | 377 | 384 | 386 |
| 5% PVA | 373 | 379 | 383 | 390 | 414 | 417 |
| 10% PVA | 379 | 383 | 384 | 385 | 392 | 400 |
| **10% MTES** | | | | | | |
| Polymer Free | 366 | 363 | 366 | 371 | 379 | 386 |
| 5% PEG 400 | 368 | 370 | 372 | 374 | 379 | 385 |
| 10% PEG 400 | 370 | 371 | 371 | 373 | 378 | 381 |
| 5% PEG 600 | 370 | 370 | 372 | 374 | 384 | 398 |
| 10% PEG 600 | 370 | 368 | 372 | 372 | 375 | 368 |
| 5% PVA | 375 | 381 | 382 | 380 | 400 | 413 |
| 10% PVA | 382 | 383 | 398 | 405 | 346* | 339* |
| **1% DMDMS** | | | | | | |
| Polymer Free[a] | 368 | 370 | 369 | 371 | 402 | - |
| 5% PEG 400 | 370 | 367 | 375 | 386 | 406 | 406 |
| 10% PEG 400 | 368 | 369 | 375 | 380 | 384 | 369 |
| 5% PEG 600 | 370 | 372 | 373 | 378 | 407 | 405 |
| 10% PEG 600 | 368 | 369 | 372 | 374 | 379 | 387 |
| 5% PVA | 372 | 379 | 381 | 384 | 414 | 420 |
| 10% PVA | 377 | 383 | 390 | 396 | 426 | 419 |
| **5% DMDMS** | | | | | | |
| Polymer Free | 368 | 369 | 367 | 368 | 385 | |
| 5% PEG 400 | - | 369 | 372 | 373 | 387 | 386 |
| 10% PEG 400 | - | 369 | 370 | 372 | 371 | 365 |
| 5% PEG 600 | - | 369 | 372 | 373 | 374 | 376 |
| 10% PEG 600 | - | 369 | 371 | 370 | 372 | 372 |
| 5% PVA | - | 381 | 384 | 384 | 410 | 420 |
| 10% PVA | - | 393 | 389 | 344* | 343* | * |

*Sample was opaque, wavelength is maximum of scattering

[a] Data from 2.5% DMDMS sample

**Table 3.13. Wavelengths of Maximum Emission of 7AI in Washed, Polymer-Doped Sol-Gel-Derived Monoliths Prepared Using Co-Hydrolyzed Silanes**

| Sample | Day 1 | Day 10 | Day 23 | Day 34 | Day 60 | Day 74 |
|---|---|---|---|---|---|---|
| **TEOS** | | | | | | |
| Polymer Free | 366 | 370 | 371 | 369 | 382 | - |
| 5% PEG 400 | - | 374 | 378 | 378 | 386 | 388 |
| 10% PEG 400 | - | 375 | 375 | 374 | 378 | 373 |
| 5% PEG 600 | - | 374 | 378 | 378 | 384 | 383 |
| 10% PEG 600 | - | 373 | 375 | 376 | 378 | 376 |
| 5% PVA | - | 386 | 392 | 397 | 411 | 414 |
| 10% PVA | - | 391 | 399 | 402 | 416 | 431 |
| **5% MTES** | | | | | | |
| Polymer Free | 367 | 374 | 373 | 375 | 385 | - |
| 5% PEG 400 | 377 | 375 | 374 | 375 | 380 | 382 |
| 10% PEG 400 | 375 | 373 | 374 | 376 | 376 | 376 |
| 5% PEG 600 | 374 | 376 | 377 | 377 | 377 | 382 |
| 10% PEG 600 | 371 | 373 | 375 | 376 | 371 | 365 |
| 5% PVA | 380 | 388 | 390 | 397 | 411 | 416 |
| 10% PVA | 387 | 396 | 404 | 415 | 425 | 427 |
| **10% MTES** | | | | | | |
| Polymer Free | 367 | 371 | 371 | 370 | 376 | - |
| 5% PEG 400 | 373 | 372 | 374 | 374 | 378 | 377 |
| 10% PEG 400 | 374 | 372 | 376 | 374 | 375 | 370 |
| 5% PEG 600 | 377 | 368 | 372 | 373 | 375 | 369 |
| 10% PEG 600 | 371 | 371 | 372 | 372 | 374 | 369 |
| 5% PVA | 383 | 384 | 388 | 393 | 399 | 403 |
| 10% PVA | 390 | 389 | 396 | 399 | 333* | 337* |
| **1% DMDMS** | | | | | | |
| Polymer Free[a] | 370 | 372 | 370 | 372 | 385 | - |
| 5% PEG 400 | 377 | 373 | 377 | 377 | 379 | 378 |
| 10% PEG 400 | 376 | 376 | 375 | 378 | 378 | 377 |
| 5% PEG 600 | 377 | 375 | 378 | 381 | 380 | 382 |
| 10% PEG 600 | 374 | 375 | 375 | 375 | 375 | 371 |
| 5% PVA | 384 | 386 | 389 | 393 | 407 | 411 |
| 10% PVA | 387 | 388 | 394 | 402 | 417 | 423 |
| **5% DMDMS** | | | | | | |
| Polymer Free | 369 | 372 | 369 | 372 | 373 | - |
| 5% PEG 400 | - | 373 | 371 | 373 | 374 | 371 |
| 10% PEG 400 | - | 373 | 372 | 373 | 374 | 370 |
| 5% PEG 600 | - | 372 | 372 | 374 | 374 | 373 |
| 10% PEG 600 | - | 372 | 371 | 372 | 371 | 370 |
| 5% PVA | - | 387 | 389 | 394 | 405 | 408 |
| 10% PVA | - | 393 | 397 | 400 | 344* | * |

*Sample was opaque, wavelength is maximum of scattering

[a] Data from 2.5% DMDMS sample

PVA, due to the presence of a higher proportion of hydroxyl groups, consistent with the observed red shift.

Full-width-at-half-maximum values for 7AI entrapped in TEOS-derived materials doped with polymer additives and aged 74 days are provided in Table 3.14. These values showed that there was no significant difference in the distribution of environments between washed and unwashed samples or when the type and amount of additive used was varied.

**Table 3.14. Full-Width-at-Half-Maximum Values for 7AI Entrapped in Materials Derived from TEOS and Doped with Polymer Additives, Aged 74 Days**

| Composition | Full-Width-at-Half-Maximum (nm) |
|---|---|
| **Washed** | |
| Pure TEOS | 97 |
| 5% PEG 400 | 98 |
| 10% PEG 400 | 91 |
| 5% PEG 600 | 101 |
| 10% PEG 600 | 82 |
| 5% PVA | 94 |
| 10% PVA | 94 |
| **Unwashed** | |
| Pure TEOS | 97 |
| 5% PEG 400 | 100 |
| 10% PEG 400 | 82 |
| 5% PEG 600 | 101 |
| 10% PEG 600 | 90 |
| 5% PVA | 93 |
| 10% PVA | 92 |

The relatively consistent full-width-at-half-maximum values suggested that the addition of polymer additives helped reduce the distribution of environments within the materials, resulting in more homogeneous materials as compared to samples prepared without polymer additives. It should also be noted that increasing the amount of PEG added to

TEOS-derived samples resulted in a decrease in the full-width-at-half-maximum values and hence, a reduced distribution of environments.

3.2.2.2. Prodan Fluorescence

Fluorescence experiments were also performed using PEG and PVA-doped TEOS and ORMOSIL-derived materials containing prodan. Spectra of prodan entrapped in TEOS-derived materials doped with different polymer additive are shown in Figures 3.5a and Figure 3.5b, for unwashed and washed samples respectively. The wavelengths of maximum emission for prodan entrapped in polymer-doped monoliths prepared using co-hydrolyzed silanes, unwashed and washed, are provided in Tables 3.15 and 3.16, respectively. For washed samples, the emission maximum was red-shifted for PVA-doped samples relative to PEG-doped samples. This was likely due to the presence of hydroxyl groups on the PVA molecules, which made the internal environment more polar and hence, caused a red shift in the emission of prodan. The addition of higher concentrations of either polymer also did not significantly affect the location of the emission maxima, and there was no general trend of a blue shift with increasing additive concentration, as had been observed for 7AI. The full-width-at-half-maximum of prodan entrapped in TEOS-derived materials doped with polymer additives, washed and unwashed and aged 74 days are given in Table 3.17. As with 7AI, the full-width-at-half-maximum values were relatively constant between washed and unwashed samples, regardless of the amount or type of polymer additive. This result suggested that the

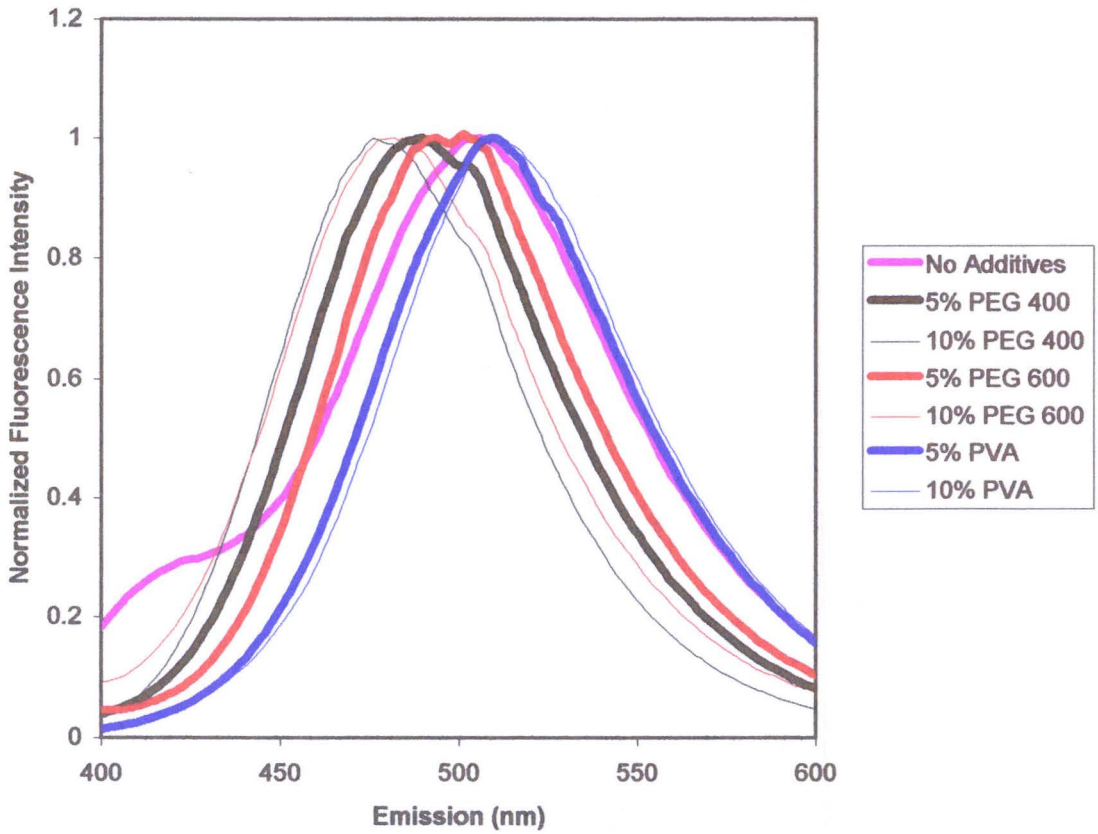


**Figure 3.5a. Emission Spectra of Prodan Entrapped in Unwashed, Polymer-Doped Materials Prepared Using TEOS**

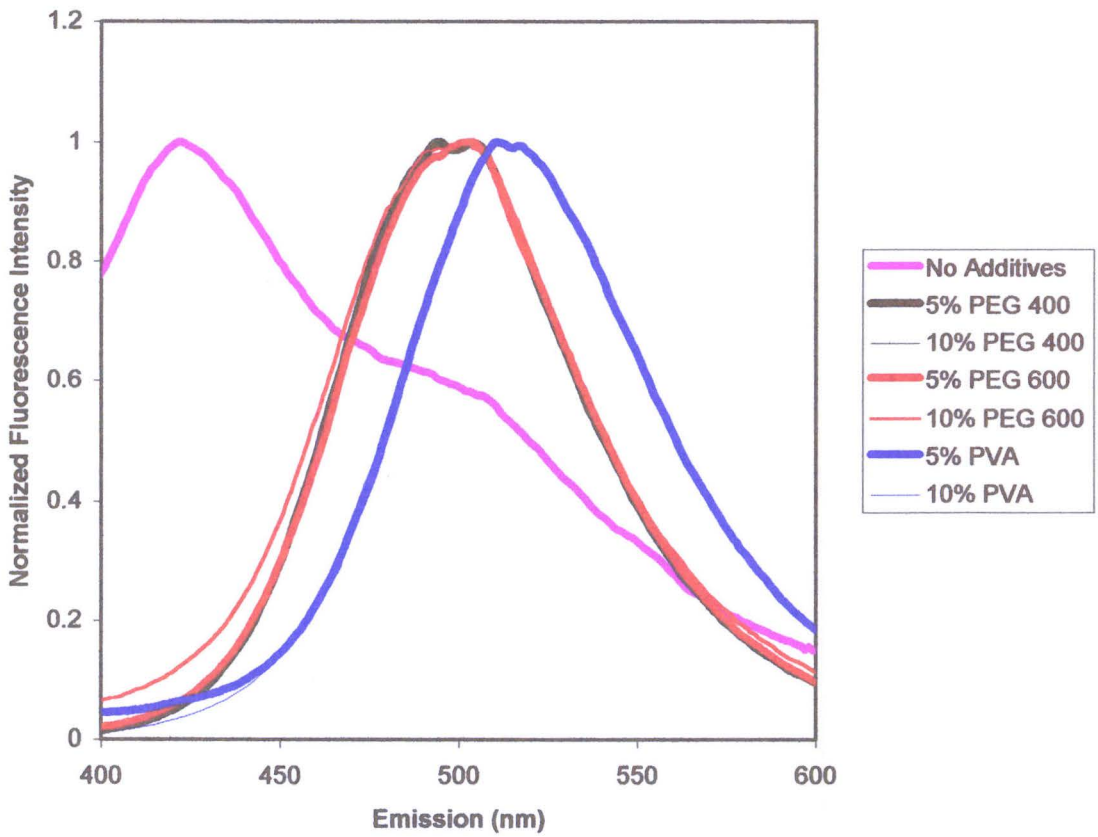


**Figure 3.5b. Emission Spectra of Prodan Entrapped in Washed, Polymer-Doped Materials Prepared Using TEOS**

**Table 3.15. Wavelengths of Maximum Emission of Prodan in Unwashed, Polymer-Doped Sol-Gel-Derived Monoliths Prepared by Co-Hydrolysis of Silanes**

| Sample | Day 1 | Day 10 | Day 23 | Day 34 | Day 60 | Day 74 |
|---|---|---|---|---|---|---|
| **TEOS** | | | | | | |
| Polymer Free | 511 | 512 | 514 | 513/435 | 516/428 | - |
| 5% PEG 400 | 510 | 512 | 513 | 509 | 499 | 489 |
| 10% PEG 400 | 510 | 510 | 511 | 508 | 492 | 479 |
| 5% PEG 600 | 511 | 512 | 513 | 510 | 500 | 497 |
| 10% PEG 600 | 508 | 509 | 508 | 505 | 495 | 481 |
| 5% PVA | 509 | 512 | 515 | 518 | 512 | 509 |
| 10% PVA | 510 | 512 | 516 | 516 | 508 | 511 |
| **5% MTES** | | | | | | |
| Polymer Free | 510 | 511 | 509 | 512/426 | 511/423 | - |
| 5% PEG 400 | 510 | 511 | 510 | 507 | 494 | 492 |
| 10% PEG 400 | 507 | 509 | 511 | 509 | 501 | 496 |
| 5% PEG 600 | 507 | 510 | 510 | 506 | 496 | 488 |
| 10% PEG 600 | 508 | 509 | 509 | 506 | 494 | 487 |
| 5% PVA | 510 | 511 | 513 | 514 | 507 | 506 |
| 10% PVA | 507 | 512 | 513 | 511 | 501 | 492 |
| **10% MTES** | | | | | | |
| Polymer Free | 512 | 509 | 508 | 506 | 502/423 | - |
| 5% PEG 400 | 509 | 510 | 508 | 503 | 489 | 486 |
| 10% PEG 400 | 506 | 509 | 507 | 506 | 496 | 490 |
| 5% PEG 600 | 510 | 509 | 507 | 506 | 491 | 487 |
| 10% PEG 600 | 507 | 507 | 506 | 505 | 494 | 490 |
| 5% PVA | 509 | 511 | 511 | 511 | 504 | 498 |
| 10% PVA | 509 | 509 | 511 | 509 | 498 | 489 |
| **1% DMDMS** | | | | | | |
| Polymer Free[a] | 511 | 510 | 513 | 508/428 | 511/426 | - |
| 5% PEG 400 | 508 | 509 | 511 | 510 | 504 | 500 |
| 10% PEG 400 | 507 | 509 | 510 | 510 | 503 | 502 |
| 5% PEG 600 | 510 | 510 | 511 | 510 | 503 | 501 |
| 10% PEG 600 | 505 | 509 | 509 | 506 | 500 | 497 |
| 5% PVA | 510 | 511 | 514 | 516 | 514 | 511 |
| 10% PVA | 508 | 510 | 512 | 513 | 512 | - |
| **5% DMDMS** | | | | | | |
| Polymer Free | 509 | 507 | 506 | 505 | 500 | - |
| 5% PEG 400 | 509 | 507 | 506 | 505 | 487 | 480 |
| 10% PEG 400 | 508 | 506 | 504 | 497 | 480 | 471 |
| 5% PEG 600 | 509 | 507 | 505 | 500 | 482 | 477 |
| 10% PEG 600 | 507 | 505 | 504 | 494 | 479 | 468 |
| 5% PVA | 509 | 506 | 508 | 504 | 493 | 491 |
| 10% PVA | 509 | 508 | 503/420 | 430/494 | 463 | 470 |

[a] Data from 2.5% DMDMS sample

**Table 3.16. Wavelengths of Maximum Emission of Prodan in Washed, Polymer-Doped Sol-Gel-Derived Monoliths Prepared Using Co-Hydrolyzed Silanes**

| Sample | Day 1 | Day 10 | Day 23 | Day 34 | Day 60 | Day 74 |
|---|---|---|---|---|---|---|
| **TEOS** | | | | | | |
| Polymer Free | 510 | 515 | 516/434 | 512/432 | 514/425 | - |
| 5% PEG 400 | 516 | 513 | 508 | 506 | 502 | 497 |
| 10% PEG 400 | 514 | 511 | 508 | 505 | 501 | 498 |
| 5% PEG 600 | 516 | 514 | 510 | 508 | 501 | 498 |
| 10% PEG 600 | 511 | 507 | 504 | 501 | 498 | 496 |
| 5% PVA | 517 | 519 | 520 | 518 | 518 | 514 |
| 10% PVA | 514 | 517 | 517 | 517 | 515 | 514 |
| **5% MTES** | | | | | | |
| Polymer Free | 511 | 514 | 514/436 | 508/429 | 505/423 | - |
| 5% PEG 400 | 514 | 510 | 506 | 506 | 499 | 496 |
| 10% PEG 400 | 512 | 509 | 506 | 504 | 498 | 496 |
| 5% PEG 600 | 513 | 509 | 507 | 505 | 498 | 494 |
| 10% PEG 600 | 509 | 507 | 505 | 501 | 496 | 493 |
| 5% PVA | 517 | 516 | 516 | 513 | 506 | 506 |
| 10% PVA | 515 | 516 | 514 | 512 | 508 | 508 |
| **10% MTES** | | | | | | |
| Polymer Free | 510 | 510 | 509 | 508 | 508/424 | - |
| 5% PEG 400 | 508 | 508 | 505 | 502 | 494 | 491 |
| 10% PEG 400 | 510 | 508 | 505 | 504 | 496 | 492 |
| 5% PEG 600 | 511 | 508 | 504 | 503 | 494 | 491 |
| 10% PEG 600 | 509 | 506 | 502 | 499 | 491 | 487 |
| 5% PVA | 513 | 512 | 511 | 508 | 502 | 498 |
| 10% PVA | 514 | 513 | 511 | 509 | 505 | 506/420 |
| **1% DMDMS** | | | | | | |
| Polymer Free[a] | 511 | 514 | 514/434 | 512/431 | 504/429 | - |
| 5% PEG 400 | 517 | 512 | 509 | 507 | 503 | 502 |
| 10% PEG 400 | 513 | 511 | 509 | 506 | 504 | 502 |
| 5% PEG 600 | 516 | 513 | 510 | 508 | 502 | 501 |
| 10% PEG 600 | 512 | 508 | 506 | 504 | 499 | 496 |
| 5% PVA | 519 | 519 | 518 | 516 | 513 | 512 |
| 10% PVA | 513 | 516 | 517 | 517 | 514 | 511 |
| **5% DMDMS** | | | | | | |
| Polymer Free | 508 | 507 | 505 | 504 | 492 | - |
| 5% PEG 400 | 508 | 503 | 496 | 494 | 481 | 478 |
| 10% PEG 400 | 507 | 504 | 497 | 494 | 483 | 484 |
| 5% PEG 600 | 508 | 501 | 495 | 492 | 479 | 476 |
| 10% PEG 600 | 506 | 501 | 493 | 490 | 482 | 477 |
| 5% PVA | 509 | 504 | 493 | 497 | 489 | 487 |
| 10% PVA | 510 | 506 | 505 | 500 | 487 | 482 |

[a] Data from 2.5% DMDMS sample

addition of PEG or PVA to the materials resulted in a much narrower distribution of environments relative to samples that were prepared in the absence of polymer additives.

**Table 3.17. Full-Width-at-Half-Maximum Values for Prodan Entrapped in Materials Derived from TEOS and Doped with Polymer Additives, Aged 74 Days**

| Composition | Full-Width-at-Half-Maximum (nm) |
|---|---|
| **Washed** | |
| Pure TEOS | >119 (aggregate) |
| 5% PEG 400 | 78 |
| 10% PEG 400 | 79 |
| 5% PEG 600 | 79 |
| 10% PEG 600 | 83 |
| 5% PVA | 82 |
| 10% PVA | 82 |
| **Unwashed** | |
| Pure TEOS | 93 |
| 5% PEG 400 | 84 |
| 10% PEG 400 | 79 |
| 5% PEG 600 | 82 |
| 10% PEG 600 | 84 |
| 5% PVA | 84 |
| 10% PVA | 83 |

Upon comparing the emission maxima for prodan entrapped in neat TEOS and ORMOSIL-derived samples relative to polymer-doped samples, it was noted that polymer-doped samples did not exhibit significant emission intensity around 420 nm. The absence of significant intensity at 420 nm suggested that the probe did not form aggregates in the polymer-doped samples and instead existed in its monomeric form. The fact that the probe was predominantly present in its monomeric form suggested that the environment within the sol-gel-derived glass was less polar (relative to polymer-free materials) in the presence of polymer additives, since the matrix was able to solvate the monomeric form of the probe. The wavelength of the emission maximum of prodan in

samples prepared using PEG as an additive was also blue shifted relative to samples that were prepared in the absence of PEG. The emission maximum of prodan near day 60 (a time at which comparisons could be made between the two samples) in TEOS-derived, co-hydrolyzed, washed, polymer-doped samples was at 502 nm. In the polymer-free sample prepared under the same conditions, the emission maximum was at 514 nm with significant intensity at 425 nm due to the aggregated form of prodan. This difference suggested that the presence of the polymer imparted a degree of hydrophobicity to the resulting material since the emission maximum was blue shifted in the polymer-doped sample. The trend was also apparent for ORMOSIL-derived samples, regardless of the composition. Hence, the location of the emission maxima of prodan in polymer-doped samples and the absence of intensity at 420 nm for these samples support the conclusion that the addition of PEG results in materials that are more hydrophobic (relative to samples prepared without PEG). However, PVA did not exhibit the same trend. In fact, PVA-doped samples exhibited emission maxima that were very close to the values determined from polymer-free samples, indicating that PVA did not have a significant effect on the polarity of the internal environment of the materials.

### *3.2.3. Summary of Studies of ORMOSIL-Derived and Polymer-Doped Materials*

In summary, the separate hydrolysis of the silane precursors resulted in materials that were more transparent and slightly more resistant to cracking than samples prepared using silane precursors that were co-hydrolyzed. However, the results of fluorescence studies showed that better control over the polarity of sol-gel-derived materials was

observed by using organically modified silane precursors that were prepared by co-hydrolysis. The differences in spectral widths of both 7AI and prodan suggested that the internal environment of samples prepared using co-hydrolyzed silanes was more homogeneous than that of samples prepared using separately hydrolyzed silanes. The spectroscopic properties of the entrapped probes also suggested that washing the materials after gelation narrowed the distribution of environments. Although addition of ORMOSILs did provide some control over polarity, the range over which the internal polarity could be controlled was limited. The addition of excessive amounts of organically modified silanes caused undesirable changes in physical characteristics such as reduction in optical clarity, decreased hardness and poorer dehydration/rehydration stability, consistent with phase separation. It was found that the use of low concentrations of ORMOSILs resulted in materials that were optically clear and were somewhat resistant to cracking upon dehydration or rehydration.

The co-entrapment of polymer additives was another useful method for modifying the internal environment of sol-gel-derived materials. The addition of PEG to TEOS and ORMOSIL-derived samples offered enhanced material properties in terms of dehydration/rehydration stability and optical clarity. However, samples doped with PVA tended to be opaque and hence, not useful for optical measurements. The incorporation of PEG also led to materials that had a much narrower distribution of internal environments compared to undoped samples, and allowed good control of the internal polarity of the materials.

Allowing the materials to dry completely resulted in cracking upon rehydration, hence, slides should be only partially dried (i.e. 21 days) and then stored in a high humidity environment or in buffer solution to prevent further drying. Storage in a high moisture environment was also useful since it is required for samples doped with proteins, since proteins cannot withstand complete dehydration without loss of activity.

## 3.3. Investigation of Sol-Gel Entrapped Proteins: The Effect of ORMOSIL and Polymer Additive Content on Entrapped Protein Function

### *3.3.1. Salicylate Binding to Human Serum Albumin (HSA)*

#### 3.3.1.1. Solution vs. Encapsulated

On the basis of the results obtained from fluorescence studies and on the need to use co-hydrolysis methods for investigation of samples containing DMDMS, all samples used for protein entrapment studies were prepared using co-hydrolyzed silanes and were washed after gelation. The samples used for entrapment of human serum albumin (HSA) were those that exhibited desirable physical characteristics such as good dehydration/rehydration stability, and high optical transparency after 21 days of aging. Based on these criteria, samples composed of TEOS alone and those with organosilane contents up to 20.0% MTES, 10.0% PTMS and 5.0% DMDMS were used for entrapment of HSA.

Figure 3.6 shows the background-corrected and normalized fluorescence emission spectra obtained from native HSA in solution, HSA in solution that was denatured using guanidine hydrochloride, and HSA entrapped in the various ORMOSIL-derived glasses described above. In most cases, the emission spectra of the entrapped protein were similar to the spectrum of native HSA in solution, exhibiting only slight blue shifts and small increases in the spectral width as ORMOSIL content was increased. The emission maxima and full-width-at-half-maximum values for HSA entrapped in the various samples are provided in Table 3.18.

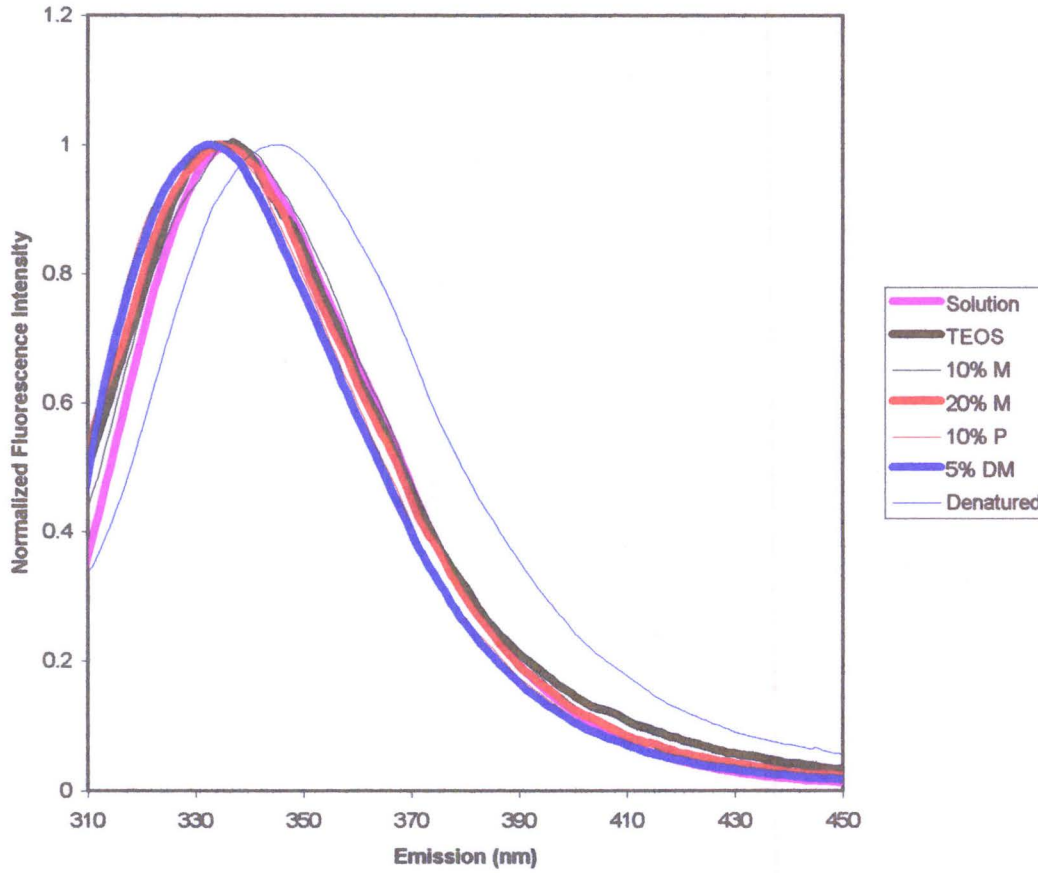


**Figure 3.6. Fluorescence Emission Spectra of HSA in Solution and Entrapped in Sol-Gel-Derived Materials Prepared by Co-Hydrolysis of Precursors**

**Table 3.18. Fluorescence Emission Maxima of HSA in Various Samples**

| Sample | Emission Maximum (nm) | Full-Width-at-Half-Maximum (nm) |
|---|---|---|
| Native HSA | 337 | 53 |
| Denatured HSA | 345 | 61 |
| TEOS | 337 | 56 |
| 10% MTES | 337 | 55 |
| 20% MTES | 334 | 57 |
| 10% PTMS | 334 | 55 |
| 5% DMDMS | 333 | 53 |

These results provided two important pieces of information. First, the sol-gel-derived hybrid materials were suitable for spectroscopic studies of entrapped proteins, even when using the ultraviolet portion of the spectrum for excitation, where light scattering is the highest. Second, based on the similarities between the spectra of native and entrapped HSA, HSA appeared to be entrapped with retention of its native conformation regardless of the ORMOSIL type or content.

In order to determine the effect of entrapment on the ligand binding ability of HSA, the entrapped protein was titrated with salicylate and the results were compared to those obtained for native and denatured HSA in solution. Since the samples were optically clear, binding could be monitored spectroscopically by quantitating the change in emission intensity of the Trp residue resulting from binding of salicylate. The results of these titrations are shown in Figure 3.7. The slopes of the binding curves, provided in Table 3.19, showed that most of the samples retained at least partial function relative to native HSA, indicating that the entrapment method did not completely alter the functional form of the protein.

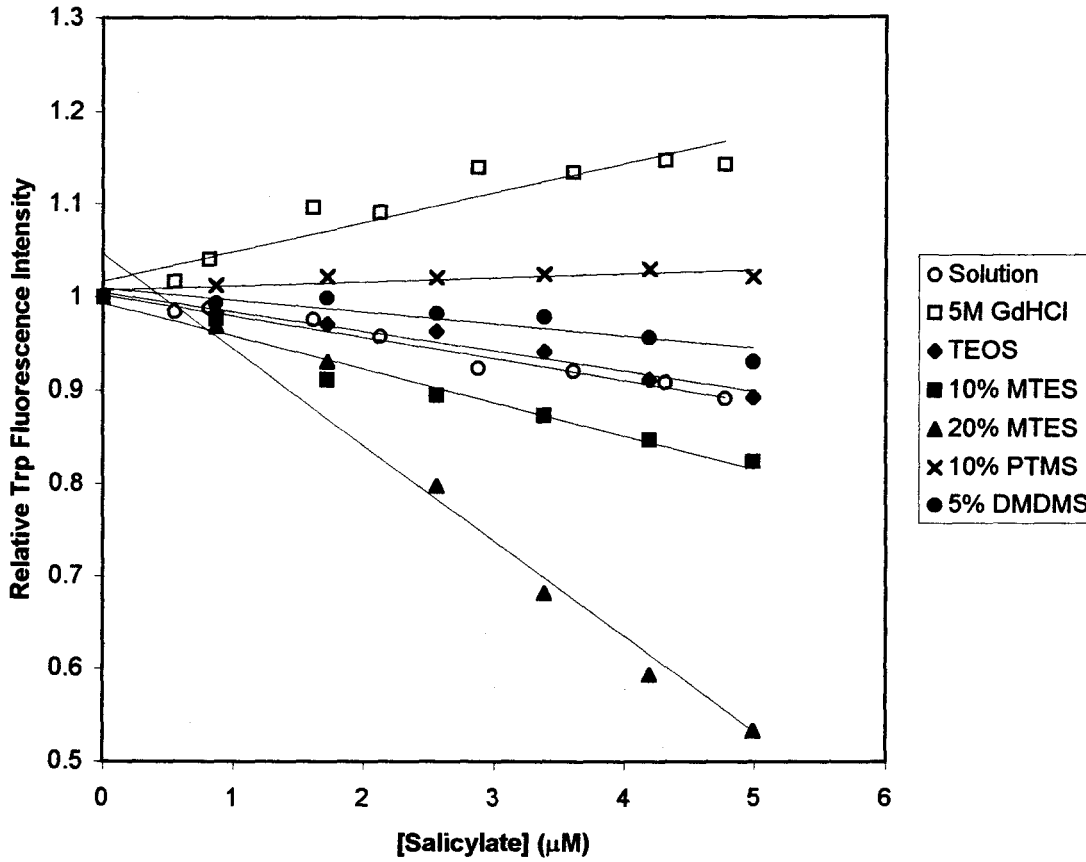


**Figure 3.7. Changes in HSA Fluorescence Intensity Resulting From Quenching by Salicylate Upon Binding**

**Table 3.19. Slopes of Salicylate Binding Curves for HSA in Various Samples**

| Sample | Slope of Binding Curve | $r^2$ |
|---|---|---|
| Native HSA | -0.023 | 0.970 |
| Denatured HSA | 0.028 | 0.882 |
| TEOS | -0.021 | 0.965 |
| 10.0% MTES | -0.036 | 0.961 |
| 20.0% MTES | -0.103 | 0.968 |
| 10.0% PTMS | 0.004 | 0.661 |
| 5.0% DMDMS | -0.013 | 0.841 |

HSA entrapped in TEOS-derived glasses showed similar sensitivity to salicylate binding as compared to the native protein in solution, suggesting that TEOS had no major effect on HSA function. The use of 5.0% DMDMS and especially 10.0% PTMS caused a reduction of protein function as shown by the more positive slopes relative to that for the solution sample. The reduced binding ability of HSA as well as the spectral blue shifts in 10.0% PTMS and 5.0% DMDMS environments were likely indicative of partial denaturation of the protein in the presence of longer or more alkyl chains. It is known that HSA is denatured by low levels of ethanol or propanol, so this result was not surprising. Entrapment of HSA into samples containing MTES resulted in enhancement of the sensitivity of HSA to salicylate as the level of MTES was increased, exhibiting an apparent binding affinity greater than that obtained in solution. Given the relatively hydrophobic nature of salicylate, the increased sensitivity to salicylate was likely the result of analyte preconcentration into the samples via a solid-phase extraction process. This preconcentration effect may be advantageous for biosensor development since the sample of interest can be selectively extracted into the matrix, providing improved sensor performance with minimization of interferences.

### *3.3.2. Lipase-Catalyzed Hydrolysis of Glyceryl Tributyrate*

#### 3.3.2.1. Effect of ORMOSIL Content and Type on Activity

Figure 3.8 shows the activity of entrapped lipase as a percentage of its activity in solution. Entrapment of lipase into TEOS-derived glasses resulted in almost complete loss of enzyme activity, in agreement with previous reports.[37] The presence of MTES resulted in improvement in protein function, which became greater as the level of MTES was increased, providing maximum activity values about three times higher than those obtained from TEOS-derived samples. The presence of PTMS provided no improvement in activity. This result suggests that PTMS may lead to enzyme denaturation, or may reduce the rate of diffusion of the analyte into or the product out of the matrix due to steric impediments from the larger alkyl chains. The presence of DMDMS also provided higher activity values, on the order of three times the activity values obtained from TEOS-derived samples. It was possible that the lower degree of cross-linking in DMDMS samples may have played a role in controlling the conformation of the enzyme, causing an enhancement in activity. Blank activity assays that were performed in the absence of lipase were typically 2-3 % of the solution activity values, and were subtracted from all assays (solution and entrapped) to account for non-enzymatic hydrolysis of the substrate.

The observation that the activity of lipase was higher in materials derived using ORMOSILs was not surprising. Previous reports[37] using sol-gel-derived powders have shown that the presence of high concentrations of organically modified silanes enhances

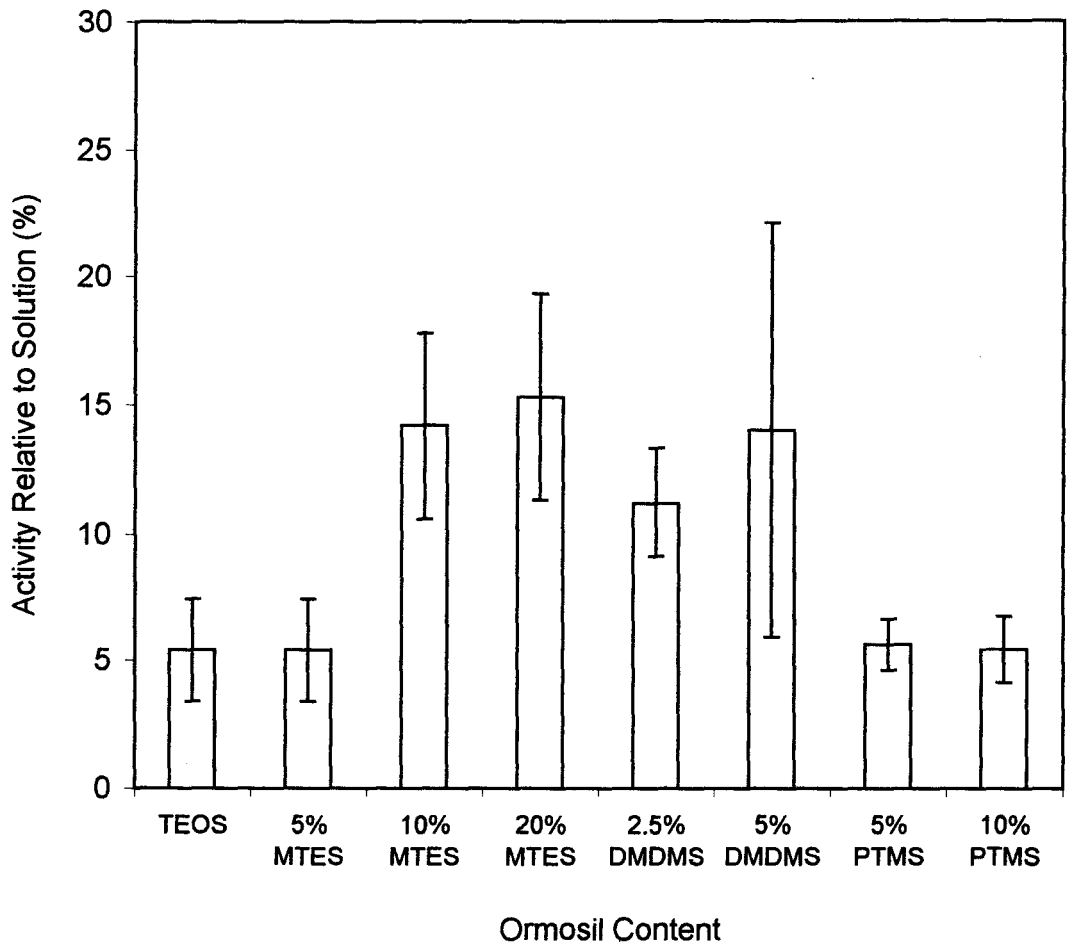


**Figure 3.8. Activity of Lipase Entrapped in TEOS and ORMOSIL-Derived Monoliths Relative to the Activity of Lipase in Solution**

the activity of lipase. Reetz[37,80] has suggested that the improved activity of entrapped may be due to the high dispersion of lipase molecules within in the gel matrix. However, the enhancement of activity in more hydrophobic media may also be due to the effect of increased interfacial activation, which is observed for many lipases present in water/organic two-phase systems. The enhanced activity results from conformational changes of the protein chain upon adhesion of the lipase to an organic/inorganic interface. It has been shown[81] that a hydrophobic α-helical lid within the structure of lipase is present over the active site and has the ability to move to associate with the interface of the organic and inorganic media, resulting in the exposure of the active site. In ORMOSIL-derived sol-gel materials, the presence of organic groups act as the hydrophobic portions whereas TEOS provides a polar, aqueous-like environment. Mixing lipase with the ORMOSIL-TEOS mixture causes the lid to swing open to adhere to the hydrophobic regions at the interface. Upon gelation, the lipase molecule may be immobilized in its active form and hence, the hydrolytic activity is enhanced relative to TEOS-derived samples, for which there is no driving force for exposure of the active site. Also, as shown in the previous section, the use of DMDMS was more likely to form phase separated materials, resulting in more interfacial area. This larger interfacial area may explain why lipase was somewhat more active in DMDMS-derived materials relative to samples prepared from MTES. The amount of PTMS used in the investigation may have been too low to provide the interfacial area required for enhanced lipase activity. However, materials prepared from PTMS in concentrations greater than 5.0 %

exhibited poor material properties. It is also possible that the longer chains denatured lipase, rendering it less active.

3.3.2.2. Effect of PVA and PEG Additives on Activity of Lipase Entrapped in Sol-Gel-Derived Slides

Further studies were done using polymer additives co-entrapped with lipase in sol-gel-derived slides. Based on the activity values from the lipase samples entrapped in ORMOSILs described above, certain ORMOSIL ratios were used chosen for co-entrapment of polymers. The ratios chosen were those that exhibited the highest activity, specifically, TEOS (for comparison purposes), 20.0% MTES and 5.0% DMDMS. The polymers used were PEG (molecular weights of 400 and 600) at concentrations of 5.0 and 10.0% (w/v in the buffer) and the samples were either washed or unwashed. PVA (molecular weight of 13 000 to 23 000) at a concentration of 10.0% (w/v) was also co-entrapped because previous reports[37] have shown that PVA has a beneficial effect on the activity of entrapped lipase.

The activity of lipase in solution containing varying levels of PVA is shown in Table 3.20. The activity of lipase in solution in the presence of PVA was significantly lower than that of free lipase in the absence of PVA. Lipase entrapped in TEOS or ORMOSIL-derived materials doped with 10.0% (w/v in the buffer) PVA also exhibited much lower activity relative to lipase entrapped without PVA. It is possible that the hydroxyl groups of PVA interacted with the protein in such a manner that the protein was in a non-active conformation, resulting in reduced activity in the presence of PVA. As a result of the

reduced activity of lipase in the presence of PVA, no further activity studies were performed using this additive.

**Table 3.20. Activity of Lipase in Solution and Entrapped in the Presence and Absence of 10% PVA**

| Sample | Activity Relative to Solution Without PVA (%) |
|---|---|
| Solution with PVA | 9.4±1.7 |
| TEOS without PVA | 4.4±1.6 |
| TEOS with PVA | 1.1±0.8 |
| 20% MTES without PVA | 3.2±1.6 |
| 20% MTES with PVA | 2.0±0.3 |
| 5% DMDMS without PVA | 14.0±8.1 |
| 5% DMDMS with PVA | 14.2±1.6 |

The effect of PEG on the activity of lipase was also investigated as a function of the molecular weight and concentration of PEG. The activity of lipase in solution in the presence of the various PEG additives is shown in Figure 3.9. It is apparent that PEG does not have a detrimental effect on the activity of lipase in solution, unlike PVA. This result in consistent with the known behaviour of PEG, which has been reported to act as an osmolyte to stabilize proteins.[82] Such compounds reduce the solubility of the peptide backbone relative to water and hence destabilize the unfolded state of a protein. Therefore, in the presence of osmolytes the protein remains folded in order to reduce the exposure of the backbone to the osmolyte solution. The osmotic effect of PEG is also more pronounced because the molecular weight of PEG used was much smaller than that of PVA. Since osmotic stabilization is dependent on the number of osmolyte molecules present, at equal concentrations (i.e. equal weight percentages), there were more molecules of PEG 400 or 600 than there were of 13 000 to 23 000 molecular weight PVA molecules available to stabilize lipase.

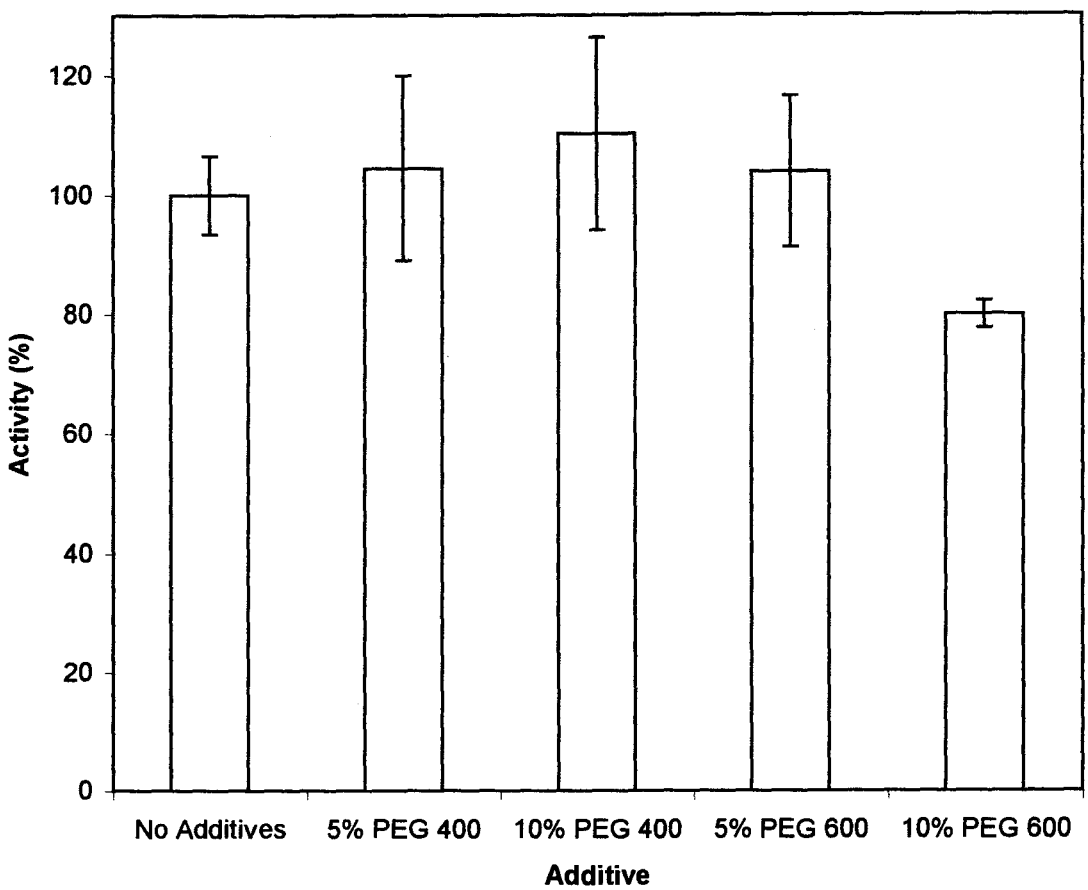


**Figure 3.9. Activity of Lipase in Solution in the Presence and Absence of PEG**

The activity values determined for sol-gel-derived samples made from TEOS, 20.0% MTES and 5.0% DMDMS are shown in Figures 3.10, 3.11 and 3.12, respectively. It was evident from these results that the co-entrapment of PEG with lipase had a significant impact on the activity of the entrapped lipase. The addition of PEG 600 at concentrations of 5.0 and 10.0% (w/v in the buffer) to unwashed TEOS-derived samples provided activity values as high as 40.0 to 50.0%, relative to solution. This activity was about ten times higher than the activity of lipase entrapped in TEOS in the absence of PEG. This was significant, since the maximum activity obtained using ORMOSILs without PEG was on the order of 15% when the sample was made of 5.0% DMDMS. This trend was also noted for samples made of 20.0% MTES and 5.0% DMDMS. However, the activity enhancements obtained from these samples were much smaller than those from TEOS-derived samples. It was expected that there may have been further enhancement of activity for ORMOSIL-derived samples in the presence of PEG owing to an additive effect of PEG and ORMOSIL content; however, this was not the case. Based on narrow full-width-at-half-maximum values for 7AI doped samples with PEG, a possible explanation for the reduction in activity is that PEG may have solubilized the organic portions of the ORMOSIL, resulting in reduced organic/inorganic interface content and hence the interfacial activation of lipase may not have occurred.

To aid in discriminating between osmolyte effects and indirect effects of PEG resulting from alterations of material properties, some of the materials were washed with fresh buffer to remove the entrapped PEG before aging. In almost all cases, washed samples exhibited significantly lower activity values as compared to unwashed samples.

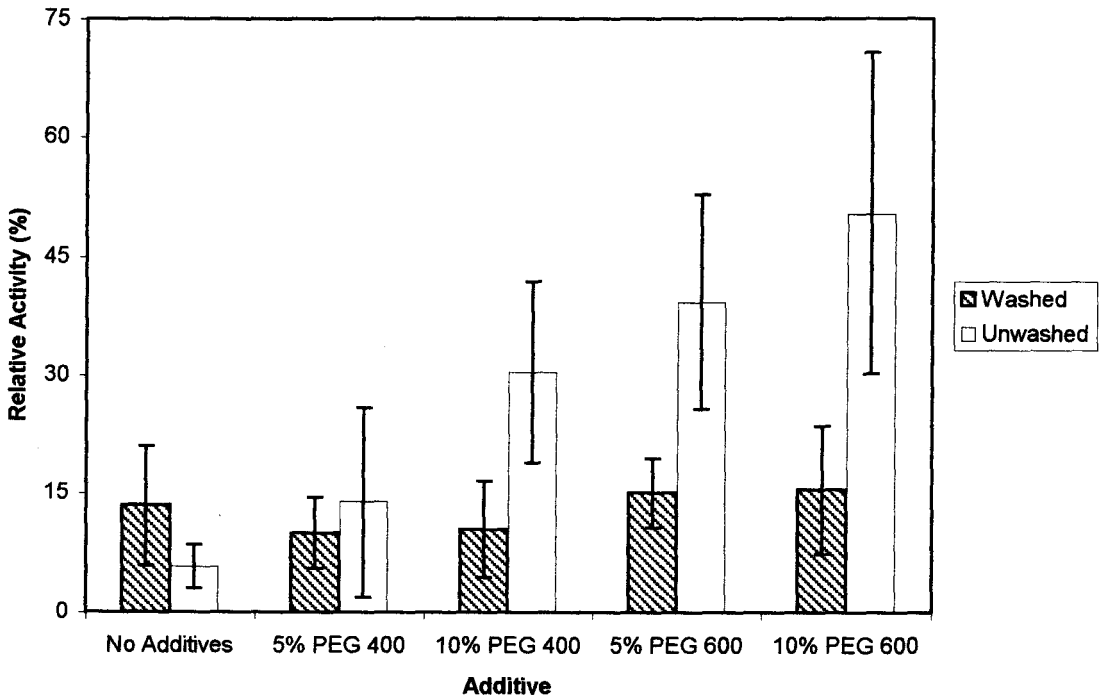


**Figure 3.10. Activity of Lipase Entrapped in TEOS-Derived Monoliths with Various Concentrations and Types of PEG**

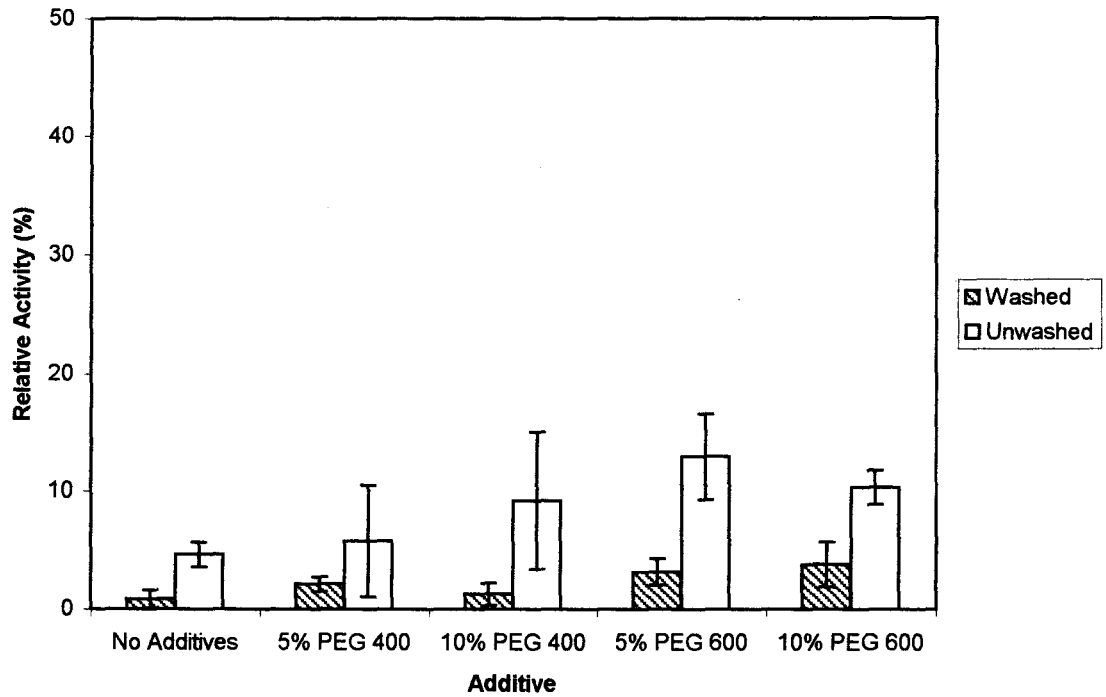


**Figure 3.11. Activity of Lipase Entrapped in 20% MTES-Derived Monoliths with Various Concentrations and Types of PEG**

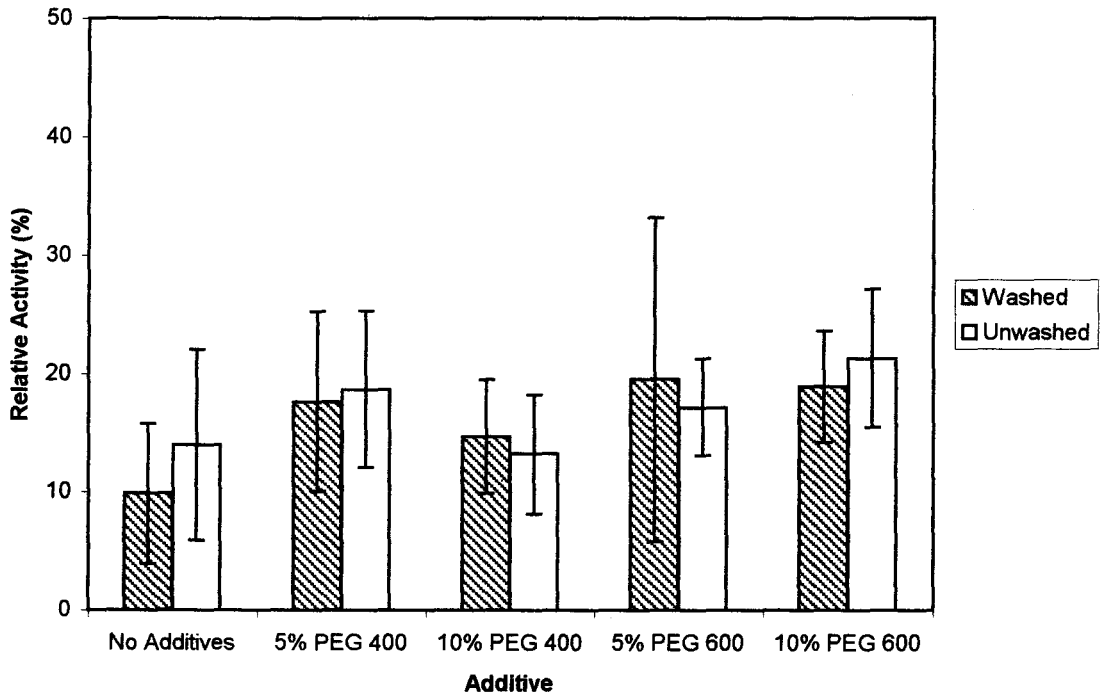


**Figure 3.12. Activity of Lipase Entrapped in 5% DMDMS-Derived Monoliths with Various Concentrations and Types of PEG**

The higher activity for unwashed samples suggested that PEG likely had a direct stabilizing effect on the entrapped lipase. It was possible that the osmotic effect of PEG protected lipase from denaturation and subsequent aggregation resulting from the ethanol encountered during entrapment.

One difficulty encountered in lipase assays was the significant amount of error associated with the lipase activity, as shown by the large error bars in Figures 3.8 to 3.12. The large errors may be due to uneven drying of the slides prior to performing activity assays, which may have caused some dissimilarity from one sample to the next in terms of slide thickness, pore size and water content. In the future, optimization of drying conditions should be investigated to ensure that drying conditions are as consistent as possible between samples. Some samples may also have been partially cracked during rehydration so the total surface area accessible to substrate during an assay may have been different, possibly leading to differences in the activity values obtained.

Overall, it was shown that the use of organically modified silanes as precursors for sol-gel processing and the incorporation of PEG allowed the preparation of functional protein-doped materials. In all cases, MTES and DMDMS provided some degree of improved protein function, while samples prepared with PTMS provided no enhancement of biomolecule function relative to samples prepared using only TEOS. The addition of polymer additives also provided a degree of improvement in the hydrolytic activity of lipase, with higher levels of PEG (but not PVA) providing improved enzyme activity.

It is important to note that in solution in the absence of polymer additives, there were no interfaces. Ideally, the activity of lipase should be lower in solution than in a

sol-gel-derived slide, due to the absence of the interfacial activation of lipase. However, this was not the case as activity values of entrapped lipase were less than 50% of those in solution, at best. This suggested that the activity of lipase was limited by the rate of diffusion of the substrate into, and fatty acid products out of the porous material. Also, the titrimetric method used for determination of lipase activity does not allow monitoring of the kinetics of the enzyme-catalyzed reaction since the progress of product formation could not be monitored with time.

## 3.4. Preparation and Characterization of Sol-Gel-Derived Thin Films for pH Sensing Applications

The results of the previous section demonstrated that it is possible to prepare optically clear hybrid organic/inorganic sol-gel-derived materials using processing conditions suitable for biomolecule entrapment, and that proteins could be entrapped into these materials with retention of at least a portion of their biological function.

Although the preparation of sol-gel-derived monoliths and slides was appropriate for spectroscopic characterization of the internal environment of the materials, there were some problems associated with the use of these formats for biomolecule immobilization. These problems included the relatively thick cross-section of the sol-gel-derived slides (0.2 cm) which leads to long response times, owing to slow diffusion of analytes in the pores of the materials.[74] In addition, such samples are fragile and are hard to mount, making spectroscopic measurements difficult to reproduce. For this reason, thin sol-gel-derived films were examined as an alternative format for sensor development.

### *3.4.1. Casting Parameters for Preparation of High-Quality Films*

Dipcasting is a well established method for preparing sol-gel-derived films,[60] however, the method used for dipcasting thin sol-gel-derived films in this research project was somewhat different from that used previously. Earlier methods used ethanol as a viscosity modifier and as a co-solvent for alkoxysilanes to aid in film formation. However, this method was not acceptable for entrapment of biomolecules since ethanol is

known to cause protein denaturation. Instead, the two-step method involving hydrolysis of the silane precursors and the addition of buffer to promote gelation for preparation of sol-gel-derived materials was applied for preparation of thin films, in order to make the processing conditions amenable to biomolecule entrapment.

Films were considered useful if they were resistant to cracking prior to and after immersion in aqueous solution and were visibly clear and homogeneous on the surface of the glass slide substrate. There were a variety of different factors that were investigated in preparation of useful sol-gel-derived thin films. These factors included silane hydrolysis conditions, film preparation temperature, buffer type and concentration, substrate withdrawal speed, substrate surface treatment prior to casting, ORMOSIL type and content and the presence of polymer additives. The sections below discuss the variables that were investigated in developing a simple protocol for preparation of dipcast sol-gel-derived thin films that was suitable for biomolecule entrapment.

3.4.1.1. Surface Pretreatment

Thin films were dipcast on glass microscope or quartz plates, which were cut to a size that could fit easily into a 1 $cm^2$ fluorimeter cuvette to allow spectroscopic characterization. Glass was used for immobilization of fluorescent probes and for preparation of lipase-doped thin films. Quartz slides were used for preparation of HSA-doped films, to allow excitation at 295 nm, which was not possible when glass slides were used owing to fluorescent impurities in the glass. Prior to use, the slides were cleaned to remove any surface adsorbed contaminants that may have interfered with film

formation or fluorescent contaminants that may have interfered with the fluorescence signals derived from solution or immobilized probe molecules. The slides were also washed to hydroxylate the surface in order to provide better adhesion of the silica films to the glass surface.

Three treatment methods were used for preparing glass slides for dipcasting: rinsing with concentrated HF solution (48% (w/v)), dilute HF solution (1% (w/v)) or 1.0 M NaOH. Samples treated with concentrated HF, became white and opaque due to extensive etching, even when treated for only a few seconds. These slides were not used for further studies. Cleaning slides with dilute HF solution for 30 seconds, followed by neutralization using 1.0 M NaOH, rinsing and drying gave samples that were clear. Simply rinsing the slides in a solution of 1.0 M NaOH for approximately 12 hours also gave clear slides. In both cases, thin films were cast onto the slides prepared using hydrolyzed TEOS and Tris buffer (10.0 mM) at pH 7.2. It was found that both the 1% HF-NaOH and the simple NaOH pretreatment methods resulted in films that were intact on the surface and crack-free. Given that there was no discernible benefit to the use of hydrofluoric acid for treatment of the slides and the extreme hazards associated with the use and handling of HF[83], all slides were prepared by rinsing with NaOH, followed by rinsing with water and air drying. The same method of slide pretreatment was applied to quartz slides with similar results.

3.4.1.2. Dependence on Buffer Salts

Another factor that was investigated for the development of a sol-gel-derived film formation protocol was the effect of type and concentration of buffer in the aqueous solution that was mixed with the hydrolyzed silane sol prior to gelation. The three buffer salts examined were potassium phosphate ($K_2HPO_4$), Trizma hydrochloride (Tris) and (N-[2-Hydroxyethyl]piperazine-N'-[2-ethane-sulfonic acid]) (HEPES). These salts were chosen because their $pK_a$ values are within the biological range of 6.5 to 8.5 necessary for biomolecules to retain optimal function and because they do not contain significant amounts of fluorescent impurities. It was found that dipcast thin films derived from TEOS cracked extensively upon drying when films were prepared with phosphate or HEPES buffer at 10.0 mM concentrations and at pH 7.2. The cracks formed were readily visible without the assistance of a microscope. These buffer salts also promoted the rapid gelation of the sol/buffer solution, making it difficult to cast more than three films from a single sol/buffer solution before the solution became too viscous to form intact films. Conversely, it was found that slides prepared using Tris buffer at a concentration of 10.0 mM, with 100.0 mM KCl and at pH 7.2 remained intact and exhibited no cracking, even when viewed under a microscope. It was also possible to prepare as many as 6 films from single casting solution, since the gelation time for Tris/sol solutions was on the order of an hour. This observation was consistent with gelation times for monoliths prepared using Tris buffer, as discussed previously. Thin films prepared using Tris/KCl buffer could be repeatedly placed in water and removed without any visible formation of cracks. It should be noted that the presence of KCl was necessary for formation of high-

quality films since films prepared in the absence of the salt were completely cracked, even when pH 7.2 Tris was used as the buffer solution to promote gelation.

3.4.1.3. Withdrawal Speed

Equation 5 from the introduction shows that the thickness of sol-gel-derived films prepared by dipcasting is dependent upon the speed at which the substrate is withdrawn from the casting solution. According to this relationship, higher casting speeds will produce thicker films. Upon testing a number of withdrawal speeds, a speed of 4 mm per minute was determined to be optimal for film formation. Speeds higher than 4 mm/minute resulted in less pristine films which often cracked or peeled from the surface, while speeds lower than 4 mm/min required too long a time to cast. A possible explanation for the cracking of rapidly cast films is that the drying rates of the films is too slow. During film formation ethanol and water are expelled from the film as it is cast, leading to thinning and drying. In thicker films, the rates of evaporation and drying in regions closer to the outer surface of the film may be faster than the rates of evaporation and drying in the inner regions of the film. The difference in drying rates may form hydrostatic pressure gradients within the film, causing fractures and peeling of the film off of the surface. This phenomenon has also been noted for slides and monoliths and documented as the dehydration/rehydration stability in previous sections.

3.4.1.4. Viscosity Effects

Another factor that has an effect on the thickness of sol-gel-derived films prepared by dipcasting is the viscosity of the solution being cast, with more viscous solutions resulting in thicker films, as shown in Equation 5. In this work, the factors that affected solution viscosity were casting temperature, casting time after solution mixing and the amount of hydrolysis of the sol before mixing with buffer. In cases where the buffer and hydrolyzed silane were held at 0°C prior to and during mixing and casting, thicker films were produced which cracked extensively. Mixing and casting at room temperature reduced the film thickness, and resulted in high-quality films.

Another factor that affected the apparent viscosity of the hydrolyzed TEOS solution was the length of time that the silane precursors were allowed to hydrolyze before use. TEOS solutions that had been stored for 7 days at -20°C, were more viscous than those that had been stored for a period of only 24 hours. This was likely due to the fact that extended hydrolysis time allowed the formation of larger colloidal particles within the sol, which made the solution more viscous. The films resulting from the use of 24-hour-old hydrolyzed TEOS tended to be more homogenous and crack resistant than those prepared from week-old TEOS, when all other casting parameters were similar. Hence, for film formation, the silane precursor used was mixed, sonicated and stored for 24 hours at -20°C prior to film casting. This method of preparation allowed multiple films to be cast within approximately 40 minutes, after which time, the solution became too viscous to prepare intact films.

3.4.1.5. Drying and Aging Conditions

The conditions that were employed for drying the films were varied in order to determine the effect of drying conditions on film stability. Tris-derived films prepared using TEOS as the silane precursor were dried and stored in sealed glass vials that were either completely dry or that had 100 μL of water at the bottom to provide a high-humidity environment. It was found that films stored in a dry environment overnight remained crack-free and resistant to cracking upon immersion in water. However, films stored in a high-humidity environment overnight exhibited extensive cracking. Therefore, dry aging was used for all films studied.

3.4.1.6. ORMOSIL and Polymer Content for Production of Useful Films

The methods described in the previous section for formation of thin sol-gel-derived films were tested using only TEOS as the silane precursor. However, given the beneficial effects of ORMOSILs and polymer additives on entrapped proteins, it was desirable to attempt to prepare sol-gel-derived thin films using organically modified silane precursors with or without polymer additives.

The organically modified silane precursors used for preparation of thin films were similar to those that provided enhanced activity for entrapped lipase. Specifically, the ORMOSIL ratios used were 5.0 and 10.0% (v/v) MTES and 1.0 and 5.0% (v/v) DMDMS. All of the films prepared using organically modified silane precursors and prepared in an identical manner to TEOS-derived films were completely crack-free, transparent and did not crack upon dehydration or rehydration, without exception. The

fact that the films produced were of exceptionally high quality was an encouraging indication that it would be possible to entrap proteins in thin films derived from ORMOSIL precursors. The results of assays using lipase entrapped in ORMOSIL-derived thin films are discussed later.

Thin films could also be prepared with entrapped polymers. However, the nature of the polymer was important for obtaining high-quality films. Thin film prepared using TEOS with PVA (molecular weight of 13 000 to 23 000) at concentrations of 5.0 and 10.0 % (w/v) resulted in thick films that were extensively cracked upon drying, even under optimized casting conditions. This cracking was likely due to the fact that the buffer solutions used for preparation of the sol-gel-derived film casting solutions were highly viscous in the presence of PVA at these concentrations. On the other hand, PEG (molecular weights of 400 or 600) doped TEOS-derived films were generally crack-free and transparent, provided that the PEG concentration was 3.0% (w/v in the buffer) or less. Above 3.0% PEG, the films tended to be cracked at the bottom edge of the cast substrate, likely due to the slow drying of the thicker film in this region. Incorporation of 1.0 to 3.0 % (w/v in the buffer) PEG into thin films derived using 5.0 and 10.0% (v/v) MTES and 1.0 and 5.0% (v/v) DMDMS also resulted in crack-free films with good optical clarity.

### *3.4.2. Entrapment of pH-Sensitive Fluorescent Probes*

Once durable films were produced, the films were used for entrapment of pH-sensitive fluorescent probes to investigate their potential for sensor applications. The

fluorescent probes chosen for this study were fluorescein and SNARF-1. Both probes were used in both their free form and when conjugated to a high molecular weight dextran backbone. The latter species were used to avoid leaching of the entrapped probe from within the material, since small molecules such as SNARF-1 or fluorescein (with molecular weights of 453.45 g/mol and 332.3 g/mol, respectively) can diffuse through the pores of the matrix, which could lead to loss of material with time.[48,49] Dextran-fluorescein and dextran-SNARF-1 are both commercially available and hence were used for testing the pH sensitivity of the probes entrapped in sol-gel-derived thin films.

The leachability of the probes was investigated by entrapping SNARF-1, dextran-SNARF-1, fluorescein and dextran-fluorescein separately in TEOS-derived thin films cast on glass slides. The films were aged for 12 or 24 hours and were then allowed to soak in 3.0 mL of pH 9.0 PBS overnight and the emission spectra of the solutions were collected in the absence of the film. The emission spectra of the solutions containing the fluorescein and dextran-fluorescein and SNARF-1 and dextran-SNARF-1 films are shown in Figures 3.13 and 3.14. It was found that SNARF-1, fluorescein and dextran-fluorescein had leached from the film after soaking for 12 hours. On the other hand, SNARF-1-labeled dextran did not leach after 12 hours of aging. Dextran-fluorescein films that had been aged for 24 hours showed no leaching, suggesting that the film structure may still be evolving after 12 hours. Hence, all films were aged for 24 hours for subsequent studies.

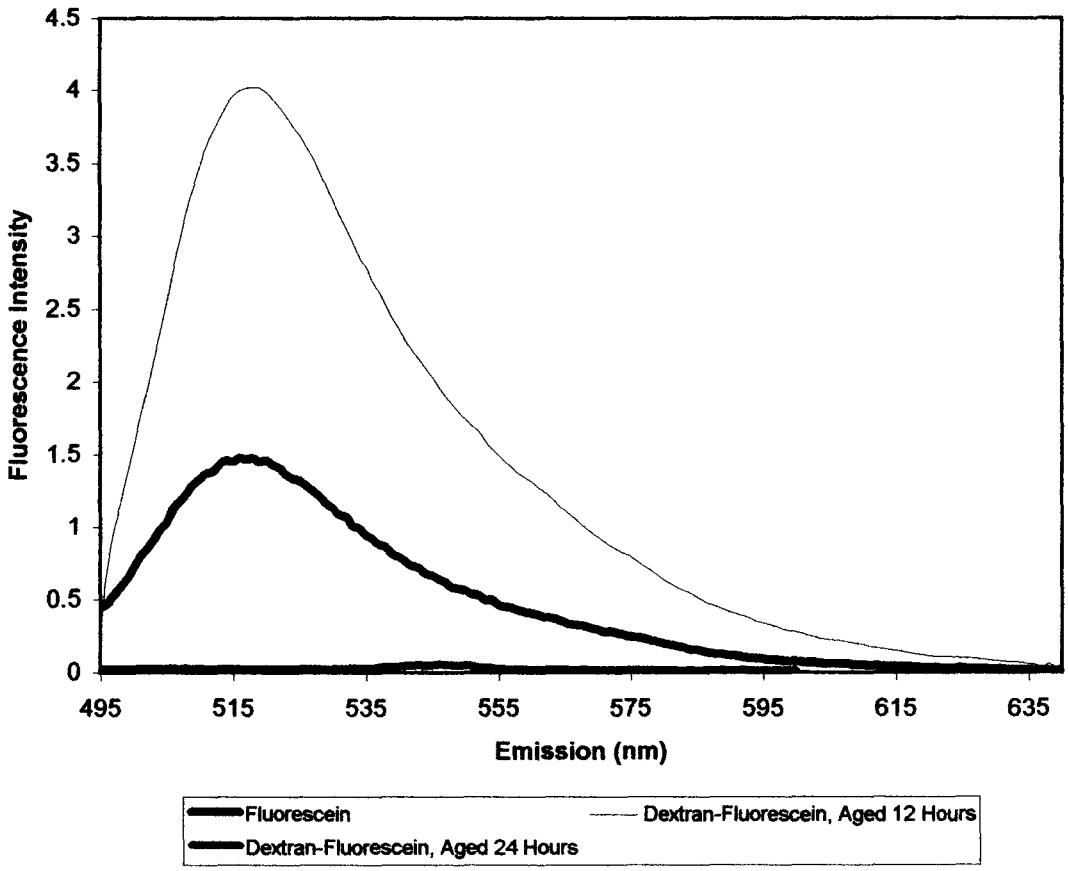


**Figure 3.13. Emission Spectra of Storage Solutions Used for Leaching of Fluorescein and Dextran-Fluorescein**

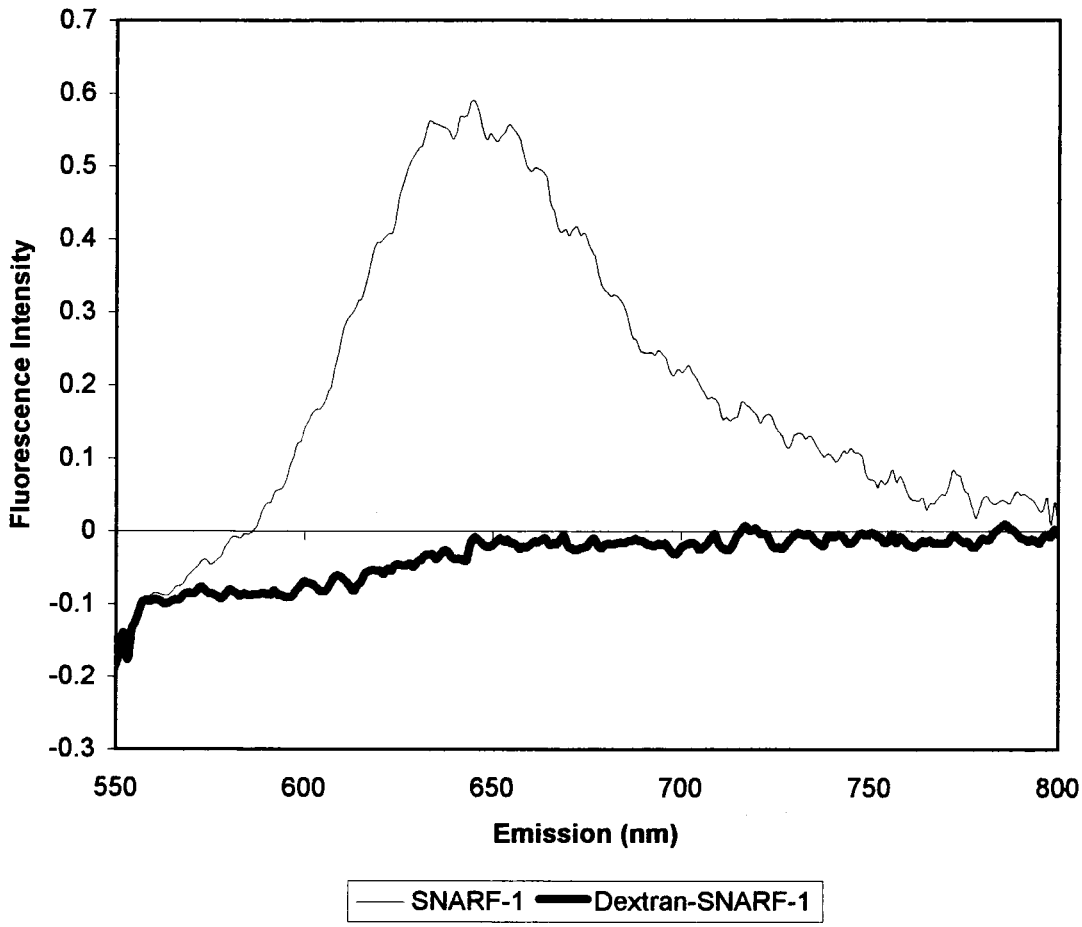


**Figure 3.14. Emission Spectra of Storage Solutions Used for Leaching of SNARF-1 and Dextran-SNARF-1**

3.4.2.1. pH Response of Fluorescein and SNARF-1 in Solution and Immobilized in Sol-Gel-Derived Films

To determine the effect of pH on the emission of fluorescein, HCl was added to the solution containing a dextran-fluorescein-doped film. Figure 3.15 shows the emission spectra of dextran-fluorescein entrapped in a TEOS-derived film aged for 24 hours and placed in a solution of pH 7.2, 10.0 mM Tris buffer as a function of added HCl (0.100 M in 5 μL aliquots). The figure shows that the intensity of emission of dextran-fluorescein decreased with each 5 μL aliquot of acid (i.e. shift to lower pH). However, after the addition of an amount of NaOH equivalent to the total amount HCl added (i.e. 30 μL of 0.100 M), the intensity of dextran-fluorescein emission returned to only 71.0% of its original intensity. Figure 3.16 shows the emission intensity of dextran-fluorescein at 520 nm as a function of time. Sequential additions of acid and base (details in figure) resulted in an initial drop in the intensity of dextran-fluorescein, followed by an increase in intensity to only 88.9 % of its initial intensity. This reduction in intensity may have been due to photodegradation of the dextran-fluorescein after continuous exposure to the excitation radiation. The negative slopes on the low intensity base lines support this suggestion. Photobleaching of a fluorescent probe used for sensing applications is undesirable since the signal from the sensor may not remain stable over time, shifting the calibration and degrading the performance of the sensor.

Given the poor results for dextran-fluorescein, dextran-SNARF-1 was investigated as an alternate pH sensitive probe, since the signal derived from the probe is ratiometric.

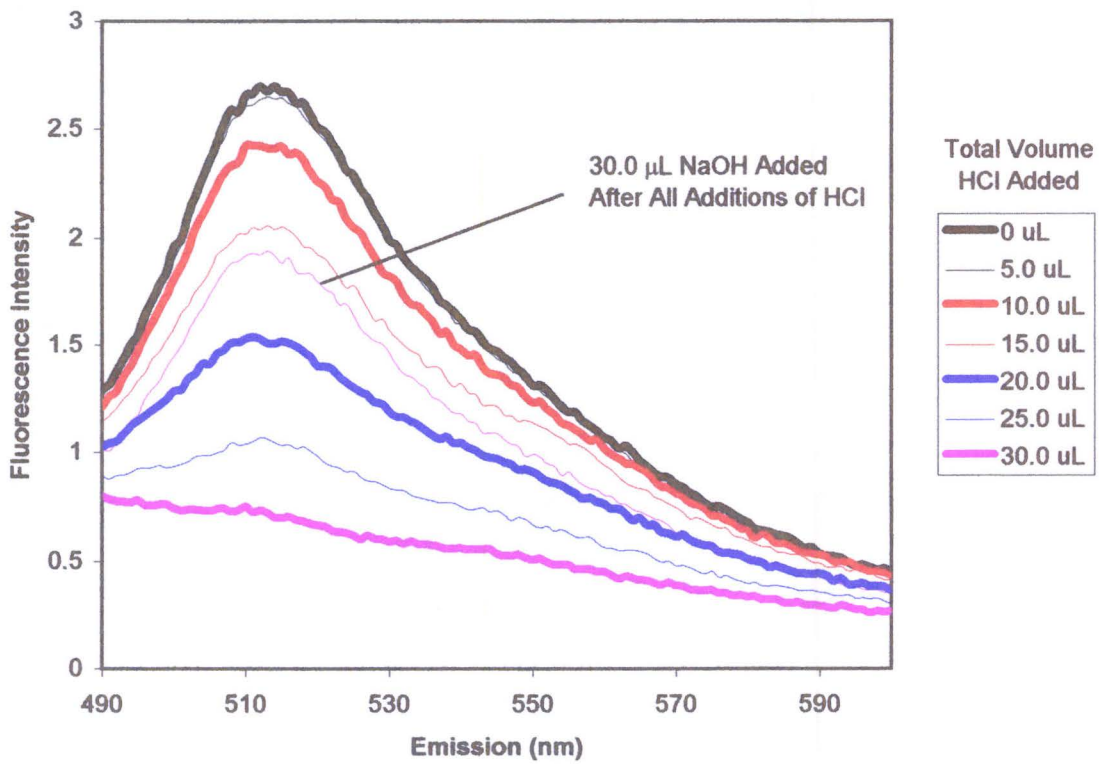


**Figure 3.15. Emission Spectra of Fluorescein Entrapped in a TEOS-Derived Film (Each Spectrum Corresponds to the Addition of 5 μL of 0.100 M HCl to 2.0 mL of pH 7.2 PBS Containing the Dextran-Fluorescein-Doped Film)**

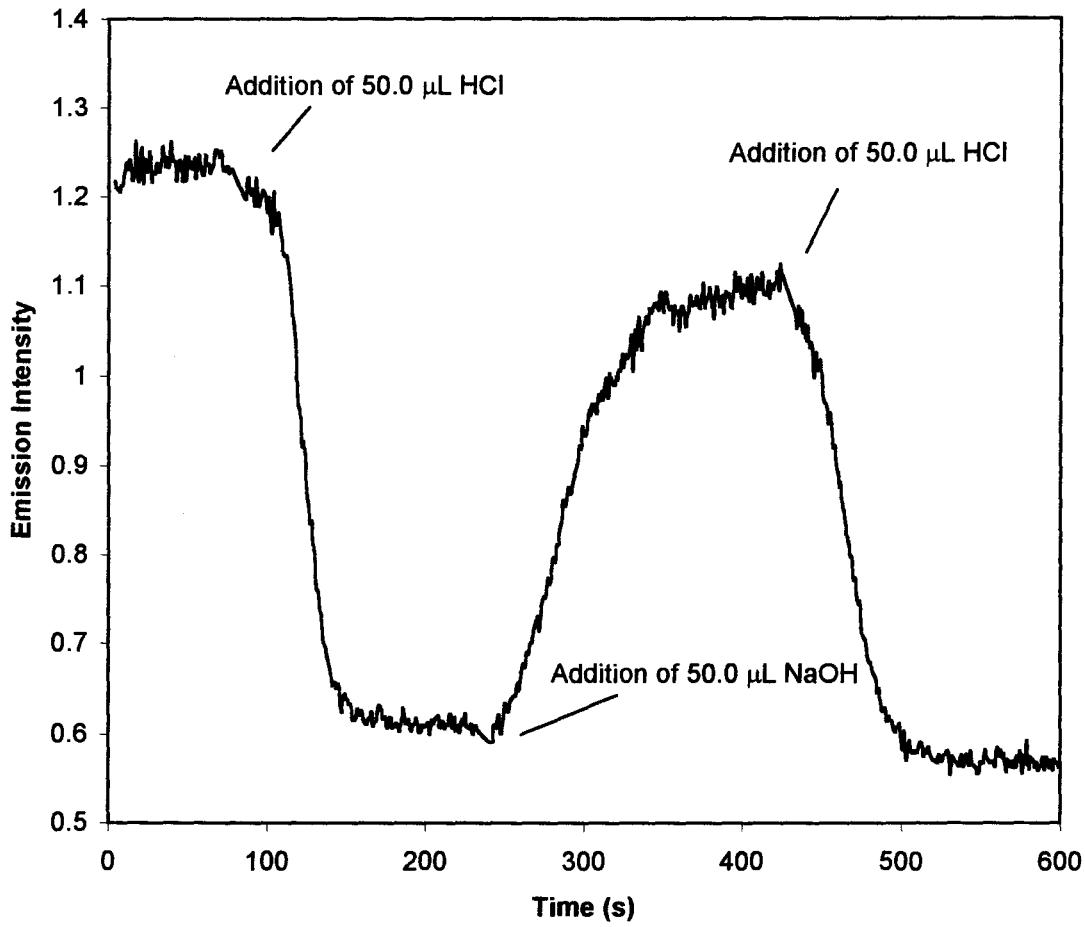


**Figure 3.16. Response of Fluorescein in Real Time as a Function of Added Acid and Base**

The use of a ratiometric probe prevents loss of signal with time due to photodegradation since the signal derived from the probe is not dependent on the concentration of the probe, but rather a ratio of intensities from two different forms of the probe, which ideally should photobleach at the same rate.

The emission spectra of dextran-SNARF-1 in solution at various pH values excited at 488 nm are shown in Figure 3.17. The emission at 640 nm corresponds to the basic form of the probe while the emission at 588 nm corresponds to the acidic form of the probe. The ratio of intensities at 588 nm and 640 nm (i.e. $I_{588}/I_{640}$) changes as a function of pH as shown in Figure 3.18. The fluorescence-based response derived from dextran-SNARF-1 is similar to any other pH indicator, appearing as a standard acid-base titration curve with its $pK_a$ near 7.0. It was possible to use other excitation wavelengths for dextran-SNARF-1. However, the pH sensitivity of dextran-SNARF-1 was dependent on the excitation wavelength used. As seen in Figure 3.19, excitation at 531 nm provided emission spectra with the highest intensity and best signal-to-noise ratio. This was important in the context of the use of dextran-SNARF-1 for thin films since the concentration of the probe in a thin film is quite low. In addition, the change in emission ratio was high for this excitation wavelength, making it sensitive to pH shifts. Hence, all films were excited at 531 nm in subsequent studies.

One advantage to the use of a ratiometric pH indicator is the ability to monitor the emission of both forms of the probe simultaneously, using a single excitation wavelength. This was possible using a fluorimeter with a T-format optical layout such as the SLM 8100, used in this research project. It should be noted that it is also possible to construct

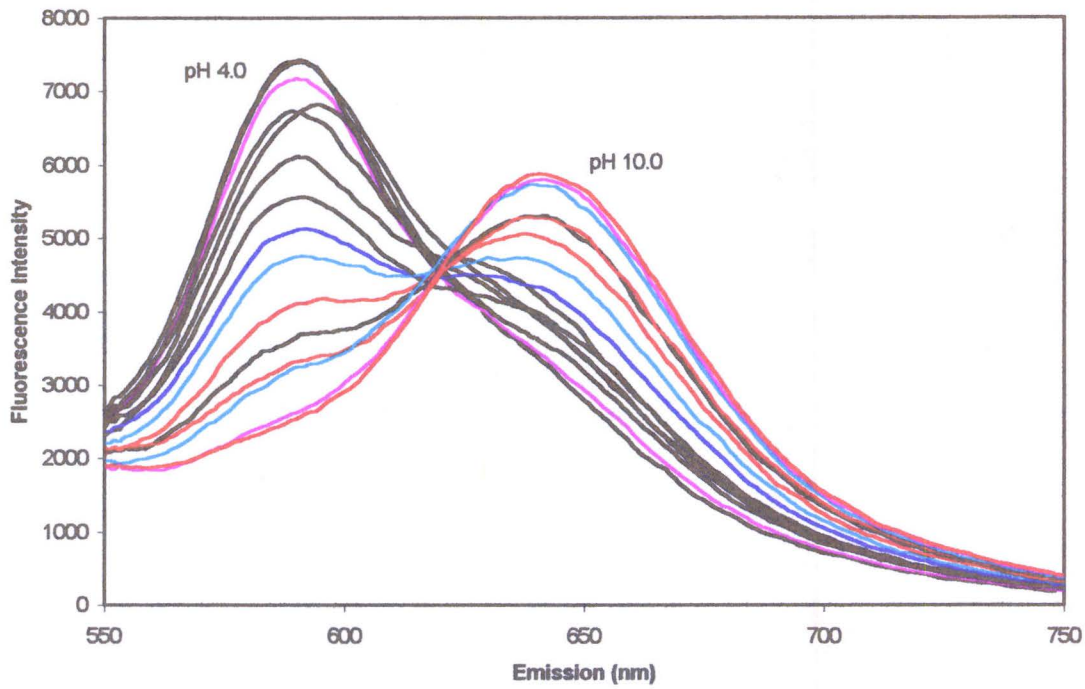


**Figure 3.17. Fluorescence Emission Spectra of Dextran-SNARF-1 (Excited at 488 nm) in Solution as a Function of pH**

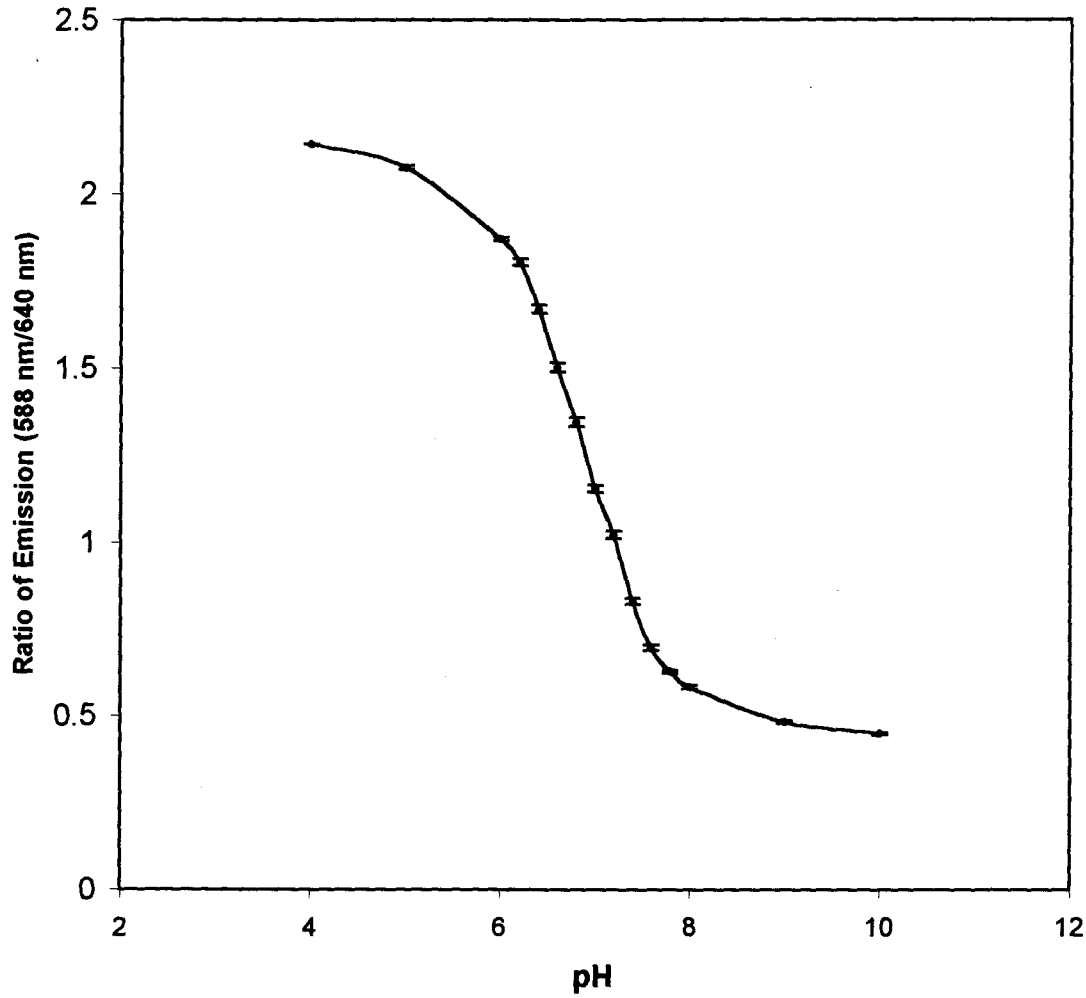


**Figure 3.18. pH Response of Dextran-SNARF-1 in Solution**

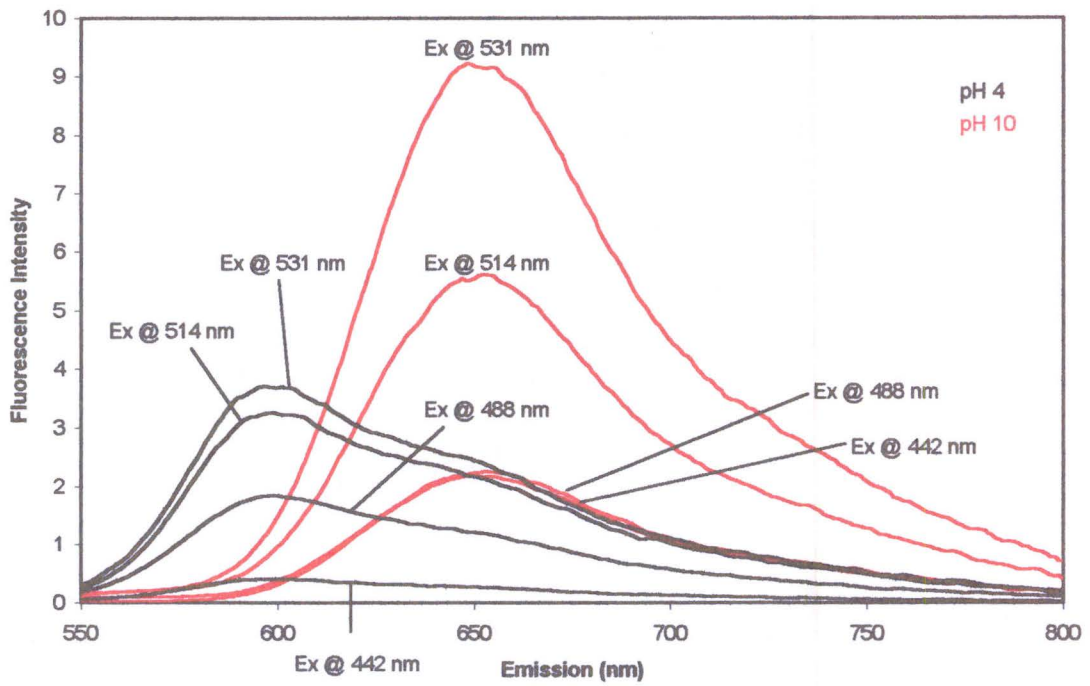


**Figure 3.19. Emission Spectra of Dextran-SNARF-1 Excited at Different Wavelengths**

a simple instrument with light emitting diodes and filters to do this measurement. Figure 3.20 shows the pH response of SNARF-1 in solution in real time, while monitoring the ratio of signals from the left (588 nm) and right (640 nm) monochromators simultaneously. The ratio of intensity increases with reduction in pH due to the addition of acid and a decrease in the ratio with increased pH due to the addition of base. This figure shows that by simultaneously monitoring the emission of the two forms of SNARF, it was possible to detect changes in pH quickly, and reproducibly. The figure also shows that the pH response is fully reversible, sensitive to small changes in pH and immune to any changes in emission intensity due to photodegradation of the probe.

The next stage of investigation of the pH response of SNARF-1 involved the entrapment of the probe in sol-gel-derived thin films. The dextran-SNARF-1 was incorporated into TEOS-derived films, aged in a sealed vial for 24 hours and suspended in a solution of pH 9.0 PBS (1.0 mM with 100.0 mM KCl). The slide was oriented as shown in Figure 2.1 with the right emission monochromator set at 588 nm and the left emission monochromator set at 640 nm. The ratio of emission was then monitored as a function of time and acid and base were added to the solution containing the film. The response of the ratio with additions of acid and base are shown in Figure 3.21. It is readily apparent that there was a much smaller change in the ratio of emission of dextran-SNARF-1 entrapped in the film relative to solution.

The poor response of thin film immobilized dextran-SNARF-1 indicated ratiometric detection of changes in pH by the simultaneous monitoring of the two emission wavelength may be difficult due to scattering artifacts in the channel that had the

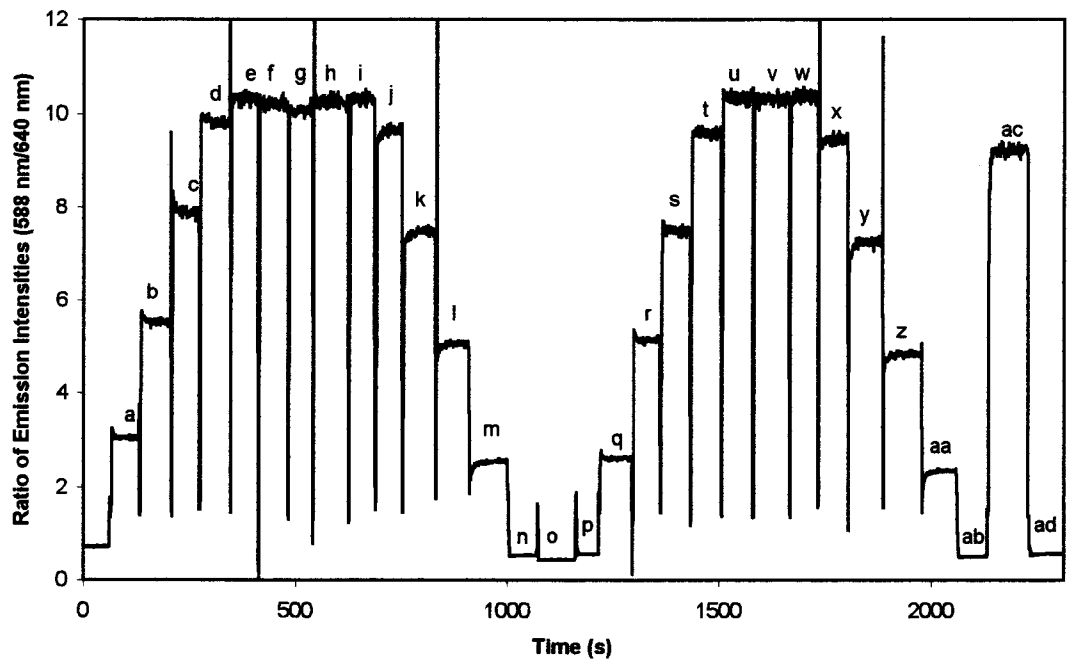


**Figure 3.20. Reversible pH Response of Dextran-SNARF-1 in Solution in Real Time as a Function of Added Acid and Base (Excitation at 531 nm). Additions (Initial Volume was 2.0 mL): 5 μL 0.100 M HCl (a-g), 5 μL 0.100 M NaOH (h-o), 5 μL 0.100 M HCl (p-v), 5 μL 0.100 M NaOH (w-ab), 20 μL 0.100 M HCl (ac), 20 μL 0.100 M NaOH (ad)**

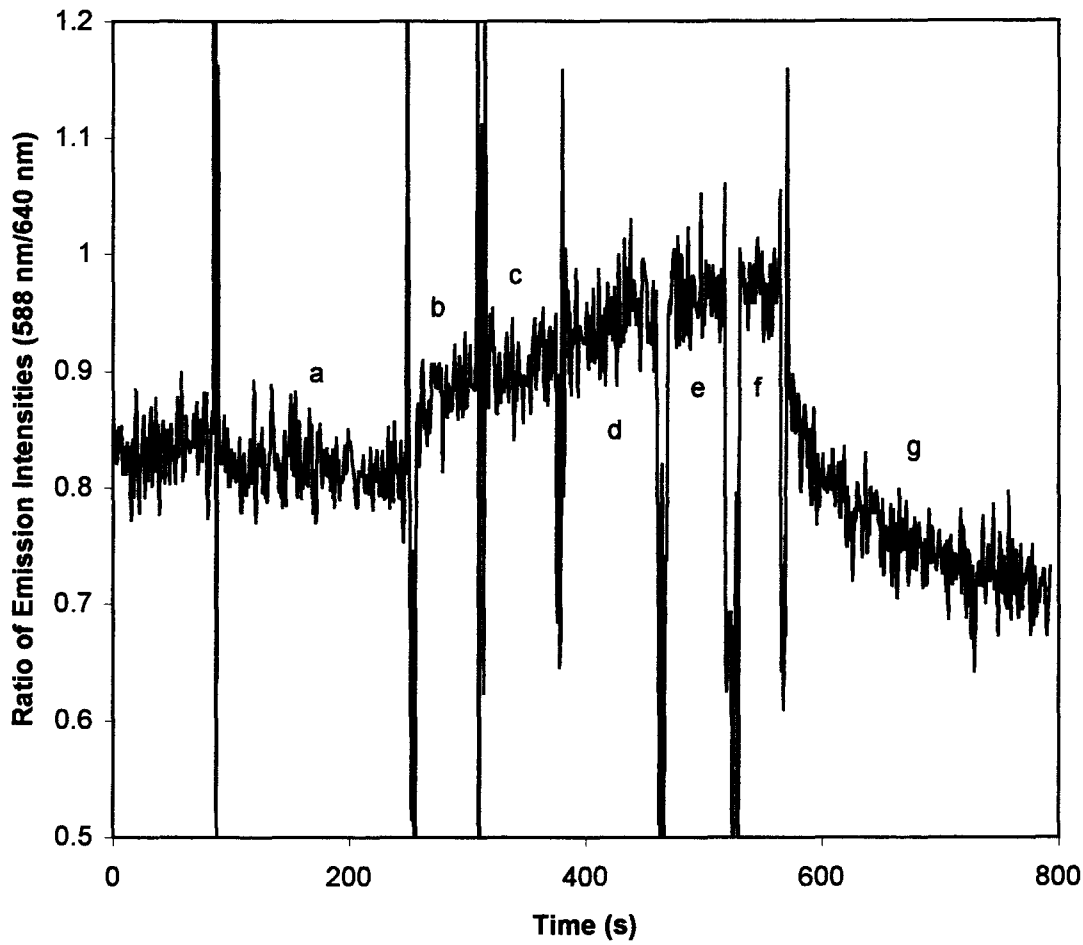


**Figure 3.21. pH Response of Dextran-SNARF-1 Entrapped in a TEOS-Derived Thin Film Using Simultaneous Detection of Emission at 588 nm and 640 nm (Excitation at 531 nm). Additions: 10 μL 0.100 M HCl (a-b), 50 μL 0.100 M HCl (c), 100 μL 0.100 M HCl (d), 100 μL 0.100 M NaOH (e-g)**

excitation intensity reflected directly into it (i.e. emission right, as in Figure 2.1). Given this problem, instead of simultaneously monitoring the ratio of emission intensities of dextran-SNARF-1, the ratio of emission of the probe was determined from emission spectra collected after each addition of acid or base, using only a single emission channel. Figure 3.22 shows the ratio of emission (588 nm/640 nm) of dextran-SNARF-1 as determined by integrating a 10 nm window in the spectra, centered at 588 and 640 nm. The figure shows that the addition of acid caused the expected increase in the ratio of emission intensities, while addition of base caused decreases in the ratio. The ratio of emission signals was also fully reversible.

In summary, a protocol for preparation of thin sol-gel-derived films that was amenable to entrapment of biomolecules was developed. The method of choice for preparation of substrate for casting of thin films involved the washing of the cut glass slides in 1.0 M NaOH overnight. TEOS or ORMOSIL-derived silane precursors were prepared by sonication until a visibly homogeneous solution resulted. The sonicated solution was then stored at -20°C for 24 hours, mixed with Tris buffer solution at a pH of 7.2 and a concentration of 10.0 mM in the presence of 100.0 mM KCl at room temperature and cast at 4 mm per minute. After casting, samples were air-dried and stored dry in sealed containers for 24 hours, which prevented cracking of the films upon dehydration and rehydration. Using this protocol, it was possible to prepare high quality films using organically modified silanes in conjunction with PEG at a maximum concentration 3.0% (w/v).

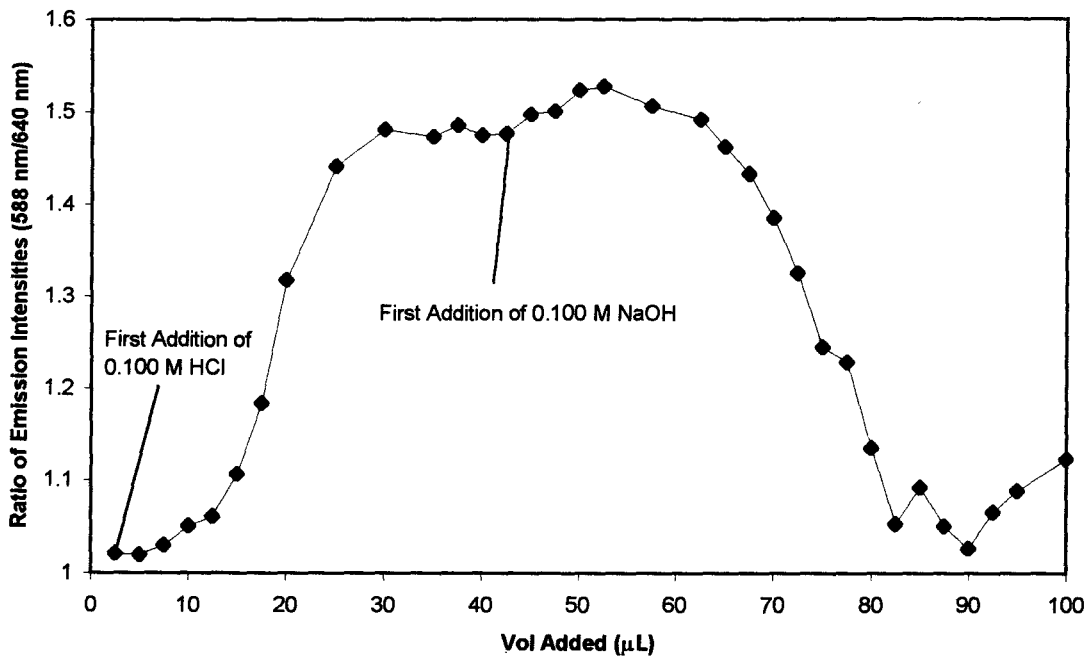


**Figure 3.22. pH Response of Dextran-SNARF-1 Entrapped in a TEOS-Derived Thin Film Determined from Emission Spectra**

Spectroscopic studies with pH-sensitive probes in solution and entrapped in the thin sol-gel-derived films showed that it was possible to detect changes in pH in real time with full reversibility. The poor response of the immobilized SNARF-1-dextran entrapped in a thin film when emission from both forms of the probe was monitored simultaneously was initially discouraging. However, it was shown that the poor response was not due to insensitivity of the entrapped probe to changes in pH, but rather was due to problems with scattering resulting from the orientation of the film-coated slide within the optical path of the fluorimeter.

## 3.5. Biosensing Using Protein-Doped Sol-Gel-Derived Films

The natural extension of the results of probe entrapment described in the previous section was the entrapment of biomolecules in thin sol-gel-derived films dipcast onto an optically clear surface. This was demonstrated using HSA entrapped in TEOS-derived thin films and lipase entrapped in TEOS and ORMOSIL-derived films, with and without added PEG.

### *3.5.1. Thin-Film HSA-Salicylate Binding Assays*

In an effort to characterize the ligand binding ability of HSA entrapped in thin films, the protein was entrapped in TEOS-derived films on quartz slides at a concentration of 66.0 ± 1.3 μM in the buffer. It was found that the use of solutions of HSA with concentrations of 10.5 ± 0.2 μM or 25.0 ± 0.5 μM were not concentrated enough to provide an adequate fluorescence signal. The thin film coated quartz slide was suspended from the top of a cuvette containing buffer and was titrated with salicylate. The emission spectrum of HSA entrapped in the TEOS-derived film is shown in Figure 3.23. The results of the salicylate titration are shown in Figure 3.24.

The slope of the linear regression line through the points was –0.093 ($r^2$ = 0.654), indicating that detection of salicylate was 2.5 times more sensitive in thin films as compared to HSA entrapped in TEOS-derived slides and native HSA in solution (-0.021 and –0.023, respectively). It is possible that a faster response time in films (~5 minutes),

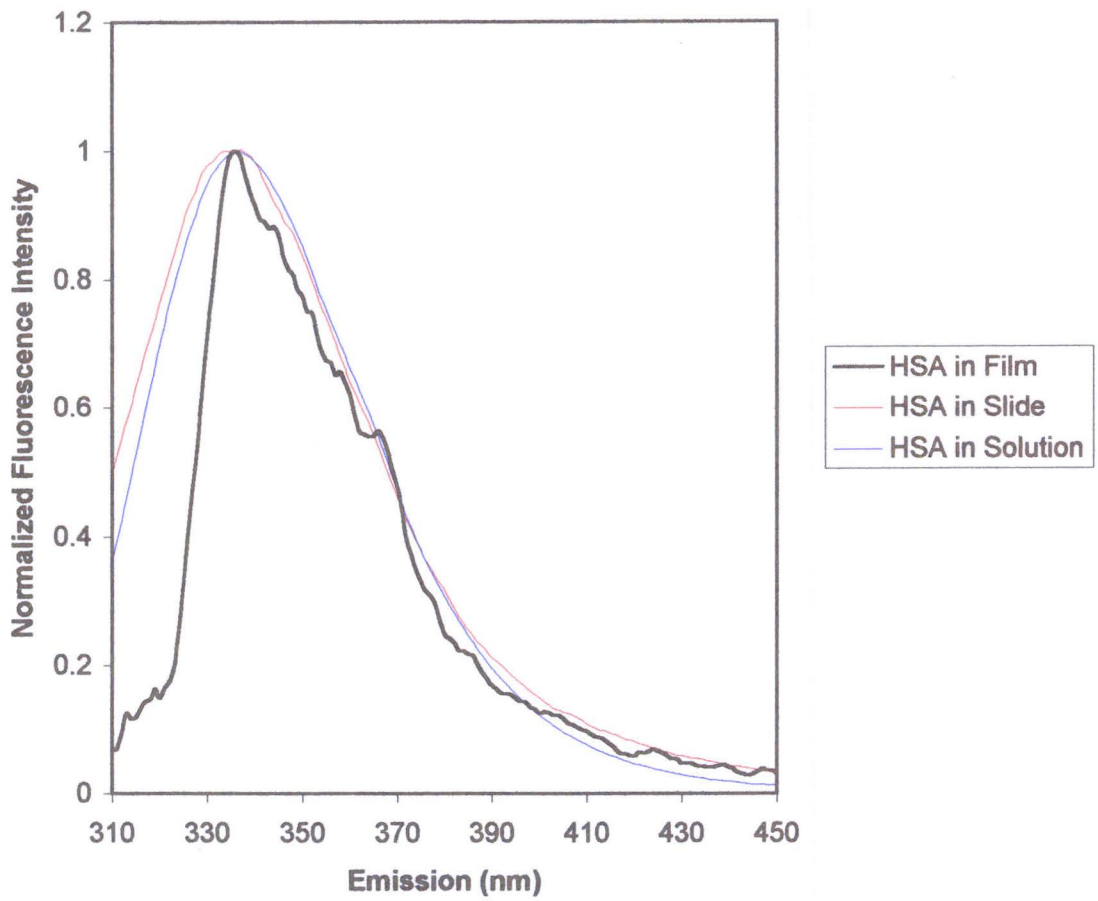


**Figure 3.23. Emission Spectra of Native HSA in Solution and Entrapped in TEOS-Derived Slides and Thin Films**

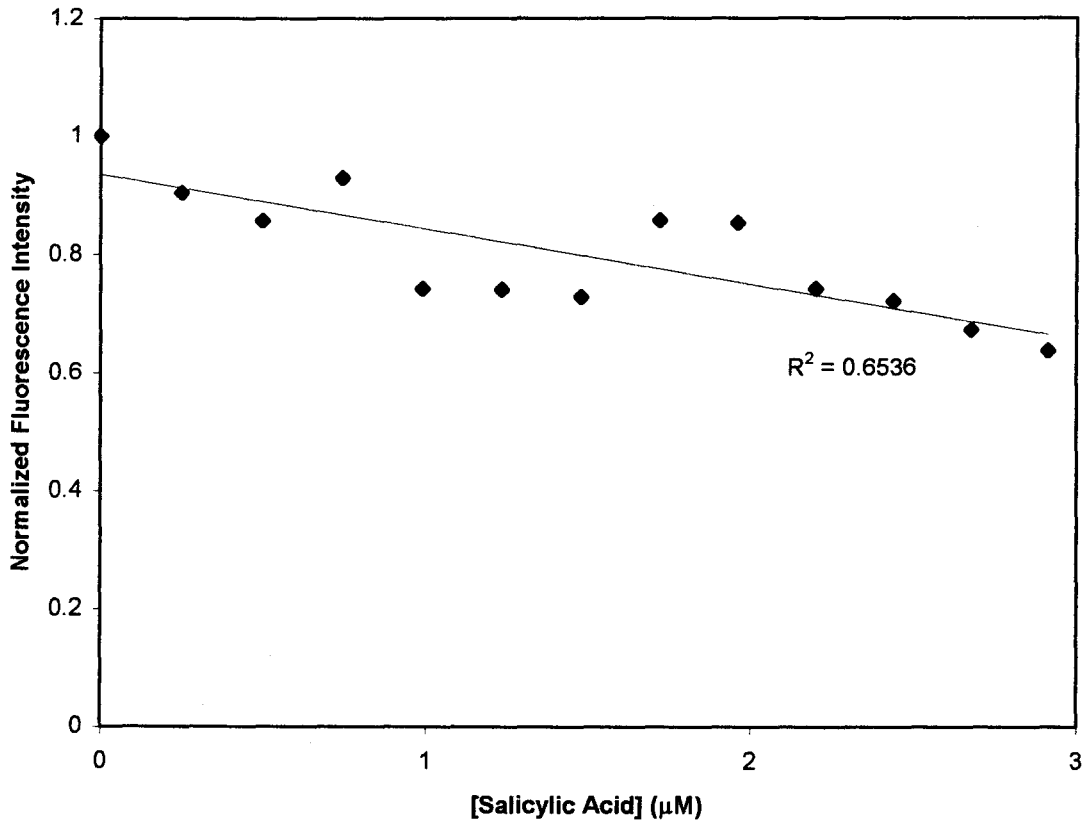


**Figure 3.24. Normalized Fluorescence Intensity of HSA Entrapped in a TEOS-Derived Thin Film as a Function of Salicylate Concentration**

coupled with a preconcentration effect may have enhanced the sensitivity. Further work is needed to more fully characterize this system.

### *3.5.2. Enzyme Activity Assays Based on Lipase-Catalyzed Hydrolysis of Glyceryl Tributyrate*

The results described above suggested that it was possible to entrap biomolecules in optically clear sol-gel-derived films with retention of their biological function. Hence, lipase was entrapped in TEOS and ORMOSIL-derived thin films coated onto glass microscope slides in the presence and absence of PEG to determine if it was possible to immobilize the enzyme in a thin film with retention of its hydrolytic activity.

The titrimetric method of quantitating the activity of entrapped lipase is problematic because it does not allow monitoring of the kinetics of the enzyme-catalyzed hydrolysis of triglycerides, it is time consuming and exhibits a low degree of reproducibility. Due to these problems, an alternate method of monitoring the activity of lipase spectroscopically was investigated and used with thin films.

#### 3.5.2.1. Absorbance-Based Assay of Thin Film Immobilized Lipase Activity

In this new method, a solution of the pH indicator phenol red (initially at pH 9.0) was added to the solution surrounding the slide to monitor the decrease in pH of the solution caused by the formation of butyric acid from the lipase-catalyzed hydrolysis of glyceryl tributyrate. The absorbance of phenol red at 560 nm drops with decreasing pH, hence it was a useful indicator for monitoring the formation of butyric acid. The

absorbance as a function of time for lipase entrapped in thin films prepared from TEOS, 20.0% MTES and 5.0% DMDMS are shown in Figures 3.25, 3.26 and 3.27, respectively.

The results of these lipase-doped thin film kinetic assays showed that the enzyme was active when entrapped within a thin film on the surface of a glass slide, relative to films that did not contain lipase. The slopes of the absorbance as a function of time were also reasonably reproducible between samples of the same silane content. The change is absorbance per unit time for lipase entrapped in each type of silane is summarized in Table 3.21.

**Table 3.21. Absorbance Change as a Function of Time for Lipase Entrapped in Thin Films of Various Compositions**

| Film Composition | Slope (ΔA/minute) |
|---|---|
| TEOS | -0.0126 ± 0.0003 |
| 20% MTES | -0.0261 ± 0.0014* |
| 5% DMDMS | -0.0041 ± 0.0007 |

*Average of slopes from t=1 to 8 min (Trial 1) and t=10 to 20 min (trials 2 and 3)

It was readily apparent from Figures 3.25 to 3.27 that lipase entrapped in the thin films remained active and was able to catalyze the hydrolysis of glyceryl tributyrate. It was also found that lipase entrapped in films prepared from 20.0% MTES seemed to be more active than when entrapped in films prepared from TEOS, which was consistent with the results obtained for lipase entrapped in sol-gel-derived slides. Contrary to previous results, it was found that lipase entrapped in films composed of 5.0% DMDMS was less active than lipase entrapped in TEOS-derived films. This result suggested that sol-gel-derived thin films may not behave in the same manner as bulk sol-gel-derived materials, due to the accelerated aging and drying processes found in films.

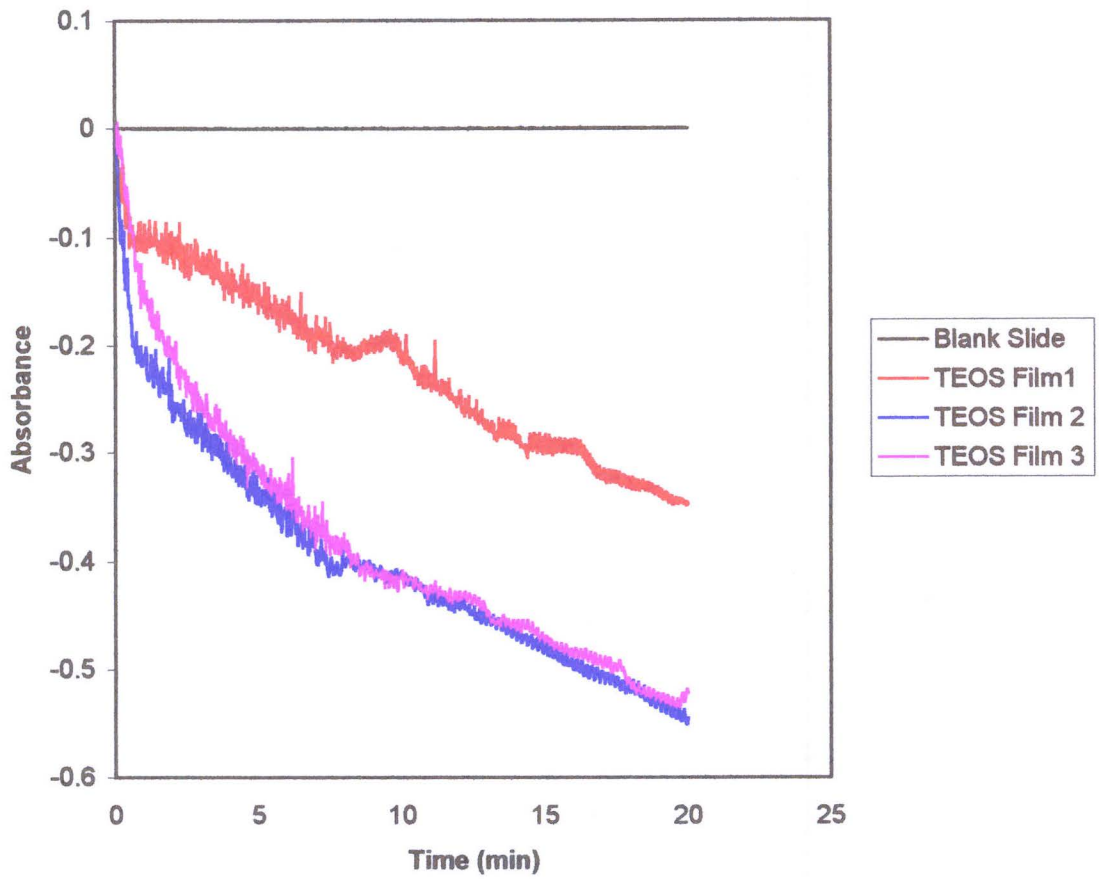


**Figure 3.25. Absorbance of Phenol Red as a Function of Time in the Presence of Lipase Entrapped in a Thin Film Derived From TEOS**

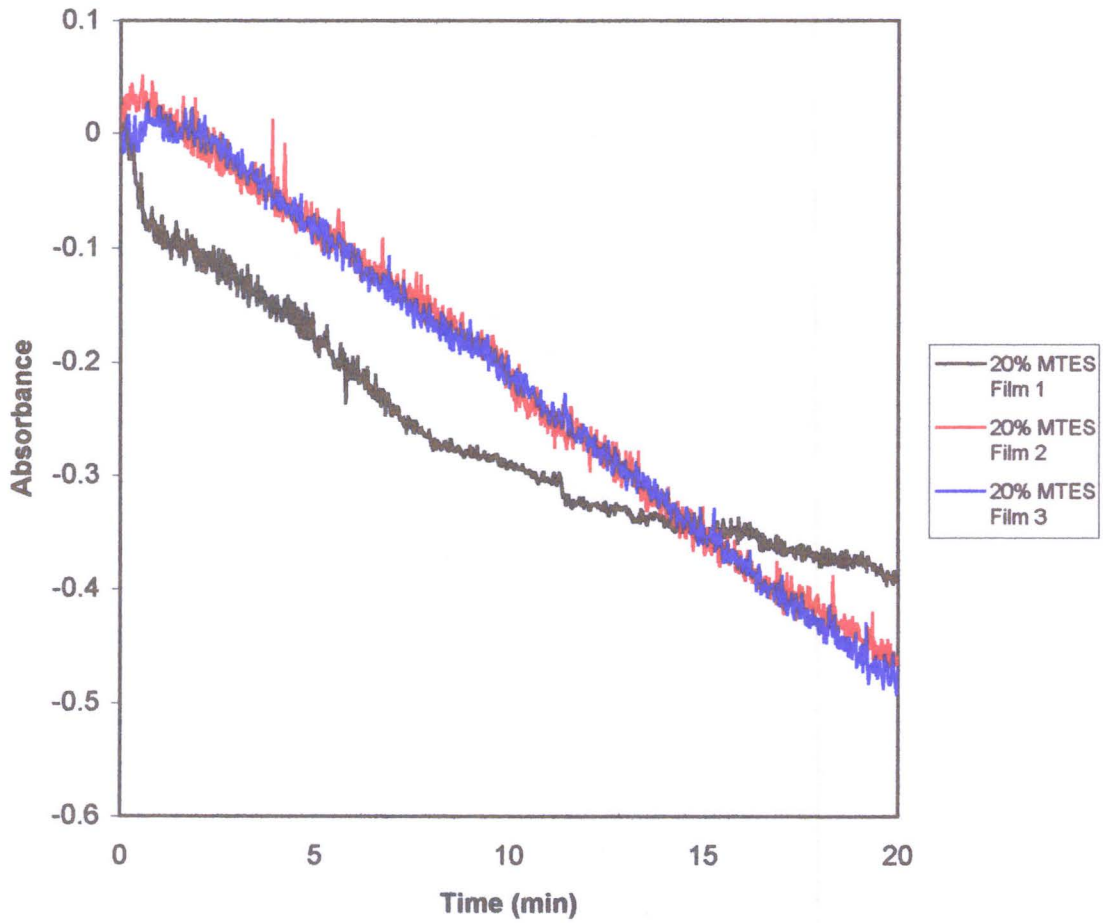


**Figure 3.26. Absorbance of Phenol Red as a Function of Time in the Presence of Lipase Entrapped in a Thin Film Derived From 20.0% MTES**

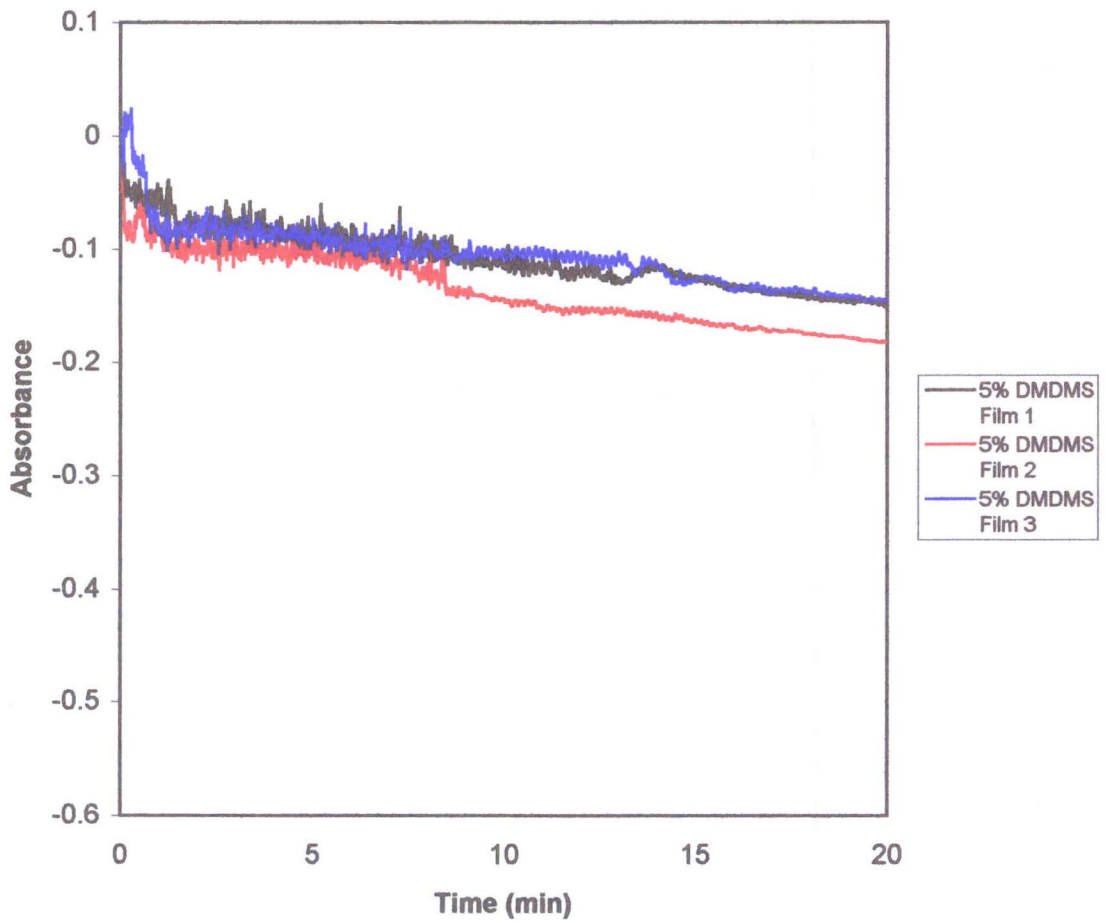


**Figure 3.27. Absorbance of Phenol Red as a Function of Time in the Presence of Lipase Entrapped in a Thin Film Derived From 5.0% DMDMS**

Spectroscopic examination of 7AI and prodan entrapped in thin films would be a useful method of monitoring the changes in film structure as the films age and dry.

Phenol red-based activity assays were also performed using lipase co-entrapped with PEG 400 and 600 in concentrations of 1.0 to 3.0% (w/v in the buffer). The slopes derived from these activity assays are provided in Table 3.22.

**Table 3.22. Absorbance Change as a Function of Time for Lipase Entrapped in TEOS-Derived Thin Films of in the Presence of Various Concentrations of PEG 400 and 600**

| Composition | Slope (ΔA/minute) |
|---|---|
| Polymer Free TEOS | -0.0126±0.0003 |
| 1.0% PEG 400 | -0.0115±0.0034 |
| 2.0 % PEG 400 | -0.0107±0.0030 |
| 3.0% PEG 400 | -0.0071±0.0023 |
| 1.0% PEG 600 | -0.0239±0.0039 |
| 2.0% PEG 600 | -0.0230±0.0055 |
| 3.0% PEG 600 | -0.0232±0.0027 |

It is evident from the slopes from the activity assays that PEG 400 in concentrations of 1.0 to 3.0 % (w/v in the buffer) did not appear to offer any enhancement in activity, and in fact reduced the activity relative to samples prepared from TEOS in the absence of additives. However, the co-entrapment of PEG 600 at concentrations of 1.0 to 3.0% (w/v in the buffer) provided enhancements in activity on the order of 1.83 to 1.90 times the activity of lipase entrapped in polymer free TEOS-derived films. It was possible that PEG 400 may have leached from within the pores of the film upon immersion into the phenol red solution used in the assay, preventing any enhancement in activity, while the larger size of PEG 600 molecules may have prevented them from leaching. The enhancement of activity with PEG 600 in TEOS is in excellent agreement with the results

obtained from bulk glasses, indicating that this is the best additive for lipase activity enhancement.

3.5.2.2. Enzyme-Catalyzed pH Change Detected by Dextran-SNARF-1 in Solution

Although it was possible to spectroscopically detect changes in pH using phenol red, this method was not well suited for sensing applications using evanescent excitation in conjunction with optical fibers or planar waveguides (a future goal of this project). This difficulty stems from the fact that the very short pathlength and scattering artifacts often make it difficult to measure small changes in absorbance using this format. For this reason, a new assay for detection of pH changes using a prototypical fluorescence-based detection scheme was investigated. This was accomplished using the pH sensitive probe dextran-SNARF-1. The initial characterization of the applicability of this probe for monitoring enzyme activity was done in solution. In this case, a solution of dextran-SNARF-1 at pH 9.0, 1.0 mM PBS was placed in a cuvette in the optical path of the fluorimeter. Glyceryl tributyrate (100 μL) was then added to the cuvette. Time traces were collected such that the ratio of signals from the left and right monochromators (set at 588 and 640 nm, respectively) was monitored in real time. At t=120 seconds, 50 μL of 0.12 mg/mL lipase (dissolved in pH 7.2, 10.0 mM Tris with 100.0 mM KCl) was added to the solution and monitoring of the ratio of emission intensities was continued. The time traces of three separate trials are shown in Figure 3.28. It is apparent from the figure that there was a significant increase in the ratio of emission of dextran-SNARF-1 upon addition of lipase to the substrate solution. This change in the ratio was due to the

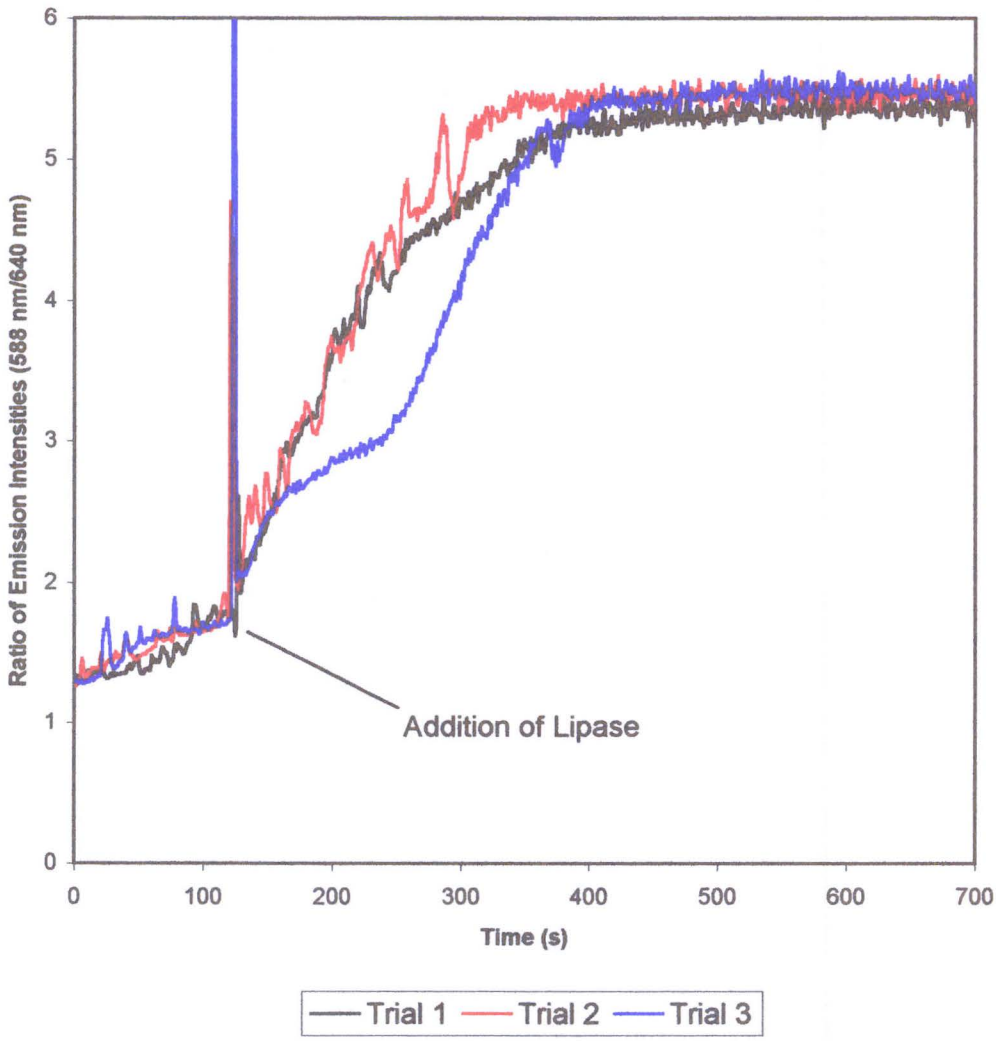


**Figure 3.28. Detection of Change of Ratio of Emission Intensities of Dextran-SNARF-1 in Solution Caused by the Lipase Catalyzed Hydrolysis of Glyceryl Tributyrate in Solution**

drop in pH of the solution caused by the lipase-catalyzed formation of butyric acid. The rate of increase in the ratio from trial to trial also showed a reasonable degree of reproducibility. The differences in the rates of change were likely due to ineffective stirring of the glyceryl tributyrate/lipase/dextran-SNARF-1 solution.

To confirm that the change in emission ratio was due to enzyme-catalyzed formation of butyric acid, a blank run was done wherein a 50 μL aliquot of pH 7.2 Tris buffer was added to a glyceryl tributyrate/dextran-SNARF-1 solution at t=120 seconds. After the ratio of emission intensity signal had equilibrated, 50 μL of lipase solution was added and the experiment was continued. The time trace for this experiment is shown in Figure 3.29. The figure shows that, as expected, there was a small increase in the ratio of emission intensities due to the addition of pH 7.2 buffer used for gelation due to the pH change from the initial value of 9.0. However, the degree of change in the ratio was not equivalent to that induced by the addition of an equivalent volume of lipase. In fact, upon subsequent addition of an equivalent volume of lipase solution, the ratio increased to approximately the same value and at the same rate as in the experiment that involved the initial addition of lipase (shown in Figure 3.28). Lipase was not dissolved in pH 9.0 Tris buffer to avoid this inherent increase in the ratio because the use of Tris at pH 9.0 causes rapid gelation, preventing formation of films.

Based on the above results, an investigation was done to determine if it was possible to monitor a change in pH using dextran-SNARF-1 in solution, induced by the hydrolysis of glyceryl tributyrate, catalyzed by lipase entrapped in a thin film. Experiments similar to those done with lipase, glyceryl tributyrate and dextran-SNARF-1 in solution were

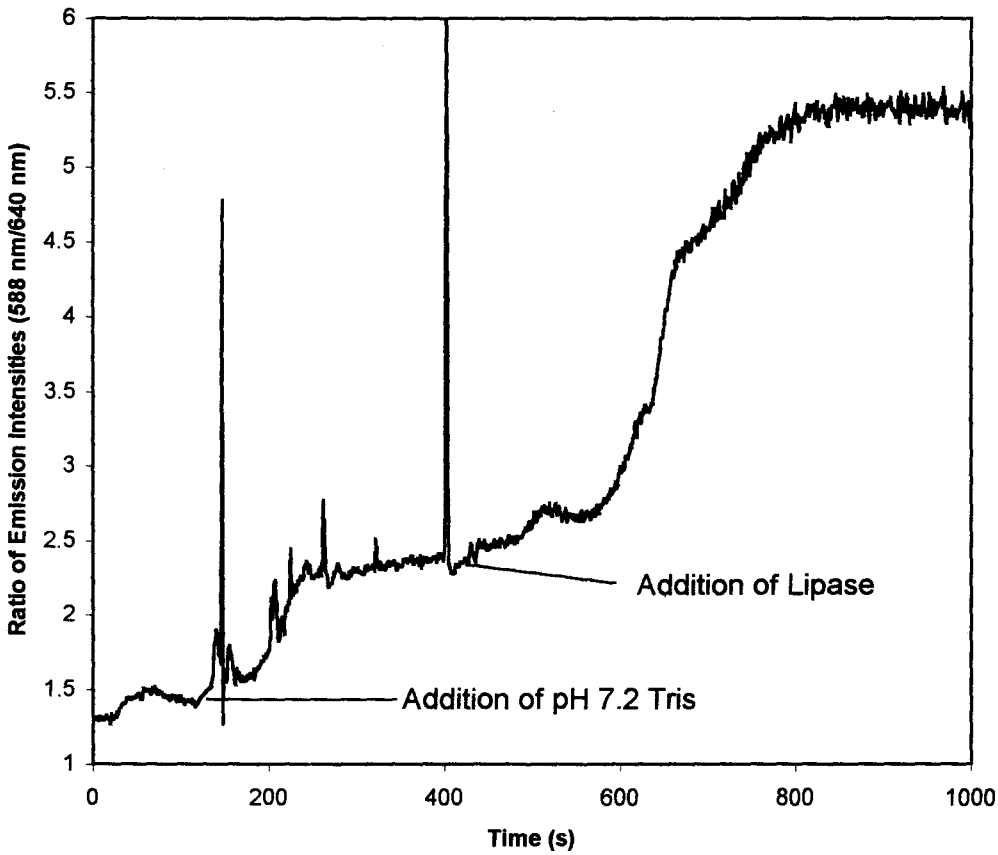


**Figure 3.29. Detection of the Change of Ratio of Emission Intensities of Dextran-SNARF-1 in Solution Caused by Sequential Additions of Blank Buffer Solution and Lipase Solution**

performed with the exception that lipase was not added to the solution. Instead, a lipase-doped TEOS-derived thin film was suspended in a solution of dextran-SNARF-1 with glyceryl tributyrate. The results (not shown) indicated that there was no significant change in pH of the solution due to the presence of the lipase-doped thin film. However, this was likely due to the orientation of the film in the optical path, which resulted in reflection artifacts and scattering of emission intensity. This configuration (i.e. thin film coated slide in a cuvette) with the indicator in solution is not the intended format for an optical sensor so the problem of scattering may not be as significant in the future when the instrument configuration is modified.

### *3.5.3. Demonstration of a Prototype for a Reagentless Optical Sensor for Triglycerides*

It is likely that the large solution volume of dextran-SNARF-1, the small amount of thin film entrapped lipase and diffusion problems within the solution may have made it difficult to measure changes in the ratiometric signal derived from dextran-SNARF-1 in the configuration described in the previous section. Therefore, TEOS-derived films were prepared with lipase co-entrapped with dextran-SNARF-1 and 3.0% PEG 600 (w/v in the buffer). 3.0% PEG 600 was used since it had been found that the presence of PEG at similar concentrations co-entrapped in sol-gel-derived slides with lipase provided an enhancement in the activity of lipase.

Figure 3.30 shows the change in the ratio of emission of dextran-SNARF-1 co-entrapped with lipase upon the addition of glyceryl tributyrate. Initially, the ratio of emission intensities remained constant, however, upon addition of substrate, the ratio of

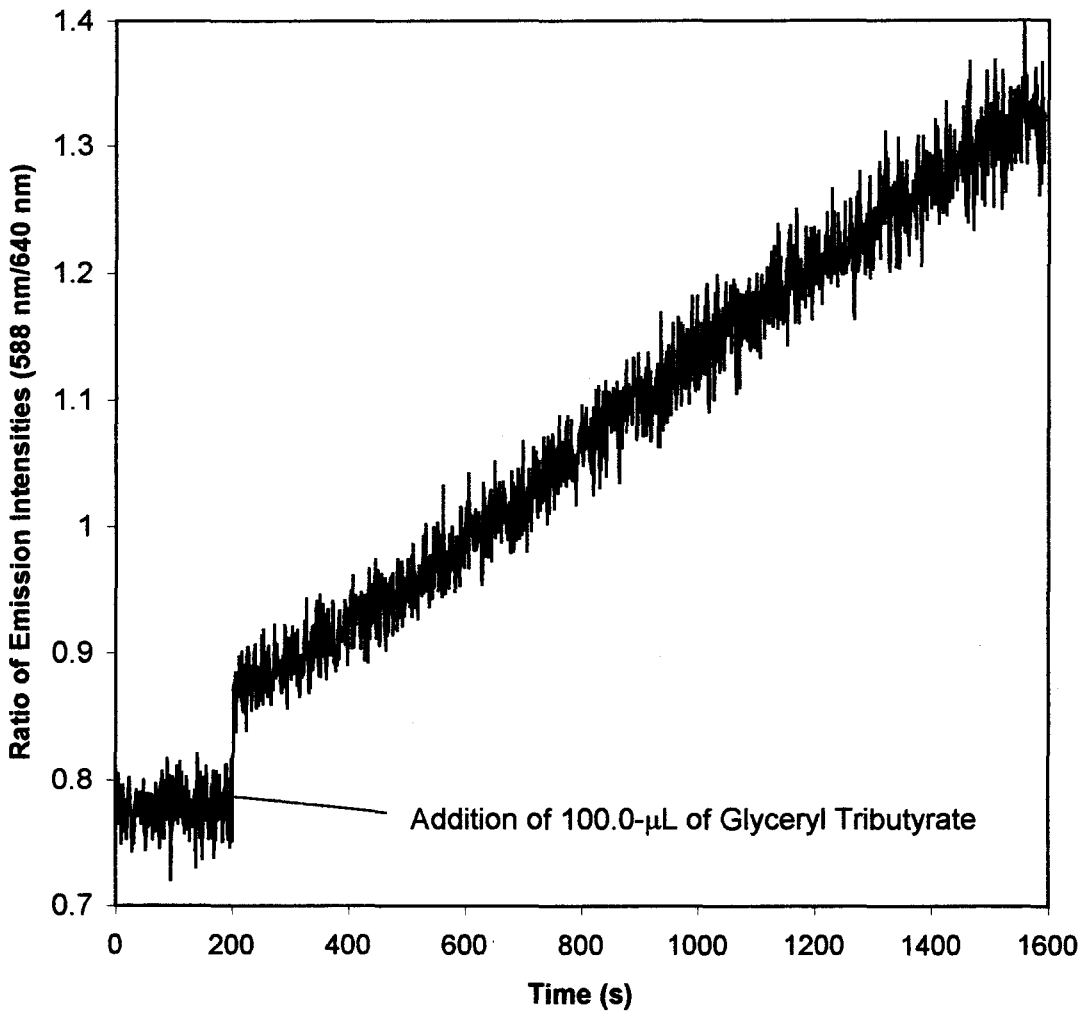


**Figure 3.30. Change in Ratio of Emission of Dextran-SNARF-1 Co-Entrapped with Lipase in a TEOS-Derived Thin Film (in the Presence of 3.0% (w/v) PEG)**

emission intensities immediately began to increase, indicating that the pH of the internal environment of the film, as detected by dextran-SNARF-1, had decreased due to the formation of butyric acid. The spectrum of the entrapped dextran-SNARF-1 was recorded prior to and after the assay was performed. These spectra are shown in Figure 3.31 and demonstrate that there was a change in pH in the region surrounding dextran-SNARF-1, as shown by the different spectral profiles before and after the assay was completed. Comparison of the ratio of emission intensities before (0.95) and after (1.00) the experiment demonstrated that the production of fatty acid products from the hydrolysis of a triglyceride could be detected without the addition of external reagents or indicators and was an important step in the development of a reagentless biosensor for triglycerides. However, due to difficulties associated with reproducibly mounting the slides in the proper orientation in the optical path of the fluorimeter, the reagentless detection method showed poor reproducibility. Further work must be done to optimize the detection of the changes in the ratio of emission intensities such that the emission of dextran-SNARF-1 is independent of the scattering of excitation or emission radiation.

In summary, the results of the studies involving entrapment of both HSA and lipase in sol-gel-derived thin films showed that both of these biomolecules retained their biological functions once entrapped. HSA was able to bind salicylate with enhanced affinity, compared to solution or entrapped in sol-gel-derived slides. The enhanced binding affinity was possibly due to preconcentration of the ligand by the film itself and/or higher accessibility of the protein entrapped in the film relative to that of HSA entrapped in a slide. It was also shown that it was possible to monitor spectroscopically

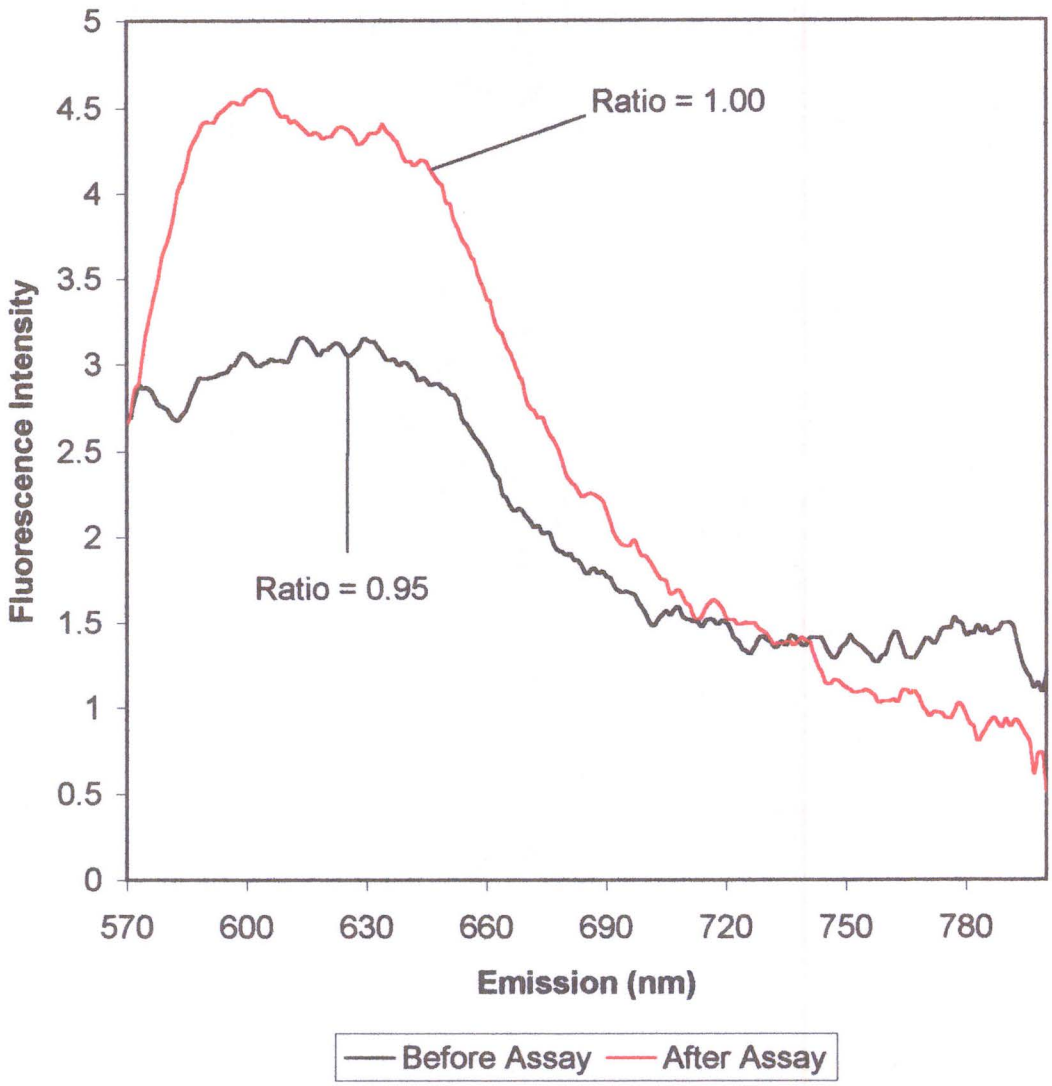


**Figure 3.31. Emission Spectra of Dextran-SNARF-1 Co-Entrapped with Lipase in a TEOS-Derived Thin Film (in the Presence of 3.0% (w/v) PEG) Prior to Addition of Glyceryl Tributyrate and After the Assay Was Completed**

the lipase-catalyzed formation of butyric acid in real time when lipase was immobilized in thin sol-gel-derived films. These spectroscopic activity assays may allow the future determination of enzyme kinetic parameters. A prototypical fluorescence-based assay for monitoring the activity of lipase was also developed with promising results. The results suggested that the assay may find application in the construction of a reagentless optical fiber or planar waveguide-based triglyceride biosensor. However, further work must be done to optimize the assay, specifically to improve the detection scheme to allow enhanced detection of the emission of dextran-SNARF-1 by avoiding the problem of scattering of the excitation and emission intensities.

# Chapter 4: Conclusions and Future Work

## 4.1. Conclusions

The overall purpose of the research project was the preparation and spectroscopic characterization of optically clear, sol-gel-derived hybrid organic/inorganic materials using protocols amenable to entrapment of biomolecules. The idea of immobilizing biomolecules in sol-gel-derived materials for preparation of biosensors is not new. However, most of the work done in this field has focused on the use of TEOS and TMOS-derived bulk glasses for entrapment of biomolecules. These materials are appropriate for immobilization of hydrophilic biomolecules due to the highly polar nature of the silica matrix. However, not all biomolecules exhibit optimal functionality in hydrophilic environments.

To maximize the functionality of sol-gel-immobilized lipophilic proteins such as lipase, it was necessary to modify the polarity of the internal environment of sol-gel-derived materials. This was accomplished using organically modified silane precursors and polymer additives during formation of the materials. The use of ORMOSILs for modification of the internal environment of sol-gel-derived materials has been demonstrated previously, however, the methods employed resulted in materials that were not optically clear and hence not amenable to spectroscopic characterization. A portion of this project, therefore, involved the development of a protocol for formation of optically clear hybrid organic/inorganic sol-gel-derived materials that was amenable to entrapment of biomolecules.

It was found that it was possible to prepare optically clear sol-gel-derived materials of varied composition that retained stable physical properties by controlling the processing conditions. Materials formed as slides could be prepared with ORMOSIL compositions of up to 20.0% MTES (v/v, with respect to TEOS), 5.0% DMDMS and 10.0% PTMS, with high optical clarity and reasonable durability if the silane precursors were co-hydrolyzed (i.e. TEOS and ORMOSIL hydrolyzed in the same solution). Compositions greater than these stated values resulted in materials that were not optically clear or that were easily fractured. It was also found that the internal polarity of the sol-gel-derived materials could be tuned by adjusting the concentration of the silane precursors used for formation of the materials. The fact that many of the samples were optically clear allowed fluorimetric determination of the internal polarity of the materials, using the environmentally sensitive probes 7AI and prodan. It was also found that washing the materials provided enhanced control of the polarity of the internal environment, allowing the preparation of materials that had a narrower distribution of internal environments, as demonstrated by the reduced degree of spectral broadening of the entrapped probes. Another method of modification of the internal environment of the materials was the incorporation of polymer additives into the matrix prior to gelation. Once again, it was shown that the resulting materials were optically clear and reasonably resistant to fracture due to dehydration and rehydration over time.

To demonstrate that the protocol adopted for preparation of optically clear hybrid materials was amenable to entrapment of biomolecules, the protein HSA and the hydrolytic, lipophilic enzyme lipase were entrapped in these materials. Their biological

functions were tested once entrapped in materials of various compositions (in terms of ORMOSIL and polymer additive content). It was found that for HSA, entrapment allowed retention of the salicylate-binding ability of the protein relative to its native state in solution. In some cases, entrapment even enhanced the affinity of the protein for its ligand, likely due to a preconcentration of the ligand by the material. For development of sensors, this preconcentration effect may be useful to allow more efficient association of the ligand with the protein.

In the case of lipase, it was found that entrapment of the enzyme in sol-gel-derived slides of various compositions allowed partial retention of its hydrolytic activity, even 21 days after entrapment. Some of the compositions of the materials resulted in better retention of the hydrolytic activity of the enzyme, likely due to an increased degree of hydrophobicity necessary for lipase function. The activity of the enzyme was only a fraction of that for the enzyme in solution, likely due to poor accessibility of the enzyme to its substrate. The poor accessibility was likely due to the slow diffusion of the substrate through the porous silica matrix. A significant finding was that the co-entrapment of PEG 600 in concentrations of 10.0% (w/v in the buffer) with lipase resulted in the greatest retention of activity of the entrapped enzyme.

The format chosen for coupling of the sol-gel-derived materials to planar waveguides was thin sol-gel-derived films. A new and simple protocol was developed for formation of thin films that allowed control of the properties of the films. By manipulating such film preparation parameters as solution viscosity, substrate withdrawal rate and buffer conditions, it was possible to dipcast films onto the surface of glass or

quartz slides that exhibited high optical clarity and excellent dehydration/rehydration stability. Biomolecules entrapped into films retained their biological function and in the case of HSA, there was an enhancement in the ligand-binding ability of the protein when entrapped in a film, likely due to higher accessibility of the protein to salicylate as well as preconcentration of salicylate by the film itself.

The initial development of a fluorescence-based assay for monitoring the rate of formation of the products of the hydrolysis of triglycerides was also performed. This assay used the pH-sensitive, ratiometric probe SNARF-1 (conjugated to a hydrophilic polysaccharide) to monitor the drop in pH induced by the lipase-catalyzed formation of butyric acid. Initial results using the probe and enzyme in solution indicated that it was possible to monitor the activity of the enzyme in real time and with reasonable degrees of reproducibility and that the pH-dependent signal derived from dextran-SNARF-1 was reversible. By using SNARF-1 labeled dextran, it was possible to reduce the degree of signal loss resulting from leaching of the entrapped probe from the sol-gel-derived matrix. The use of this fluorescent probe entrapped in a thin film with retention of pH sensitivity was also a step forward in the development of an optical sensor of pH that could be coupled to planar waveguides or optical fibers.

The most significant result of this project was the ability to monitor a change in pH, as detected by thin film immobilized dextran-SNARF-1, resulting from the lipase catalyzed hydrolysis of glyceryl tributyrate to form butyric acid, within a self contained sensor without the need for external reagents. The demonstration of the ability to detect

the presence of triglycerides indicates that, with optimization of the detection scheme, a reagentless optical biosensor for triglycerides can be constructed.

## 4.2. Future Work

The results of this research project have shown that it is possible to entrap biomolecules in optically clear hybrid organic/inorganic sol-gel-derived materials with retention of their biological function. However, for these materials to be used for preparation of a viable optical sensor or biosensor, some further work must be undertaken. First, a new method of mounting glass slides coated with SNARF-1-dextran-doped thin films in the optical path of the fluorimeter must be developed. The current method of orienting the slide in the optical path does not provide efficient detection of intensity from one form of the probe, when using a T-format for simultaneous monitoring of the emission of the acidic and basic forms of the probe in real time. Possible detection schemes may involve evanescent excitation of the probe entrapped in a film on the surface of a glass slide or optical fiber. Surface immobilization would allow coupling of the pH-dependent emission of the two forms of the probe back into the waveguide which could then be detected simultaneously using separate detectors (such as photodiodes) for each wavelength. Since it was possible to excite dextran-SNARF-1 at a variety of wavelengths, small, inexpensive excitation sources such as light emitting diodes could be used to allow miniaturization of the sensor. This may allow detection of fluorescence intensity that is not dependent on the orientation of the slide itself.

The results of this research project have demonstrated that lipase retains its activity when entrapped in sol-gel-derived thin films, that dextran-SNARF-1 also retains its pH sensitivity when entrapped and that it is possible to detect enzyme induced changes in pH when the lipase and dextran-SNARF-1 are co-immobilized. This method could also be extended to application with other hydrolytic enzymes such as acetylcholinesterase or urease. Both of these enzymes form hydrolysis products that cause changes in the pH of the surrounding solution, which could be monitored by co-entrapped SNARF-1-dextran.

## References


1. Hall, E. A. H.; *Biosensors*, Prentice Hall, **1991**, 6-7.
2. Paddle, B.M.; *Biosensors and Bioelectronics*, **1996**, 11, 1079-1113.
3. Collings, A.F.; Caruso, F.; *Rep. Prog. Phys.*, **1997**, 1397-1445.
4. Brennan, J.D.; Accepted for publication in *J. Fluorescence*, **1999**.
5. Brennan, J.; *Appl. Spec.*, **1999**, 53, 106A-121A.
6. Voet, D.; Voet, J.G.; *Biochemistry, 2nd Edition*, John Wiley and Sons, Inc., **1995**, 332-333.
7. Weetall, H.H.; *Appl. Biochem. Biotechnol.* **1993**, 41, 157-188.
8. O'Driscoll, K.F; *Methods Enzymol.*, **1976**, 44, 169-183.
9. Brinker, C.J.; Scherer, G.W.; *Sol-Gel Science: The Physics and Chemistry of Sol-Gel Processing*, Academic Press, **1990**.
10. Hench, L.L; West, J.K; *Chem. Rev.*, **1990**, 90, 33-72.
11. Braun, S.; Rappoport, S.; Zusman, R.; Avnir, D.; Ottolenghi, M.; *Mat. Lett.*, **1990**, 10, 1-5.
12. Ellerby, L.M.; Nishida, C.R.; Nishida, F.; Yamanaka, S.A.; Dunn, B.; Valentine, J.S.; Zink, J.I.; *Science*, **1992**, 255, 1113-1115.
13. Braun, S.; Shtelzer, S., Rappoport, S.; Avnir, D., Ottolenghi, M.; *J. Non-Crys. Solids*, **1992**, 147&148, 739-743.
14. Avnir, D.; Braun, S.; Lev, O.; Ottolenghi, M.; *Chem. Mater.*, **1994**, 6, 1605-1614.
15. Dave, B.C.; Dunn, B.; Valentine, J.S.; Zink, J.I.; *Anal. Chem.*, **1994**, 66, 1120A-1127A.
16. Dave, B.C.; Miller, J.M.; Dunn, B.; Valentine, J.S.; Zink, J.I.; *J. Sol-Gel Sci. Tech.*, **1997**, 8, 629-634.
17. Dunn, B.; Miller, J.M.; Dave, B.C.; Valentine, J.S.; Zink, J.I.; *Acta. Mater.*, **1998**, 46, 737-741.
18. Lev, O.; *Analusis*, **1992**, 20, 543-553.
19. *The Chemistry of Organic Silicon Compounds, Vol. 2.;* Rappoport, Z., Apeloig, Y., Eds., John Wiley and Sons, Ltd., **1998**, pp. 2317-2361.
20. Lev, O.; Tsionsky, M.; Rabinovich, V.; Glezer, S.; Sampath, I.; Pankratov, J. G.; *Anal. Chem.*, **1995**, 67, 22A-30A.
21. Narang, U.; Jordan, J.D.; Bright, F.V.; Prasad, P.N.; *J. Phys. Chem.*, **1994**, 98, 8101-8107.
22. Lobnik, A.; Wolfbeis, O.S.; *Analyst*, **1998**, 123, 2247-2250.
23. Flora, K.K.; Brennan, J.D.; Baker, G.A.; Doody, M.A.; Bright, F.V.; *Biophys. J.* **1998**, 1084-1096.
24. Flora, K.K.; Brennan, J.D.; *Anal. Chem.*, **1998**, 70, 4505-4513.
25. Chen, Q.; Kenausis, G.L.; Heller, A.; *J. Am. Chem. Soc.*, **1998**, 120, 4582-4585.
26. Wang, R.; Narang, U.; Prasad, P.N.; Bright, F.V.; *Anal. Chem.*, **1993**, 65, 2671-2675.
27. Shabat, D.; Grynszpan, F.; Saphier, S.; Turniansky, A.; Avnir, D.; Keinan, E.; *Chem. Mater.*, **1997**, 2258-2260.

28. Dosoretz, C.; Armon, R.; Starosvetzky, J.; Rothschild, N.J.; *J. Sol-Gel Sci. Technol.* **1996**, 7, 7-11.
29. Flora, K.K.; Dabrowski, M.; Musson, S.; Brennan, J.D.; Accepted for Publication in *Can. J. Chem.*, **1999**.
30. Rottman, C.; Grader, G.S.; De Hazan, Y.; Avnir, D.; *Langmuir*, **1996**, 12, 5505-5508.
31. Schubert, U.; Husing, N.; Lorenz, A.; *Chem. Mater.*, **1995**, 7, 2010-2027.
32. Kim, G-D.; Lee, D-A.; Kim, J-D.; Moon, J-W.; Lee, H-L.; *J. Sol-Gel Sci. Tech.*, **1997**, 10, 283-289.
33. Baker, G.A.; Pandey, S.; Maziarz, E.P.; Bright, F.V.; *J. Sol-Gel Sci. Tech.*, **1999**, 15, 37-48.
34. Wen, J.; Wilkes, G.; *Chem. Mater.*, **1996**, 8, 1667-1681.
35. Reetz, M.T.; Jaeger, K-E.; *Chem. Phys. Lipids*, **1998**, 93, 3-14.
36. Reetz, M.T.; Zonta, A.; Simpelkamp, J.; *Angew. Chem. Int. Ed. Engl.*, **1995**, 34, 301-303.
37. Reetz, M.T.; Zonta, A.; Simpelkamp, J.; *Biotech. Bioeng.* **1996**, 49, 527-534.
38. Negrerie, M.; Gai, F.; Bellefeuille, S.M.; Petrich, J.W.; *J. Phys. Chem.*, **1991**, 95, 8663-8670.
39. Chapman, C.F.; Maroncelli, M.; *J. Phys. Chem.*, **1992**, 96, 8430-8441.
40. Chen, Y.; Rich, R.L.; Gai, F.; Petrich, J.W.; *J. Phys. Chem.* **1993**, 97, 1770-1780.
41. Rich, R.L.; Chen, Y.; Neven, D.; Negrerie. M.; Gai, F.; Petrich, J.W.; *J. Phys. Chem.*, **1993**, 97, 1781-1788.
42. Weber, G.; Ferris, F.J.; *Biochem.*, **1979**, 18, 3075-3078.
43. Sun, S.; Heitz, M.P.; Perez, S.A.; Colon, L.A.; Bruckenstein, S.; Bright, F.V.; *Appl. Spec.*, **1997**, 51, 1316-1322.
44. Carter. D.C.; Ho, J.X.; *Adv. Protein Chem.*, **1994**, 45,153-203.
45. Kuncova, G.; Guglielmi, M.; Dubina, P.; Safar, B.; *Collect. Czech. Chem. Commun.*, **1995**, 60, 1573-1577.
46. Flora, K.K.; Brennan, J.D.; Accepted for publication in *The Analyst*, **1999**.
47. MacCraith, B.D.; *Sens. and Actuators B*, **1993**, 11, 29-34.
48. Plaschke, M.; Czolk, R.; Reichert, J.; Ache, H.J.; *Thin Solid Films*, **1996**, 279, 233-235.
49. Baker, G.A.; Watkins, A. N.; Pandey, S.; Bright, F.V.; *Analyst*, **1999**, 124, 373-379.
50. Whitaker, J.E.; Haughland, R.P.; Prendergast, F.G.; *Anal. Biochem.*, **1991**, 194, 330-344.
51. Parker, J.W.; Laksin, O.; Yu, C.; Lau, M-L.; Klima, S.; Fisher, R.; Scott, I.; Atwater, B.W.; *Anal. Chem.*, **1993**, 65, 2329-2334.
52. Lakowicz, Joseph R.; *Principle of Fluorescence Spectroscopy*, Plenum Press, 1983, 1-6.
53. Lakowicz, Joseph R.; *Principle of Fluorescence Spectroscopy*, Plenum Press, 1983, 9-11.
54. Lakowicz, Joseph R.; *Principle of Fluorescence Spectroscopy*, Plenum Press, 1983, . 189-190.

55. Wehry, E.L.; In *Practical Fluorescence, 2nd Ed.*, Edited by Guilbault, G.G.; Marcel Dekker, Inc., 1990, 133.
56. Wehry, E.L.; In *Practical Fluorescence, 2nd Ed.*, Edited by Guilbault, G.G.; Marcel Dekker, Inc., 1990, 137.
57. Matsui, K.; Matsuzuka, T.; Fujita, H.J.; *J. Phys. Chem.*, **1989**, 93, 4991-4994.
58. Wehry, E.L. In *Practical Fluorescence, 2nd Ed.*, Edited by Guilbault, G.G.; Marcel Dekker, Inc., 1990, 166.
59. Guglielmi, M.; Colombo, P.; Peron, F.; Esposti, L.M.D.; *J. Mat. Sci.*, **1992**, 27, 5052-5056.
60. Nishida, F.; McKiernan, J.M.; Dunn, B.; Zink, J.I.; Brinker, J.C.; Hurd, A.J.; *J. Am. Ceram. Soc.*, **1995**, 78, 1640-1648.
61. Reuter, H.; Brandherm, M-T.; *Angew. Chem. Int. Ed. Engl.*, **1995**, 34, 1578-1579.
62. Dunawila, D.D.; Torgerson, B.A.; Chang, C.K.; Berglund, K.A.; *Anal. Chem.*, **1994**, 66, 2739-2744.
63. Jordan, J.D.; Dunbar, R.A.; Bright, F.V.; *Anal. Chim. Acta.*, **1996**, 332, 83-91.
64. Jordan, J.D.; Dunbar, R.A.; Hook, D.J.; Zhuang, H.; Gardella, J.A.; Colon, L.A.; Bright, F.V.; *Chem. Mater.*, **1998**, 10, 1041-1051.
65. Malins, C.; Fanni, S.; Glever, H.G.; Vos, J.G.; MacCraith, B.D.; *Anal. Commun.*, **1999**, 3-4.
66. McDonagh, C.; MacCraith, B.D.; McEvoy, A.K.; *Anal. Chem.*, **1998**, 70, 45-50.
67. Krihak, M.K.; Shahriari, M.R.; *Electron. Lett.*, **1996**, 32, 240-241.
68. MacCraith, B.D.; McDonagh, C.M.; O'Keefe, G.; Keyes, E.T.; Vos, J.G.; O'Kelly, B.; McGilp, J.F.; *Analyst*, **1993**, 118, 385-388.
69. Dunbar, R.A.; Jordan, J.D.; Bright, F.V.; *Anal. Chem.*, **1996**, 68, 604-610.
70. Lee, J.E.; Saavedra, S.S.; *Anal. Chim. Acta.*, **1994**, 265-269.
71. Butler, T.M.; MacCraith, B.D.; McDonagh, C.; *J. Non-Crys. Sol.*, **1998**, 224, 249-258.
72. Collino, R.; Therasse, J.; Chaput, F.; Boilot, J-P.; Levy, Y.; *J. Sol-Gel Sci. Tech.*, **1996**, 7, 81-85.
73. MacCraith, B.D.; Ruddy, V.; Potter, B.; O'Kelly, B.; McGilp, J.; *Electron. Lett.*, **1991**, 27, 1247-1248.
74. Zheng, L.; Reid, W.R.; Brennan, J.D.; *Anal. Chem.*, **1997**, 3940-3949.
75. Brown, K.F.; Crooks, M.J.; *Biochem. Pharmacol.*, **1976**, 25, 1175-1178.
76. Miller, J.M.; Dunn, B.; Valentine, J.S.; Zink, J.I.; *J. Non-Crys. Solids*, **1996**, 202, 279-289.
77. Livage, J.; *Curr. Opin. Solid-State Mater. Sci.*, **1997**, 2, 132-138.
78. Zarzycki, J.; Prassas, M.; Phalippou, J.; *J. Mater. Sci.*, **1982**, 17, 3371-3379.
79. Miller, J. M.; Dunn, B.; Valentine, J. S.; Zink, J. I.; *Chem. Mater.*, **1993**, 5, 115-120.
80. Reetz, M.Z.; *Adv. Mater.*, **1997**, 9, 943-954.
81. Brzozowski, A.M.; Derewenda, U.; Derewenda, Z.S.; Dodson, G.G.; Lawson, D.M.; Turkenburg, J.P.; Bjorkling, F., Huge-Jensen, B.; Patkar, S.A.; Thim, L.; *Nature*, **1991**, 491-494.

82. Bolen, D.; Liu, Y.; *Biochem.*, **1995**, 34, 12884-12891.
83. Peters, D., Miethchen, R.; *J. Fluorine Chem.*, **1996**, 79, 161-165.